

**DEVELOPING A NESTED FINITE-ELEMENT HYDRODYNAMIC
MODEL TO PREDICT PHASE AND AMPLITUDE MODIFICATION OF THE
TIDE WITHIN NARROW FJORDS**

by

Ian Church

B.Sc.Eng. Geomatics and Geodesy, University of New Brunswick, 2006

A Thesis Submitted in Partial Fulfillment of
the Requirements for the Degree of

Master of Science in Engineering

In the Graduate Academic Unit of Geodesy and Geomatics Engineering

Supervisor: John E. Hughes Clarke, Ph.D., Geodesy and Geomatics Engineering

Examining Board: Marcelo C. Santos, Ph.D., Geodesy and Geomatics Engineering
Susan P. Haigh, Ph.D., Geodesy and Geomatics Engineering

External Examiner: Charles G. Hannah, Ph.D., Ocean Sciences Division, Bedford
Institute of Oceanography

This thesis is accepted by the

Dean of Graduate Studies

THE UNIVERSITY OF NEW BRUNSWICK

September, 2008

©Ian Church, 2008

DEDICATION

To Erin, Gwen and Jim for their continued support, encouragement and patience.
This wouldn't have been possible without them.

ABSTRACT

A long term monitoring project to measure the inter-annual change in pro-glacial deltaic sediments has been initiated in Oliver Sound, one of a cluster of fjords that lie off Eclipse Sound at the northern tip of Baffin Island, Canada. In order to confidently identify the decimetre-level changes in seabed morphology from multibeam surveys, adequate tidal control is required. Surveying in such remote locations presents conditions, logistics and time constraints that prohibit the installation of tide gauges throughout the survey area and existing predicted tide stations are separated from the survey area by complex fjords and islands. To overcome these hurdles, a high resolution hydrodynamic model simulation has been constructed to predict the tides throughout the survey region which accounts for the changes in tidal phase and amplitude within the complex fjords. The simulation results are compared to existing lower resolution tidal models, nearby predicted tides and Globally Corrected GPS data from survey vessels working and transiting throughout the area.

ACKNOWLEDGEMENTS

I would like to thank Dr. John Hughes Clarke for supervising this project and providing invaluable information, Susan Haigh for spending hours going over concepts and procedures with me and Charles Hannah for helping me bring this work together.

The following people also provided me with essential information over the past two years.

- The Canadian Hydrographic Service (CHS) for the bathymetric data within the region of my project.
- NSERC from providing funding which allowed work to be completed on this project.
- ArcticNet NCE for providing funding and the platform to obtain data vital towards the completion of this project.
- Everyone within the Ocean Mapping Group for answering any question I had about software or programming.
- Dave Greenberg for tips and tricks associated with running the hydrodynamic models

- Rodrigo Leandro for providing information on and access to the online GAPS processing software.
- The sponsors of the chair in Ocean Mapping at the university of New Brunswick (U.S. Geological Survey, Kongsberg Maritime, Fugros Pelagos, Royal (U.K) Navy, Rijkswaterstaat and the Route Survey Office of the Canadian Navy)

TABLE OF CONTENTS

	Page
Dedication.....	ii
Abstract.....	iii
Acknowledgements.....	iv
Table of Contents.....	vi
List of Tables.....	viii
List of Figures.....	ix
List of Symbols, Nomenclature or Abbreviations.....	xiv
Chapter 1. Introduction.....	1
Chapter 2. Background.....	5
2.1 Tides.....	6
2.1.1 Tidal Prediction.....	9
2.1.2 Assessing Predicted Tides.....	12
2.2 Hydrodynamic Model.....	23
2.3 QUODDY.....	28
2.3.1 Input Parameters.....	29
2.4 Arctic8c Model.....	31
2.5 GPS Processing.....	34
2.5.1 CNav GcGPS.....	36
2.5.2 GPS Processing.....	39
Chapter 3. Experimental Design.....	41
3.1 Constructing the Grid.....	41
3.2 Grid Creation Process.....	43
3.3 Running the Model with the Constructed Grid.....	45
3.4 Results.....	46
3.5 Applications of the Developed Hydrodynamic Model.....	52
Chapter 4. Analysis.....	55
4.1 Model Results vs. Arctic8c Model.....	55
4.1.1 Comparison at the Head of Oliver Sound.....	59
4.2 Model Results vs. GPS.....	60
4.2.1 Amundsen 2004.....	61
4.2.2 Amundsen 2005.....	66
4.2.3 Amundsen 2006.....	71
4.2.4 Amundsen 2007.....	78
4.2.5 Using CNav to Observe Tides.....	83
4.2.6 Apparent Drift within Navy Board Inlet.....	84
4.3 Model Results vs. Predicted Tides.....	86

4.3.1	Pisiktarfik Island.....	86
4.3.2	Koluktoo Bay	87
4.3.3	Milne Inlet	88
4.4	Misfit Analysis	89
4.4.1	Predicted Tides	90
4.4.2	Arctic8c Model.....	93
4.5	Model Applied to Multibeam	95
4.5.1	Amundsen EM300 Data	96
4.5.2	Heron EM3002 data	98
Chapter 5.	Recommendations	101
Chapter 6.	Conclusions	103
Bibliography	106
Appendix A	110
Appendix B	121

Curriculum Vitae

LIST OF TABLES

	Page
Table 2.1 – Doodson Fundamental Tidal Frequencies (Modified from [Stewart, 2005]) ..	7
Table 2.2 – Doodson Numbers used with principal harmonic constituents (Modified from [Stewart, 2005])	8
Table 2.3 – Record Length Required to Resolve Principle Harmonic Constituents	11
Table 2.4 – CHS Bluefile Constituents vs. T_TIDE output for Koluktoo Bay 1964 and 1965. Amplitude in Metres and Phase in Degrees.....	13
Table 2.5 – T_TIDE Comparison for 1964 and 1965 at Koluktoo Bay	15
Table 2.6 – Wave Speed Equation.....	19
Table 2.7 – Resonant Wavelength for M2 and K1 Constituents	19
Table 2.8 – Tidal Propagation for M2 and K1 though Predicted Tide Stations	21
Table 2.9 – Amplification Calculation within the Inlet between the Pisiktarfik and Koluktoo Stations (Equation from [Forrester, W. D., 1983]).....	23
Table 2.10 – Navier-Stokes Equations.....	27
Table 2.11 – QUODDY Simulation Input Parameters	30
Table 2.12 – Inverse Barometer Effect Calculation Showing Change in Water Level with Pressure Change.....	38
Table 4.1 – Potential Relative Error Between using a Tidal Prediction from the Developed Hydrodynamic Model and the Existing Arctic8c Grid.....	60
Table 4.2 – Misfit Calculation	90
Table 4.3 – Amundsen Multibeam Comparison Results	97
Table 4.4 – 0.2% Water Depth Accuracy for the Five Comparison Locations	98
Table 4.5 – Heron Multibeam Comparison Results.....	99

LIST OF FIGURES

	Page
Figure 1.1 – Hydrodynamic Model Region located at the Northern Tip of Baffin Island .	4
Figure 2.1 – Oliver Sound Multibeam Bathymetry from CCGS Amundsen and CSL Heron within Oliver Sound.....	5
Figure 2.2 – Classification of Tides in Canadian Waters with Example Power Spectrum from the Arctic8c grid of Dunphy et al. [2005] within the Enclosed Waters of Bylot Island. Circled Area indicates Model Region (from [Forrester, W. D., 1983]).....	9
Figure 2.3 – Locations of CHS Predicted Tide Stations within the Enclosed Waters of Bylot Island.....	11
Figure 2.4 – CHS Bluefile Constituents vs. T_TIDE output for Amplitude and Phase of Koluktoo Bay Records from 1964 and 1965	14
Figure 2.5 – T_TIDE Comparison for 1964 and 1965 at Koluktoo Bay	15
Figure 2.6 – T_TIDE Constituent Amplitudes for 1964 and 1965 with Associated Confidence Intervals	16
Figure 2.7 – T_TIDE Constituent Phases in Degrees for 1964 and 1965 with Associated Confidence Intervals (degrees)	17
Figure 2.8 – T_TIDE Constituent Phases in Hours for 1964 and 1965 with Associated Confidence Intervals (hours).....	18
Figure 2.9 –Propagation of the Tidal Wave through Predicted Tide Stations	20
Figure 2.10 – The Area between the Tide Stations Divided into Sections to aid Tidal Wave Propagation Determination.....	20
Figure 2.11 – Finite Element Mesh with Varying Resolution	25
Figure 2.12 – Three Dimensional Mesh input to QUODDY (from [Ip and Lynch, 1995])	29
Figure 2.13 – Arctic8c Grid.....	32
Figure 2.14 – Arctic8c model M2 Amplitude with co-tidal lines. Phase contours at 0.5 degrees which equates to approximately 1 minute.	33

Figure 2.15 – Arctic8c model S2 Amplitude with co-tidal lines. Phase contours at 0.5 degree which equates to approximately 1 minute.....	33
Figure 2.16 – Arctic8c model N2 Amplitude with co-tidal lines. Phase contours at 0.5 degrees which equates to approximately 1 minute.	33
Figure 2.17 – Arctic8c model K1 Amplitude with co-tidal lines. Phase contours at 0.5 degree which equates to approximately 2 minutes.	34
Figure 2.18 – Arctic8c model O1 Amplitude with co-tidal lines. Phase contours at 0.5 degree which equates to approximately 2 minutes.	34
Figure 2.19 – The North-South Extent of Two GPS Satellites.....	35
Figure 3.1 – Source Bathymetry (Red = CHS Soundings, Yellow = Amundsen Multibeam Data).....	43
Figure 3.2 – Interpolated and Gridded Bathymetry (Depth in metres).....	44
Figure 3.3 – Resulting TIN from Coastline and Bathymetry.....	44
Figure 3.4 – Outline of Developed Bylot Model Grid for Constrained Waters of Bylot Island Overlaid on Existing Arctic8c Grid	46
Figure 3.5 – Initial M2 Amplitude.....	47
Figure 3.6 – Altered Eastern Boundary Initial M2 Amplitude	48
Figure 3.7 – M2 Amplitude with co-tidal lines. Phase contours at 0.5 degrees which equates to approximately 1 minute.	49
Figure 3.8 – S2 Amplitude with co-tidal lines. Phase contours at 0.5 degree which equates to approximately 1 minute.	50
Figure 3.9 – N2 Amplitude with co-tidal lines. Phase contours at 0.5 degree which equates to approximately 1 minute.	50
Figure 3.10 – K1 Amplitude with co-tidal lines. Phase contours at 0.5 degree which equates to approximately 2 minutes.....	51
Figure 3.11 – O1 Amplitude with co-tidal lines. Phase contours at 0.5 degree which equates to approximately 2 minutes.....	51
Figure 4.1 – Arctic8c Model Subtracted from Developed Model. Comparison of M2 Amplitude	56

Figure 4.2 – Arctic8c Model Subtracted from Developed Model. Comparison of S2 Amplitude	56
Figure 4.3 – Arctic8c Model Subtracted from Developed Model. Comparison of N2 Amplitude	56
Figure 4.4 – Arctic8c Model Subtracted from Developed Model. Comparison of K1 Amplitude	56
Figure 4.5 – Arctic8c Model Subtracted from Developed Model. Comparison of O1 Amplitude	57
Figure 4.6 – Arctic8c Model Subtracted from Developed Model. Comparison of M2 Phase	58
Figure 4.7 – Arctic8c Model Subtracted from Developed Model. Comparison of S2 Phase	58
Figure 4.8 – Arctic8c Model Subtracted from Developed Model. Comparison of N2 Phase	58
Figure 4.9 – Arctic8c Model Subtracted from Developed Model. Comparison of K1 Phase	58
Figure 4.10 – Arctic8c Model Subtracted from Developed Model. Comparison of O1 Phase	59
Figure 4.11 – 2004 Amundsen Ship Track through Model Domain with Arrow Indicating Transit Direction	61
Figure 4.12 – Amundsen Velocity 2004	62
Figure 4.13 – Amundsen Height above the Geoid Corrected for Pressure and Squat.....	63
Figure 4.14 – Amundsen 2004 Inverse Barometer Effect	64
Figure 4.15 – Hydrodynamic Model Output Corresponding to 2004 Ship Track	64
Figure 4.16 – Amundsen 2004 Difference between Corrected Height above Geoid and Model Output	65
Figure 4.17 – Amundsen 2004 Number of Satellites and Solution Type	66
Figure 4.18 – 2005 Amundsen Ship Track through Model Domain with Arrow Indicating Transit Direction	67
Figure 4.19 – Amundsen Velocity 2005	68

Figure 4.20 – Amundsen Height above the Geoid Corrected for Pressure and Squat. The Area to the Left of the Black Vertical Line was Removed for Analysis	69
Figure 4.21 – Amundsen 2005 Inverse Barometer Effect	69
Figure 4.22 – Hydrodynamic Model Output Corresponding to 2005 Ship Track	70
Figure 4.23 – Amundsen 2005 Difference between Corrected Height above Geoid and Model Output	70
Figure 4.24 – Amundsen 2005 Number of Satellites and Solution Type	71
Figure 4.25 – 2006 Amundsen Ship Track through Model Domain with Arrow Indicating Transit Direction	72
Figure 4.26 – Amundsen 2006 Speed	73
Figure 4.27 – Original Amundsen Height above the Geoid without Post-Processing.....	73
Figure 4.28 – Amundsen Height above the Geoid Corrected for Pressure and Squat with Post-Processing	74
Figure 4.29 – Hydrodynamic Model Output Corresponding to 2006 Ship Track	75
Figure 4.30 – Amundsen 2006 Difference between Corrected Height above Geoid and Model Output	76
Figure 4.31 – Amundsen 2006 Number of GPS Satellites and Solution Type.....	77
Figure 4.32 – Amundsen 2006 Inverse Barometer Effect	77
Figure 4.33 – 2007 Amundsen Ship Track through Model Domain with Arrow Indicating Transit Direction	78
Figure 4.34 – Amundsen 2007 Speed	79
Figure 4.35 – Amundsen Height above the Geoid Corrected for Pressure and Squat.....	80
Figure 4.36 – Amundsen Height above the Geoid with Extended Scale.....	80
Figure 4.37 – Amundsen 2007 Number of GPS Satellites and Solution Type.....	81
Figure 4.38 – Hydrodynamic Model Output Corresponding to 2007 Ship Track	82
Figure 4.39 – Amundsen 2007 Difference between Corrected Height above Geoid and Model Output	82
Figure 4.40 – Amundsen 2007 Inverse Barometer Effect	83

Figure 4.41 – Navy Board Inlet section of the 2004 Amundsen Difference	85
Figure 4.42 – Navy Board Inlet section of the 2005 Amundsen Difference	85
Figure 4.43 – Pisiktarfik Tidal Constituent Comparison	87
Figure 4.44 – Koluktoo Bay Tidal Constituent Comparison	88
Figure 4.45 – Milne Inlet Tidal Constituent Comparison.....	89
Figure 4.46 – Misfit Calculation.....	90
Figure 4.47 – Pisiktarfik Misfit Analysis.....	91
Figure 4.48 – Koluktoo Bay 1964 Misfit Analysis.....	92
Figure 4.49 – Milne Inlet Misfit Analysis	93
Figure 4.50 – M2 Component of Misfit between Arctic8c Model and Bylot Model	94
Figure 4.51 – N2 Component of Misfit between Arctic8c Model and Bylot Model.....	94
Figure 4.52 – S2 Component of Misfit between Arctic8c Model and Bylot Model	94
Figure 4.53 – K1 Component of Misfit between Arctic8c Model and Bylot Model.....	94
Figure 4.54 – O1 Component of Misfit between Arctic8c Model and Bylot Model.....	95
Figure 4.55 – Amundsen Multibeam Comparison Locations.....	96
Figure 4.56 – Heron Multibeam Comparison Locations	99
Figure 4.57 – Three Minutes of Raw Heave Data, Long Period Heave, Actual Heave and Speed from the Heron	100

LIST OF SYMBOLS, NOMENCLATURE OR ABBREVIATIONS

GcGPS – Globally Corrected Global Positioning System

IOS – Institute of Ocean Sciences

RTG – Real-Time Gipsy

PPP – Precise Point Positioning

BIO – Bedford Institute of Oceanography

ISLW – Indian Spring Low Water

RMS – Root Mean Square

CHAPTER 1. INTRODUCTION

A long term monitoring project has begun using multibeam bathymetry within the Oliver Sound fjord on the northern tip of Baffin Island, Canada. One goal of the project is to measure decimetre level vertical changes in the seabed morphology over time. In order to monitor these changes, stable vertical control is required to relate subsequent survey datasets. The major limitation to this objective is attaining a measurement of the tidal elevation at the time of survey.

The primary focus of the project is on the proglacial deltas within the fjord. Examining the deltas provides an indication of environmental changes due to processes such as river discharge, ice scouring, tidal scouring, mass wasting and bedform migration. A number of proglacial deltas have been identified for study within the fjord and multibeam surveys will be performed annually or biannually to observe transformations on the seabed in this region.

For comparisons to be constructed between subsequent survey datasets, large systematic errors associated with the bathymetry must be removed. To achieve this objective, tidal control must be established to provide knowledge of the tidal regime. Tidal control is sparse, at best, within the Canadian Arctic and reaching the ageing benchmarks to set up a tide gauge can be time consuming and hazardous. In the event that a traditional tide gauge could be erected, the nearest vertical benchmark is over 100

kilometres from the survey site and the amplitude and phase modification of the tidal wave as it propagates between deltas, up the fjord, is unknown.

Each summer the CCGS Amundsen travels from Quebec City, Canada, up into the Canadian Arctic Archipelago as part of the Arcticnet research program. The CCGS Amundsen is a 97 metre, 1200 class icebreaker which has been converted for scientific operations [Bartlett et al., 2004]. The vessel is equipped with a Simrad EM300 30 kHz multibeam sonar and a 3.5 kHz sub-bottom echosounder. During the journey to the Canadian Arctic, Eclipse Sound and Oliver Sound are visited each year. Arcticnet has teamed with Parks Canada to start a long term monitoring project within Oliver Sound, which is located in the Sirmilik National Park. The summer of 2006 was the first year that the CCGS Amundsen ventured into the Oliver Sound fjord to establish baseline information on oceanography, biology and seabed morphology. 2006 was also the first year that the CCGS Amundsen was accompanied by the Ocean Mapping Group's survey launch, the CSL Heron. At 10 metres in length and with a draft of 1.15 metres, the CSL Heron is equipped to survey the shallow Arctic deltas with the use of a Simrad EM3002 300kHz multibeam sonar, 200kHz Knudsen Sidescan, 3.5kHz sub-bottom echosounder and a MVP-30 Sound Velocity Profiler. While the CSL Heron surveys the shallow deltas, the CCGS Amundsen surveys the remainder of the fjord, where depths reach up to 500 metres.

CNav Globally corrected GPS (GcGPS) observations were obtained on both the CCGS Amundsen and the CSL Heron during the Oliver Sound survey. Under normal

circumstances these observations could be used to determine the elevation of the tides during the survey to a multi-decimetre level precision [Hughes Clarke et al., 2005]. The CNav correction signals from geosynchronous satellites, however, were only received intermittently during the Oliver Sound survey due to poor satellite visibility caused by the steep fjord walls and thus the accuracy of the GPS signal was not sufficient to detect tidal signatures for the majority of the survey. Even if continuous CNav corrections had been received, the resulting tidal elevation would not have exhibited sufficient precision to detect the desired sub-decimetre changes in the seabed.

Predicted tides could be extracted for the survey from the WebTide tidal prediction interface which accesses a hydrodynamic model data set entitled Arctic8c covering the entire Arctic Archipelago developed by Dunphy et al. [2005], but the resolution of the model is not sufficient to delineate the fjords in the survey region. The effects of the fjord and nearby islands on the tide as it reaches the head of the fjord are unknown. Predicted tides could also be obtained from nearby historic tide stations, but they are far from the survey area and separated by complex and restricted bay geometries.

To overcome the hurdles posed by these options, a hydrodynamic circulation model has been developed to encompass the Oliver Sound fjord and surrounding regions (Figure 1.1). The model is nested within the Arctic8c grid of Dunphy et al. [2005] and provides the resolution required to observe alterations to the tidal wave as it propagates up the narrow fjords. The new model can predict the phase and amplitude of the five main

principal tidal constituents for any point within the model domain which includes the head of the Oliver Sound fjord.

The results from the new model can be compared to post-processed CNav GcGPS observations from the CCGS Amundsen, the existing Dunphy et al. [2005] solutions and the predicted tides at local tide stations. Each of these sources will be used to provide some model validation.

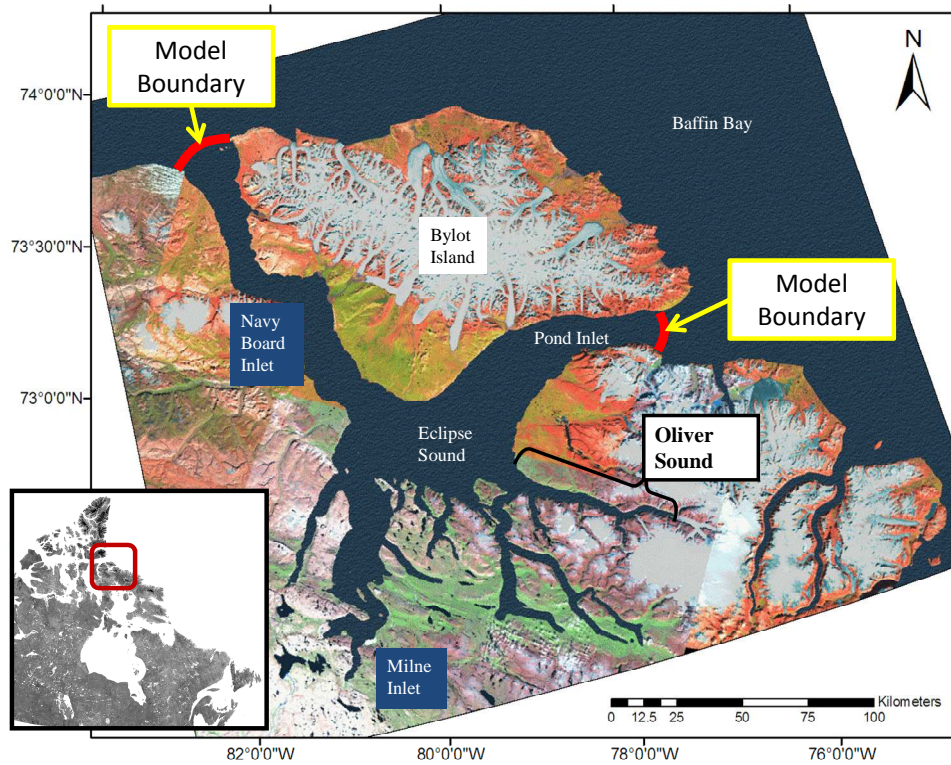


Figure 1.1 – Hydrodynamic Model Region located at the Northern Tip of Baffin Island

CHAPTER 2. BACKGROUND

The initial complete multibeam sonar bathymetric survey of Oliver Sound was performed in 2006 using both the CSL Heron and the CCGS Amundsen. This survey, along with biological and oceanographic measurements, will be used as baseline information towards a long term monitoring project in the area. Figure 2.1 displays the bathymetric data collected by the Heron and the Amundsen within Oliver Sound. The collected bathymetric data was tidally reduced using the Arctic8c grid of Dunphy et al. [2005] with interpolation into the fjord based on the nearest node in Eclipse Sound.

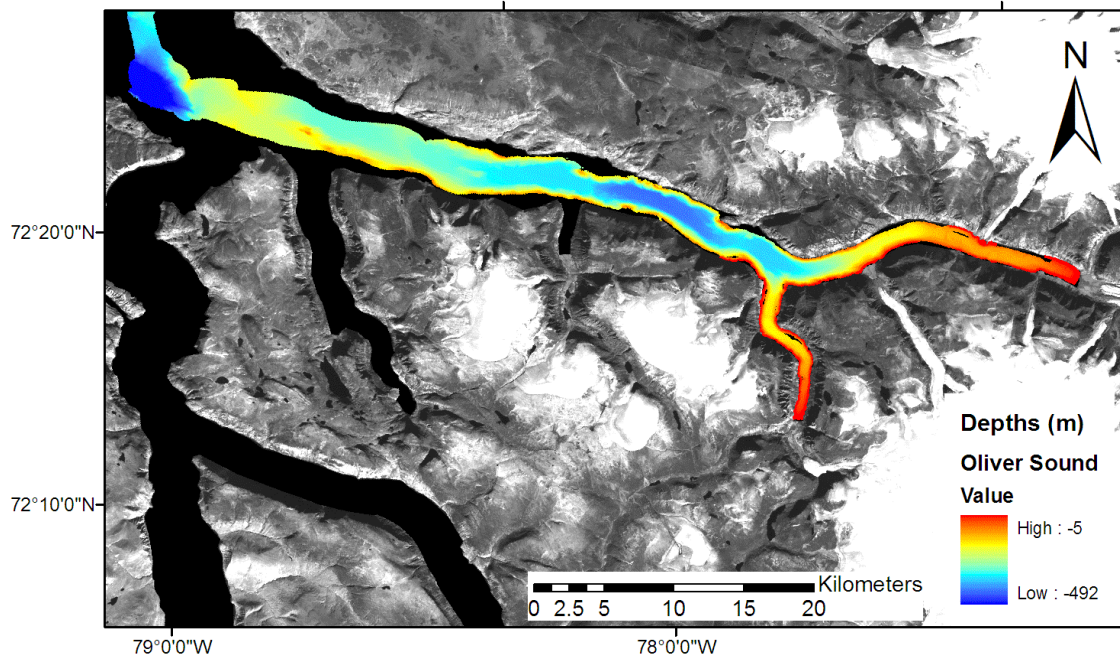


Figure 2.1 – Oliver Sound Multibeam Bathymetry from CCGS Amundsen and CSL Heron within Oliver Sound

2.1 Tides

In order to develop a hydrodynamic model for the Eclipse Sound region, the forces affecting the tides need to be understood and the principal constituents that should be modelled must be determined. These factors will influence the construction of the hydrodynamic model grid and the type of model used to simulate the tides.

The celestial driving forces for the tides within the world's oceans are based on six fundamental, known frequencies. The six frequencies result from interactions between the earth, moon and sun. The first frequency results from the interaction between the earth and the moon as the earth makes one complete rotation with respect to the moon, known as the lunar day. The second frequency results from the time required for the moon to make a full orbital rotation about the earth with respect to the sun, known as the lunar month. The third frequency results from the time required for the earth to make a full orbital rotation about the sun, known as the solar year. The fourth frequency results from the precession of the lunar equinoxes, which is the movement of the intersection between the earth's celestial equator and the orbit of the moon. The fifth frequency is a result of the movement of the moon's orbit with respect to the ecliptic, the plane of the earth's orbit. The sixth frequency results from the precession of the solar equinoxes, which is otherwise known as the movement of the intersection point of the earth's celestial equator and the ecliptic. The fundamental frequencies along with their period and source are described in table 2.1.

	Frequency (°/hour)	Period		Source
f_1	14.49205211	1	lunar day	Local mean lunar time
f_2	0.54901653	1	month	Moon's mean longitude
f_3	0.04106864	1	year	Sun's mean longitude
f_4	>0.00464184	8.847	years	Longitude of Moon's perigee
f_5	-0.00220641	18.613	years	Longitude of Moon's ascending node
f_6	0.00000196	20,940	years	Longitude of sun's perigee
$f = n_1 f_1 + n_2 f_2 + n_3 f_3 + n_4 f_4 + n_5 f_5 + n_6 f_6$				

Table 2.1 – Doodson Fundamental Tidal Frequencies (Modified from [Stewart, 2005])

Doodson used the fundamental frequencies outlined in table 2.1 to construct an expression which represents every harmonic constituent, as shown in the last row of table 2.1 [Stewart, 2005]. The fundamental frequencies are labelled f_1 through f_6 and the variables n_1 through n_6 are Doodson values (integer numbers between -5 and 5) [Stewart, 2005].

The principal diurnal and semi-diurnal tidal harmonic constituents are laid out in table 2.2 with their associated Doodson integer numbers. Each constituent is made up of combinations of the different fundamental frequencies. The sixth frequency is usually omitted because of its long period [Stewart, 2005]. The harmonics are divided into two main groups of either diurnal or semi-diurnal. Within these groups there are small

modulations about the central frequency which creates hundreds of lower amplitude constituents.

Tidal Species	Name	n1	n2	n3	n4	n5	Equilibrium Amplitude	Period
Semidiurnal								
Principal Lunar	M2	2	0	0	0	0	0.242334	12.4206
Principal Solar	S2	2	2	-2	0	0	0.112841	12.0000
Lunar Ecliptic	N2	2	-1	0	1	0	0.046398	12.6584
Diurnal								
Lunisolar	K1	1	1	0	0	0	0.141565	23.9344
Principal Lunar	O1	1	-1	0	0	0	0.100514	25.8194

Table 2.2 – Doodson Numbers used with principal harmonic constituents (Modified from [Stewart, 2005])

Within the model region on northern Baffin Island, inside the enclosed waters of Bylot Island as shown in figure 1.1, the tide is mixed, mainly semi-diurnal, as shown in figure 2.2. This indicates that the principle harmonic constituent with the greatest amplitude will be M2 with some influences from K1 and other diurnal and semi-diurnal constituents. This conclusion is reinforced in the later chapter on the Arctic8c model.

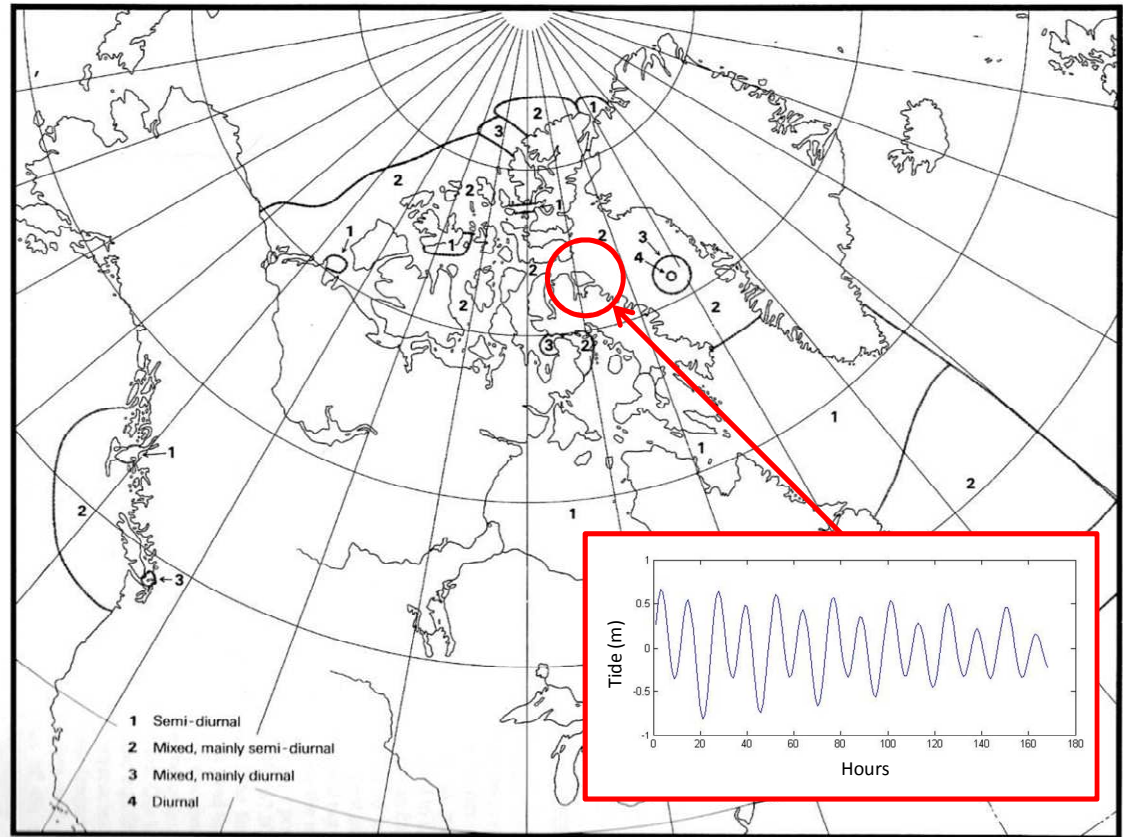


Figure 2.2 – Classification of Tides in Canadian Waters with Example Power Spectrum from the Arctic8c grid of Dunphy et al. [2005] within the Enclosed Waters of Bylot Island. Circled Area indicates Model Region (from [Forrester, W. D., 1983])

2.1.1 Tidal Prediction

There are a number of different methods available for obtaining a prediction of the tides. All predictions are based on reconstructing the tidal signature of an area for a given time using calculated tidal harmonic constituents. Traditionally tidal predictions were available only at ports where tide gauges were installed. The observed tide was broken down into its harmonic constituents and those constituents could be used to construct a

predicted tide at anytime in the future. The prediction would only truly be valid at the gauge as the propagation and modification of the tide along the coast or within a bay was unknown. Interpolations could be performed between gauges, but these methods usually assume a linear trend between gauges which may not be the true case.

A new method of predicting the tides was developed using a model of a body of water along with governing equations. The model takes true observations as input and propagates them throughout the domain based on physical laws and constraints. The theory of this approach, entitled hydrodynamic modelling, is discussed in chapter 2.2.

Within the model domain of this research, there are three tide stations for which predicted tides have been established. The stations are labelled as Pisiktarfik Island, Koluktoo Bay and Milne Inlet, as shown in figure 2.3. At Pisiktarfik Island tides were measured for 15 days in 1966. At Koluktoo Bay tides were measured for 31 days in 1964 and then again for 36 days in 1965. At the Milne Inlet benchmark, tides were measured for 63 days in 1965. It is upon these observations that harmonic constituents were established and used to create predicted tides for the region. Table 2.3 shows that 15 days of observations is barely enough to capture the S2 and O1 constituents and 30 days is just enough to capture the N2 constituent.

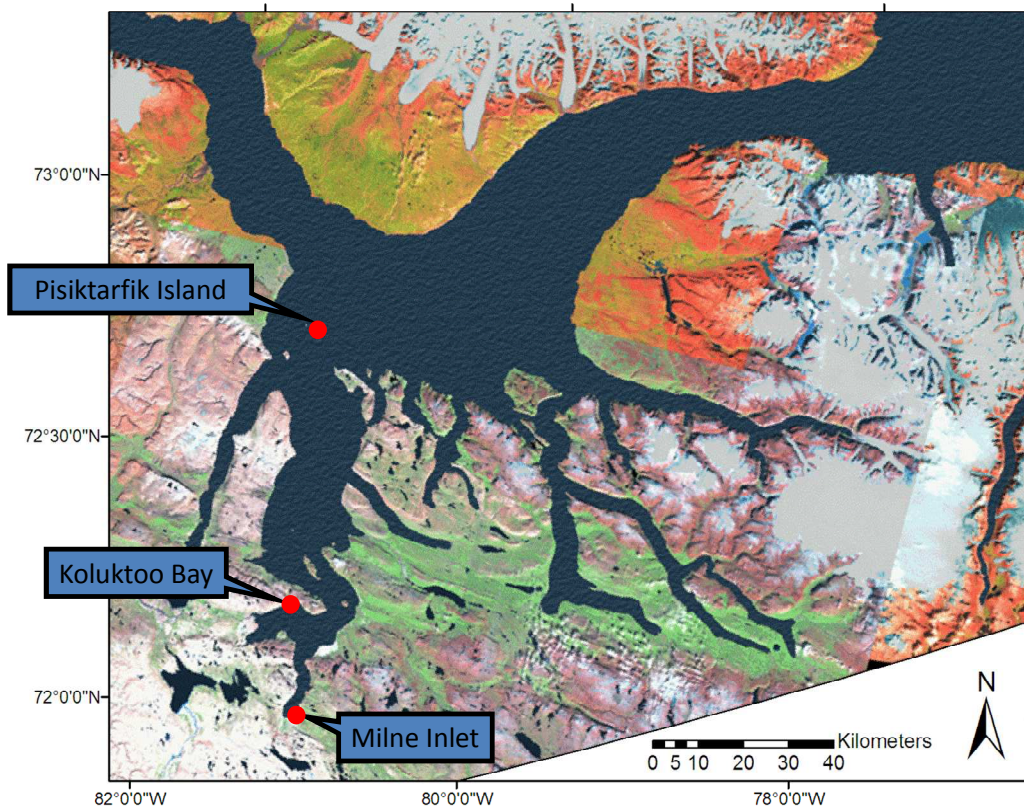


Figure 2.3 – Locations of CHS Predicted Tide Stations within the Enclosed Waters of Bylot Island

Constituent Name	Required Record Length for Analysis (days)
M2	0.54
S2	14.8
N2	27.6
K1	1
O1	13.7

Table 2.3 – Record Length Required to Resolve Principle Harmonic Constituents

2.1.2 Assessing Predicted Tides

The two Koluktoo Bay datasets can be compared to assess the repeatability of the harmonic constituent extraction from observed data and to validate published station constituents. The Canadian Hydrographic Service (CHS) provides harmonic constituents for all its tide stations across Canada in the CHS Bluefile. The method, data source and uncertainty for these constituent determinations are unknown, but they can be used for comparisons to other sources of constituent information. When there is only one recorded dataset for a specific station available, it is assumed that the constituents were derived from that record.

The water level heights from Koluktoo Bay were analyzed using a set of routines entitled T_TIDE to determine the harmonic constituents which make up the tidal regime for the 1964 and 1965 water level observations [Pawlowicz et al., 2002]. These determinations can be compared to the CHS constituents, and to each other, to determine which record was used for the CHS Bluefile prediction and to assess the repeatability of the harmonic constituent estimation. Differences between the constituent determinations from the CHS and T_TIDE can also be examined and compared to estimated variances output from T_TIDE.

T_TIDE was developed by Rich Pawlowicz as a modified and modernized version of the IOS Tidal Package developed by Mike Foreman at IOS [Pawlowicz, 2007] [Foreman, 2006]. It is a package of routines implemented in MATLAB to perform classical harmonic analysis with nodal corrections [Pawlowicz et al., 2002]. It also calculates

confidence intervals for each constituent which allows the user to distinguish true constituent frequencies from noise in the signal. Confidence intervals are calculated through forming estimates of the characteristics of the residual noise in the data and converting the estimates to confidence intervals for the standard parameters [Pawlowicz et al., 2002]. More detailed information on the development of confidence intervals for the harmonic constituents can be found in Pawlowicz et al. [2002].

The tidal records for 1964 and 1965 at Koluktoo Bay were input to the T_TIDE program and amplitudes and phases were determined and extracted for the five principal diurnal and semi-diurnal constituents. The constituents' phase and amplitude are compared to the CHS Bluefile constituent information in table 2.4 and figure 2.4.

1964	M2		S2		N2		K1		O1	
	Amp	Phase	Amp	Phase	Amp	Phase	Amp	Phase	Amp	Phase
CHS	0.573	139.92	0.204	184	0.128	103.19	0.256	248.20	0.082	209.71
T_TIDE	0.5767	139.79	0.1933	196.66	0.1288	105.2	0.2583	264.24	0.079	213.04
Diff	-0.0037	0.13	0.0107	-12.66	-0.0008	-2.00	-0.0023	-16.03	0.003	-3.32
1965	M2		S2		N2		K1		O1	
	Amp	Phase	Amp	Phase	Amp	Phase	Amp	Phase	Amp	Phase
CHS	0.573	139.92	0.204	184	0.128	103.19	0.256	248.20	0.082	209.71
T_TIDE	0.5111	106.82	0.1601	158.74	0.1521	92.15	0.255	247.26	0.0848	189.88
Diff	0.0619	33.100	0.043	25.26	-0.0241	11.04	0.001	0.94	-0.0028	19.83

Table 2.4 – CHS Bluefile Constituents vs. T_TIDE output for Koluktoo Bay 1964 and 1965. Amplitude in Metres and Phase in Degrees.

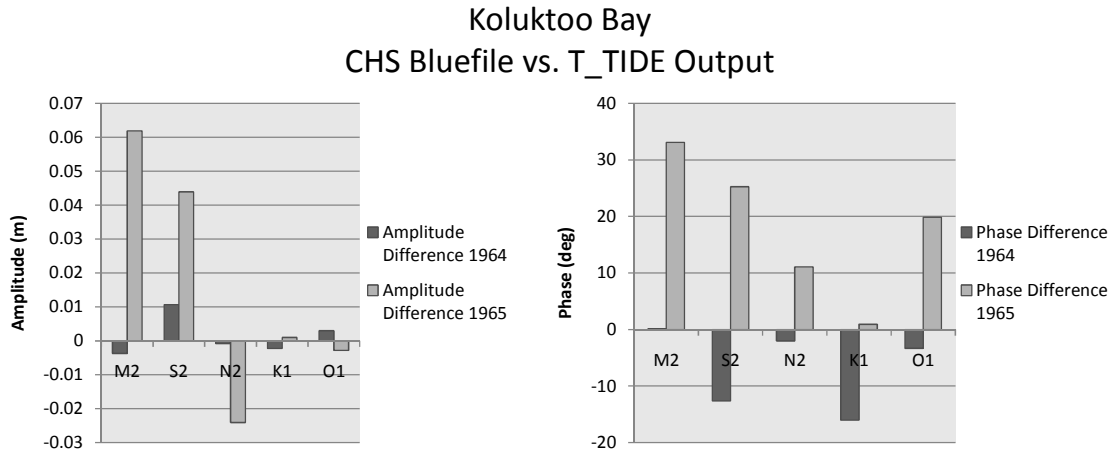


Figure 2.4 – CHS Bluefile Constituents vs. T_TIDE output for Amplitude and Phase of Koluktoo Bay Records from 1964 and 1965

As can be observed in figure 2.4, the T_TIDE output from the 1964 Koluktoo Bay dataset provides a closer match to the CHS Bluefile than the 1965 dataset. This indicates that the CHS Bluefile constituents for Koluktoo Bay were likely obtained using the original 1964 tidal record. The second note is that there is a difference between the T_TIDE output from 1964 and 1965 Koluktoo Bay datasets, as noted in table 2.5 and figure 2.5. Both the 1964 and 1965 datasets were from August and only separated by one year; therefore one would expect that the constituent extraction results from T_TIDE should be almost the same between the two records. Differences likely exist due to different ice conditions which affect the tidal regime, meteorological events, equipment inadequacies, the short observation period and potential operator error. The significance of the difference is displayed in figure 2.6 through examination of the T_TIDE confidence intervals.

Koluktoo Bay	M2		S2		N2		K1		O1	
	Amp	Phase	Amp	Phase	Amp	Phase	Amp	Phase	Amp	Phase
T_TIDE 1964	0.5767	139.79	0.1933	196.66	0.1288	105.2	0.2583	264.24	0.079	213.04
T_TIDE 1965	0.5111	106.82	0.1601	158.74	0.1521	92.15	0.255	247.26	0.0848	189.88
Diff	0.0656	32.97	0.0332	37.92	-0.023	13.05	0.0033	16.98	-0.006	23.16

Table 2.5 – T_TIDE Comparison for 1964 and 1965 at Koluktoo Bay

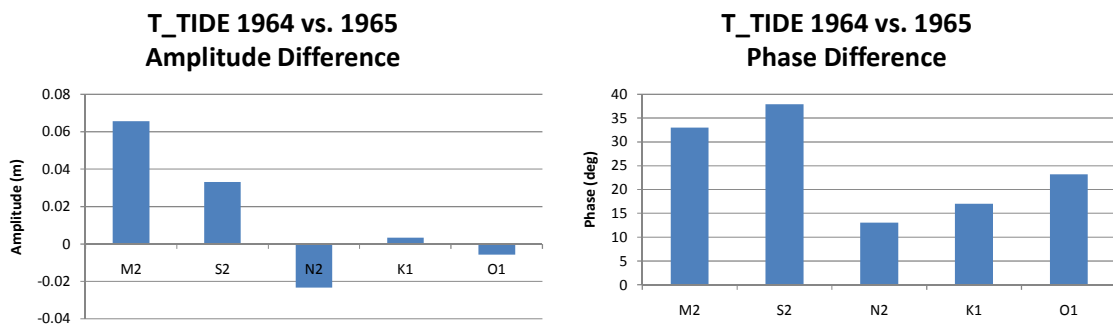


Figure 2.5 – T_TIDE Comparison for 1964 and 1965 at Koluktoo Bay

The plot in figure 2.6 displays the amplitude of the five harmonic constituents (M2, S2, N2, K1 and O1) output from T_TIDE, along with their associated confidence levels. The confidence levels are shown as the coloured bars which coincide to the point colours. For each constituent shown in figure 2.6 the confidence levels overlap, therefore the determinations from 1964 and 1965 are statistically similar.

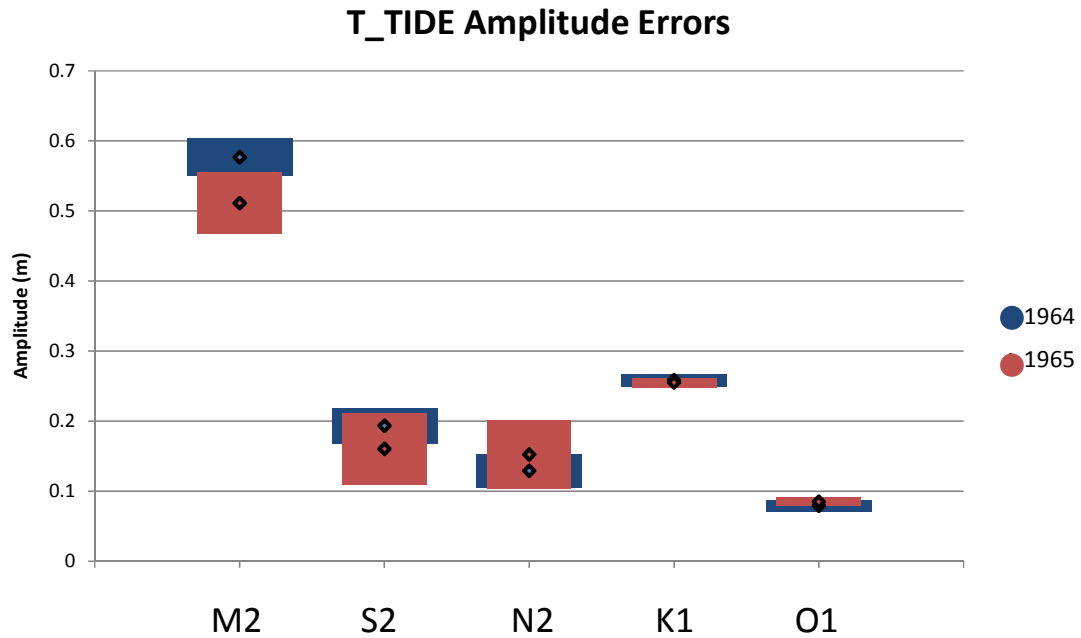


Figure 2.6 – T_TIDE Constituent Amplitudes for 1964 and 1965 with Associated Confidence Intervals

One cannot come to the same conclusions when examining the phase output from T_TIDE along with its associated confidence intervals, as shown in figures 2.7 and 2.8 in units of degrees and hours with respect to Greenwich respectively. The figures show that the phase determinations from 1964 and 1965 are significantly different. The only constituent that provides a match between the two years, within the tolerance of the confidence intervals, is the N2 constituent. As can be noted in table 2.5, the phase determination from 1964 is almost offset systematically from the phase determination for 1965. This could indicate that there is a time offset in one of the datasets. As the comparison is relative, the incorrect dataset cannot be identified. If the error exists in the

1964 dataset, it could indicate that the phase values for the harmonic constituents located in the CHS Bluefile for Koluktoo Bay are likely incorrect.

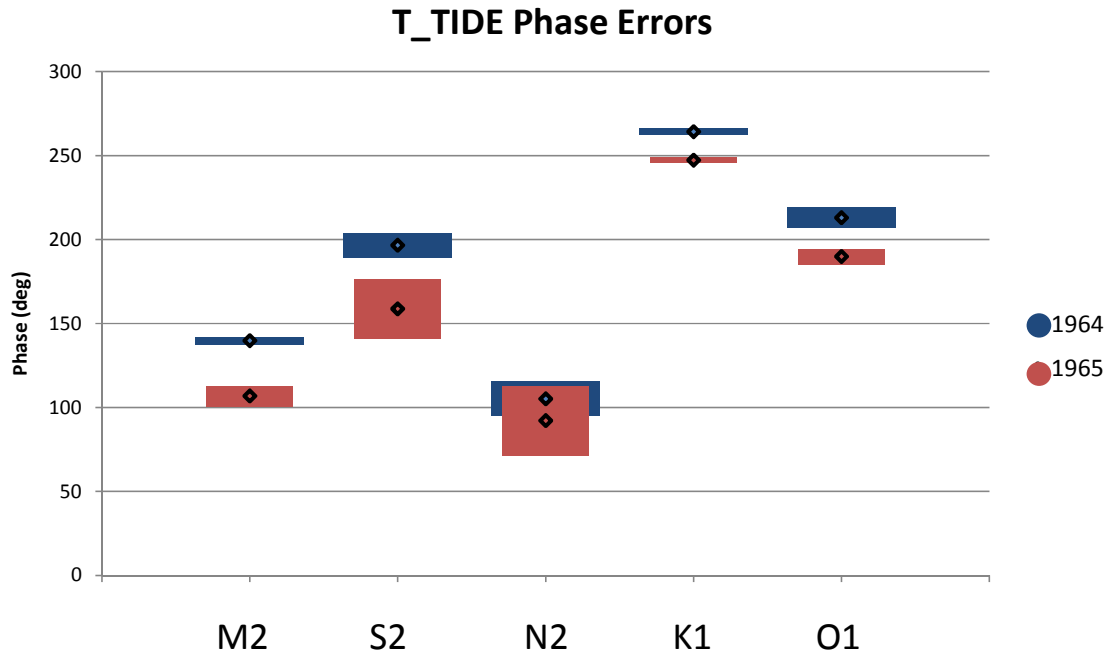


Figure 2.7 – T_TIDE Constituent Phases in Degrees for 1964 and 1965 with Associated Confidence Intervals (degrees)

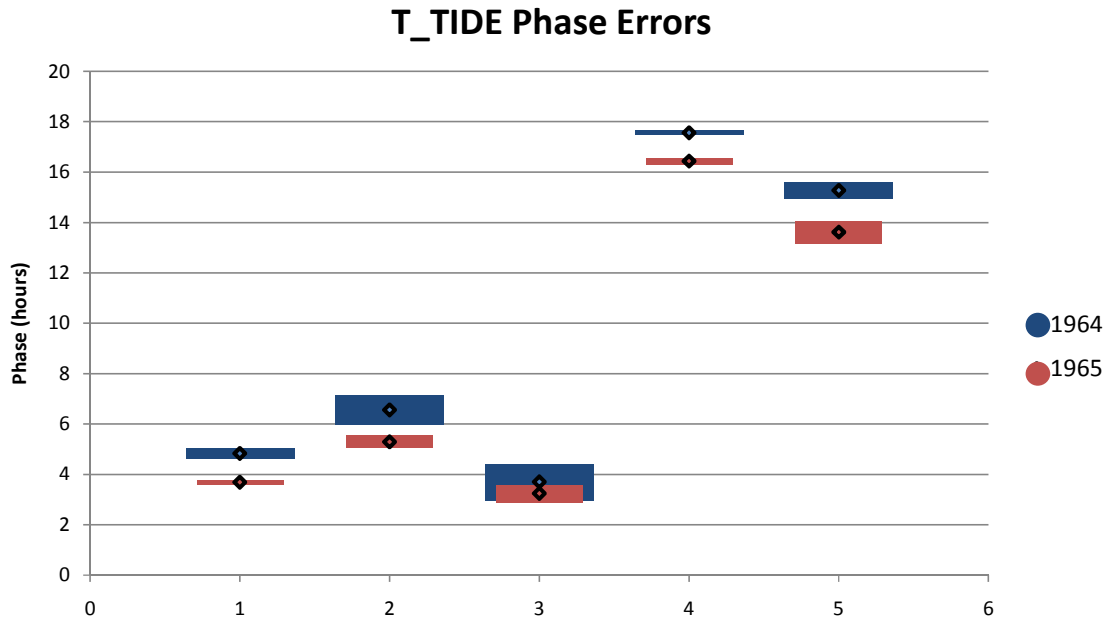


Figure 2.8 – T_TIDE Constituent Phases in Hours for 1964 and 1965 with Associated Confidence Intervals (hours)

In an effort to determine which dataset from Koluktoo Bay is incorrect, the output harmonics from T_TIDE from 1964 and 1965 can be compared to the CHS Bluefile constituents for the two neighbouring stations of Pisiktarfik Island and Milne Inlet.

It first must be determined if the tidal wave that flows through the region, described in figure 2.9, is a standing wave. This will affect the determination of the wave's propagation through the area. If the bay's geometry is such that a standing wave results from resonance within the area then the tidal wave will not propagate through the bay like a progressive wave but will appear to be stationary, with just a rising and falling of the tide at the antinodes. A standing wave results when two waves, with the same amplitude and wavelength, meet while travelling at the same speed but in opposite

directions within a resonant bay [Nave, 2006]. Resonance is created when the geometry of an open bay is such that the length is equal to some multiple of a quarter the wavelength of the tidal wave. To determine if a standing wave is present within the region, the average tidal wave speed must first be calculated. This is determined using the equation in table 2.6 and the average depth along the inlet, which was calculated by segmenting the inlet as shown in figure 2.10. The average depth for the inlet was determined to be approximately 410 metres. Using this information an average wave speed of 64 m/s was determined. The average wave speed is used in conjunction with the known period of the M2 and K1 tidal constituents to determine the wavelength. The results are shown in table 2.7. As the inlet is approximately 105 km long, it does not correspond to a standing wave structure for either the principal diurnal or semidiurnal constituent; therefore the tidal wave entering the inlet should act more like a progressive wave than a standing wave.

Surface Wave Speed Equation for Non-Dispersive Long or Shallow-Water waves (g: Gravity, h: Water Depth)	$C = \sqrt{gh}$
--	-----------------

Table 2.6 – Wave Speed Equation

Constituent	Velocity (m/s)	Period (h)	Wavelength (km) <i>λ = Period * V</i>	³ / ₄ Wavelength (km)	¹ / ₂ Wavelength (km)	¹ / ₄ Wavelength (km)
M2	64	12.421	2862	2146	1431	715
K1	64	23.93	5513	4135	2757	1378

Table 2.7 – Resonant Wavelength for M2 and K1 Constituents

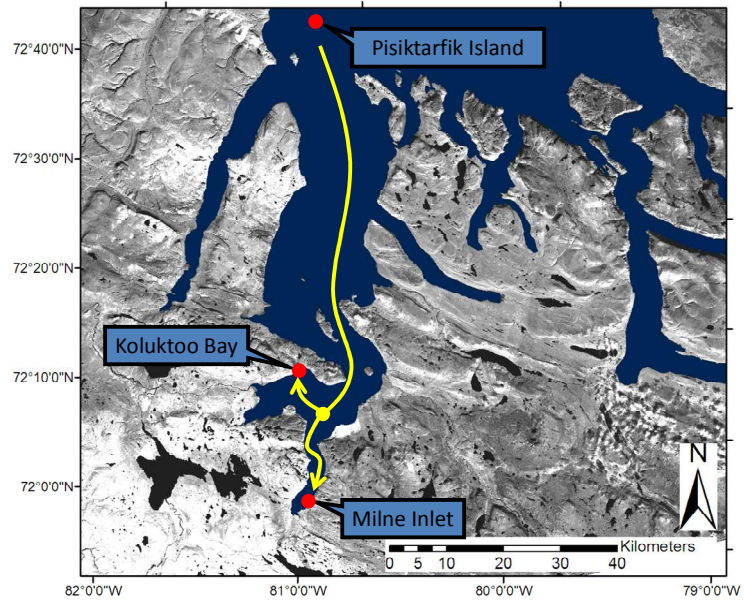


Figure 2.9 – Propagation of the Tidal Wave through Predicted Tide Stations

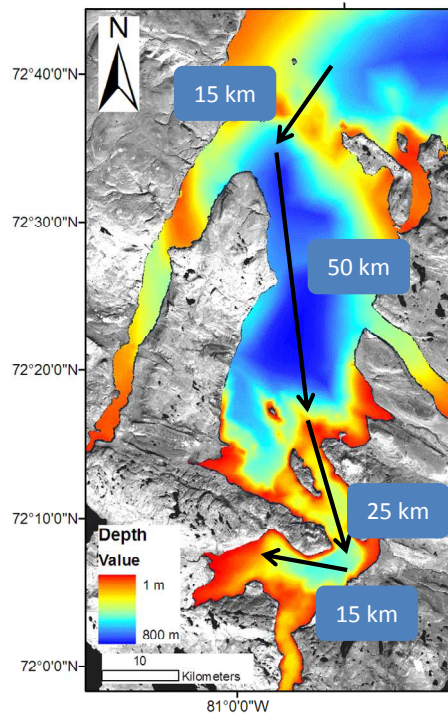


Figure 2.10 – The Area between the Tide Stations Divided into Sections to aid Tidal Wave Propagation Determination

Having determined a likely propagation of the tidal wave, the phase determination at Koluktoo Bay which is possibly correct can be identified. The three tide stations are shown in figure 2.9 along with the likely propagation of the tide. As the wave is primarily progressive, high tide should occur at Pisiktarfik Island first, followed by Koluktoo Bay and then shortly after by Milne Inlet.

The most influential diurnal and semi-diurnal constituents are compared to examine the predicted propagation of the tide between the 3 stations. The phases for the M2 and K1 constituents at the three predicted tide stations are listed in table 2.8. As can be noted in the table, the hypothesised progressive propagation of the tide is upheld by the output from the 1964 Koluktoo Bay observations, when examining the output from T_TIDE for each station, as the phase value increases from the Pisiktarfik station to the Milne Inlet and Koluktoo stations. Therefore, it is likely that the 1964 water level observations at Koluktoo Bay are correct while the 1965 observations appear to be affected by a time offset.

T_TIDE	M2	K1
	Phase (deg)	Phase (deg)
Pisiktarfik	134.5	250.86
Koluktoo 64	139.79	264.24
Koluktoo 65	106.82	247.26
Milne Inlet	137.36	263.66

Table 2.8 – Tidal Propagation for M2 and K1 though Predicted Tide Stations

The likely amplification of the tide can also be calculated from the above information. Knowing the approximate length of the inlet, the wave speed and the known M2 and K1 periods, and ignoring friction, the estimated amplification can be calculated using the equation described in table 2.9. The results of the calculation are also shown in table 2.9. The amplification calculation has the M2 component increasing by 1.5cm, referenced to the Pisiktarfik station, and the K1 component increasing by 0.2 cm, or effectively 0 cm. When the results from the amplification calculation are compared to the predicted amplitudes for within the inlet from the CHS Bluefile, as shown in table 2.10, the M2 amplifies by 2.2 cm, which is very close to the predicted 1.5 cm amplification. For the K1 constituent the Bluefile describes a decrease in amplitude by 7cm, unlike the 0 cm amplification predicted. This is likely a result of the fact that the equation assumes that amplification is required and because the inlet is very far from the resonant size for the K1 wavelength, the wave is actually attenuating as it enters the bay.

Equation for tidal amplification due to resonance $H_2 = \frac{H_1}{\cos\left(\frac{2\pi L}{cT}\right)}$ <p> H_2 • Tidal Amplitude at Head of Inlet H_1 • Tidal Amplitude at Entrance of Inlet L • Length of Inlet c • Wave Speed T • Period </p>					
Calculated Amplification From Entrance (H1) to Head of Inlet (H2)					
	H1 (m) -- from Pisiktarfik CHS Bluefile Station	L (km)	c (m/s)	T (h)	H2 (m)
M2	0.551	105	64	12.421	0.566
K1	0.332	105	64	23.93	0.334
Predicted From CHS Bluefile					
	Pisiktarfik		Koluktoo		
M2	0.551		0.573		
K1	0.332		0.256		

Table 2.9 –Amplification Calculation within the Inlet between the Pisiktarfik and Koluktoo Stations (Equation from [Forrester, W. D., 1983])

2.2 Hydrodynamic Model

A hydrodynamic model consists of a representation of a body of water in a mathematical form. The continuous mass of water is broken into discrete volumes so that the effects of a particular volume on another can be analyzed. The model domain becomes a mesh that covers the model region. The model mesh is fed to a computer along with a series of governing equations which determine how each of the mesh

volumes interacts. Simulations can be run using the hydrodynamic model, which comprises the model mesh and the governing equations, to analyze how changing conditions at a certain location affects the rest of the model.

Hydrodynamic model simulations can entail changing criteria such as the tide or other boundary conditions such as wind, surface heating, pressure gradient, temperature and salinity of the water column [Ip and Lynch, 1995]. Changing any of these variables at some specific point or within some area of the model domain will affect the rest of the model in some fashion depending on the governing equations. In this case, the effects of adding different tidal forces to the open water boundary of the hydrodynamic model will be examined.

A model is a representation of some actual phenomena. For a hydrodynamic model, the phenomenon is water and the representation is in discrete elements, to enable computation. The computation involves describing the physics of the body of water using equations based on the fundamental physical principles upon which all fluid dynamics is based [Department of Oceanography, 2003]. These principles include the continuity equation, which states that mass is conserved; the momentum equation, which states that force is equal to mass multiplied by acceleration (Newton's second law) and the energy equation, which states that energy is conserved [Wendt, 1992].

In order to transform the continuous water object into a discrete representation, the entire body of water within the model domain is divided into elements, which creates a mesh that covers the area. In this case a finite-element model with a mesh of irregular triangular elements was used. Each element is constructed of three nodal points with lines connecting them. It is essentially the process of creating a triangulated irregular network (TIN). The size of the elements depends on a number of factors. The computational complexity of the model and the computing resources available will determine the resolution of the mesh. Small elements and complex relationships between them will take a long time to compute on average computers. Usually a compromise is made with high resolution small elements used in areas of specific interest, such as shallow areas or areas with complex structures, and lower resolution large elements are used elsewhere. Figure 2.11 shows small elements in the shallow waters near the shorelines and larger elements in the deeper open water.

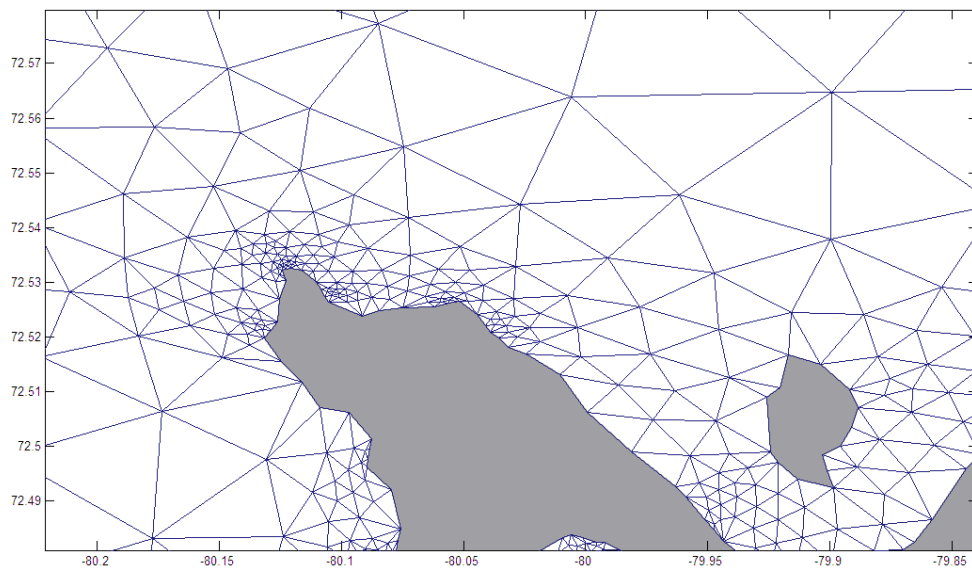


Figure 2.11 – Finite Element Mesh with Varying Resolution

Variable forces are input to drive the model and the resulting flow is analyzed. The forcing is performed at either one or many nodes. Each node is tied to a number of other nodes by the lines joining the elements. As one node moves, or is affected by some variable change, it will affect the nodes it is connected to and so on, until every node has been affected by the input variable. The particular effect of one node on another often depends on the distance between the nodes; therefore it is possible in a large grid for some nodes to not be effected by the input driving force.

Each element in the mesh has a matrix associated with it that includes the positions of the three nodes [Funnell, 2005]. To understand how applying a certain force causes the surrounding node to react, a force vector is applied to the element matrix. The result of combining these two matrices is a displacement vector which indicates how much the applied force caused the nodes to move. In a hydrodynamic model there are often thousands of elements and they all share some nodes in common with other elements. After combining matrices from different elements, with common nodes, the effects of different magnitude forces from different directions can be analyzed to understand the implications of the input forcing on the entire area [Funnell, 2005].

One of the equations for the movement of ocean waters consists of the terms which describe the force balance on a parcel of water. They are known as the Navier-Stokes equations [Department of Oceanography, 2003]. The basic equation is described in table 2.10.

$\frac{Dv}{Dt} = 2\Omega \sin \theta * v - \frac{1}{\rho} \nabla p + g + \nabla \phi_t + \frac{F_{fr}}{\rho}$	
$\frac{Dv}{Dt}$	Acceleration: Change in velocity over time
$2\Omega \sin \theta * v$	Coriolis Force: Apparent force by the rotation of the earth. Depends on rotation speed and latitude. The addition of velocity gives the inertial frequency [Department of Oceanography, 2003].
$\frac{1}{\rho} \nabla p$	Pressure Gradient: Baroclinic or Barotropic
g	Gravity
$\nabla \phi_t$	Gravitational Tidal Potential: Ocean Tides
$\frac{F_{fr}}{\rho}$	Frictional Forces: Windstress and bottom stress

Table 2.10 – Navier-Stokes Equations

A number of approximations are made to simplify the Navier-Stokes equations. The first is the Boussinesq Approximation. This approximation states that density gradients can be ignored except when they appear in terms multiplied by g, the acceleration due to gravity [Department of Oceanography, 2003]. The second is the hydrostatic approximation. It states that because the ocean's width is much greater than its depth,

vertical accelerations are small relative to gravitational acceleration and the pressure at any point in the ocean is due only to the weight of the water above it [Department of Oceanography, 2003].

2.3 QUODDY

QUODDY is a three dimensional finite-element computer simulation program for coastal ocean circulation modeling [Ip and Lynch, 1995]. It uses the conventional 3D shallow water equations to resolve the tides within a user defined domain [Ip and Lynch, 1995]. The equations solved are the Reynolds-averaged Navier-stokes equations for an incompressible, hydrostatic, Boussinesq fluid with a free surface [Li et al., 2003]. The model was developed at the Numerical Methods Laboratory at Dartmouth College in Hanover, NH, USA, and is written in ASCII FORTRAN 77 [Ip and Lynch, 1995].

Quoddy takes a triangulated mesh as input with boundary forcing conditions. The mesh is constructed of simple linear elements in 3 dimensions. The horizontal elements are triangular and the vertical elements are constructed using a terrain-following vertical sigma-coordinate system [Ip and Lynch, 1995]. At each node, the water column is divided into a number of layers. The number of layers is independent of depth and thus follows the terrain, as illustrated in figure 2.12.

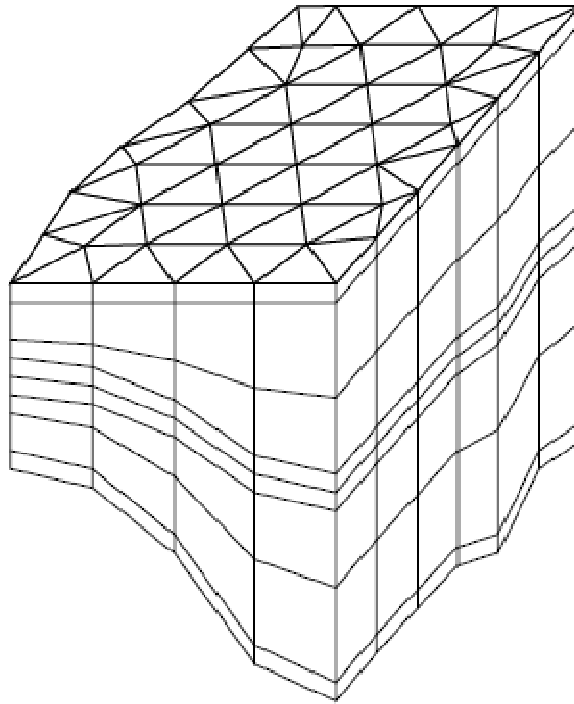


Figure 2.12 – Three Dimensional Mesh input to QUODDY (from [Ip and Lynch, 1995])

2.3.1 Input Parameters

At runtime an input file must be given to QUODDY to define a number of parameters for the model simulation. Within the input file variables can be set for items such as the working units, the coordinate system, scaling factors, central latitude, simulation length, time step, bottom friction, barotropic or baroclinic pressure, turbulence closure, temperature and salinity, advection and horizontal diffusion, minimum and maximum values for bottom friction and viscosity, quadratic drag coefficient, constituent name and output variables [Ip and Lynch, 1995]. Many other options are available for

different simulations. For this simulation, the input parameters used are outlined in table 2.11.

Parameter	Value	Units	Description
Coordinates	Cartesian		Position units were input as metres instead of degrees.
Latitude	72	Degrees	Central latitude of grid. Important for coriolis calculation. It assumes that the north-south variation in coriolis is negligible.
Minimum Depth	10	metres	
Simulation Length	536544	Seconds	Determined as 12 cycles of the M2 tide
Time Step	0.5	Seconds	Time step increment
Vertical Nodes	10		Number of levels of division vertically. See figure 2.11
Pressure	Barotropic		Indicates pressure computation
Mass Variable	None		No variables implemented. Temperature, Salinity and density are homogenous and fixed.
Cd	0.005		Quadratic Drag Coefficient. Used recommended value.
OUTPUT	va, e, z, v		va: Vertically Averaged Velocity at Timestep e: Elevation at Timestep z: Sigma-Levels at Timestep v: (u,v) Velocity Components at Timestep

Table 2.11 – QUODDY Simulation Input Parameters

As noted in table 2.11, the coordinate system for the QUODDY simulation was chosen as Cartesian instead of spherical. This uses a central latitude value, in this case 73 degrees, for the coriolis calculation over the entire grid. As the model stretched over only 2 degrees of latitude and the main open water region of Eclipse Sound was located at the specified central latitude, a single value for coriolis was deemed appropriate. The coriolis frequency calculation also varies with the sin of the latitude, as shown in table 2.10, and

the gradient of the change in frequency thus decreases with increasing latitude. This places less importance on varying the latitude within the calculation of Coriolis frequency at high latitude sites, such as the enclosed waters of Bylot Island.

2.4 Arctic8c Model

A hydrodynamic model of the Arctic Island Archipelago has already been developed by researchers within the Ocean Science Division at the Department of Fisheries and Oceans (DFO) [Dunphy et al., 2005]. The model covers the entire Arctic region and provides a good estimate of predicted tides. The limitation of the model is that due to its size and coverage, it was created using a low resolution approximation of the coastline and depth distribution. All fjords and small islands within the model domain were ignored for developmental and computational simplicity; therefore the model does not take into account the modifications to the tide caused by the shape and depth distribution of islands and fjords within the constrained waters behind Bylot Island. The model does however provide a good approximation of the tides for open water within the domain and has been used to reduce the tides for the majority of the CCGS Amundsen transit data through Arctic waters [Beaudoin et al., 2008]. The extents of the Arctic8c model can be viewed in figure 2.13.

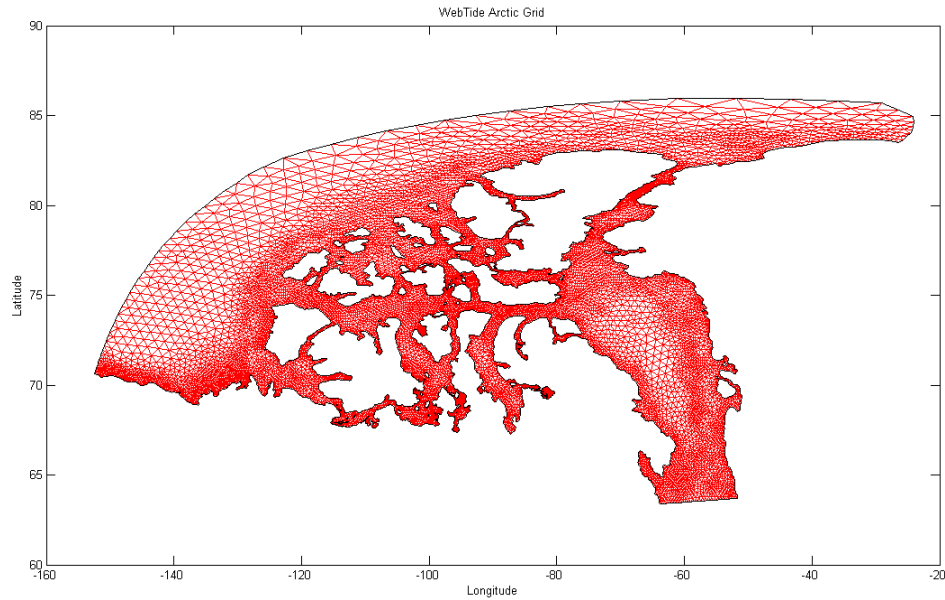


Figure 2.13 – Arctic8c Grid

The predicted tidal amplitude and phase of the Arctic8c model around Bylot Island for the two main diurnal and three main semidiurnal tidal constituents is shown in figures 2.14 through 2.18. The amplitude of the tidal constituents through the area is displayed through the colour scale while phase contours are overlaid.

Figures 2.14, 2.15 and 2.16 demonstrate that the M2, S2 and N2 component of the tidal wave progresses through Navy Board Inlet, Eclipse Sound and Pond Inlet in 7, 11 and 8 minutes respectively. That is much quicker than the K1 and O1 constituents, in figures 2.17 and 2.18, which get restrained by the Navy Board Inlet constriction. Also, none of the figures show any amplification of the tide within the waters constrained by Bylot Island.

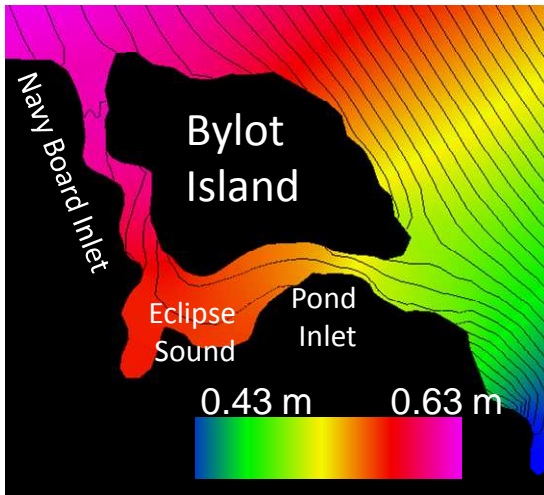


Figure 2.14 – Arctic8c model M2 Amplitude with co-tidal lines. Phase contours at 0.5 degrees which equates to approximately 1 minute.

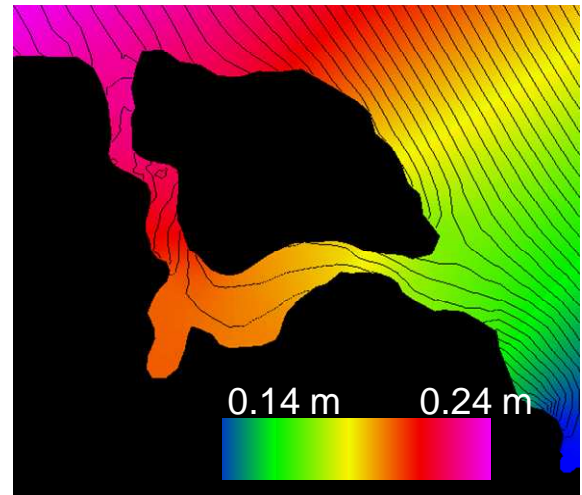


Figure 2.15 – Arctic8c model S2 Amplitude with co-tidal lines. Phase contours at 0.5 degree which equates to approximately 1 minute.

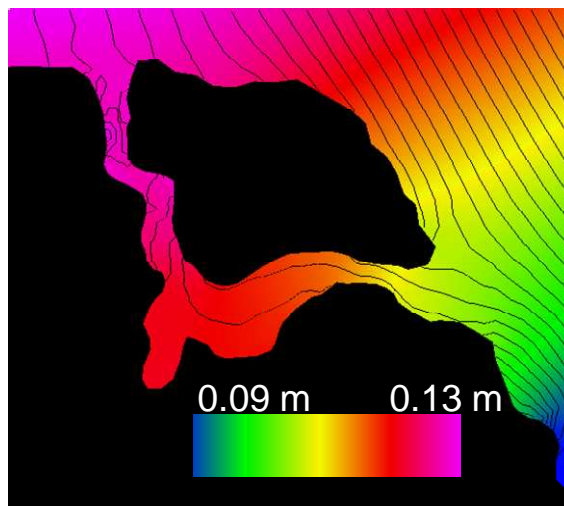
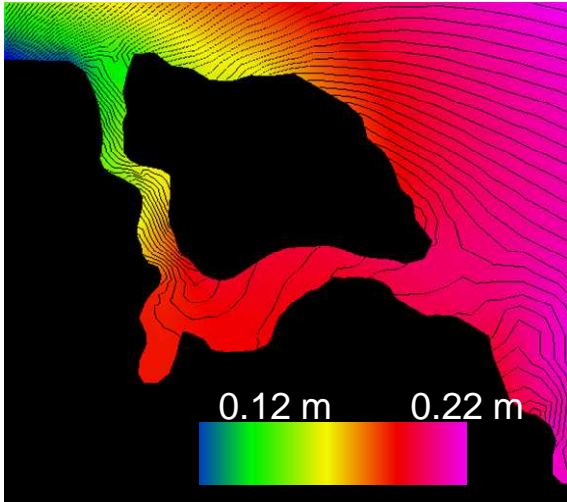
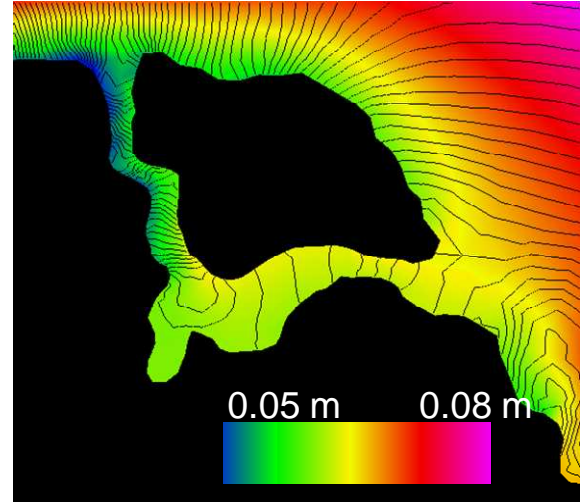


Figure 2.16 – Arctic8c model N2 Amplitude with co-tidal lines. Phase contours at 0.5 degrees which equates to approximately 1 minute.



**Figure 2.17 – Arctic8c model K1
Amplitude with co-tidal lines. Phase
contours at 0.5 degree which equates to
approximately 2 minutes.**



**Figure 2.18 – Arctic8c model O1
Amplitude with co-tidal lines. Phase
contours at 0.5 degree which equates to
approximately 2 minutes.**

2.5 GPS Processing

GPS data was collected onboard the Amundsen and the Heron during their transits through the hydrodynamic model domain on northern Baffin Island. CNav GcGPS data is collected 24 hours a day onboard the Amundsen and is available for each transit through the model domain (2004, 2005, 2006 and 2007). GcGPS data is collected on the Heron during survey operations, which occurred during the Oliver Sound survey in 2006. Corrections were not always received via geostationary satellites due to the high latitude of the region and large cliff faces which acted as southerly obstructions. In these cases, the dual frequency GPS data was post processed using the GPS data Analysis and Positioning Software (GAPS) package, as discussed in section 2.5.2.

At high latitude sites, such as Oliver Sound, the GPS constellation is not optimized to provide the optimal solution. Due to the 55 degree inclination in the polar orbit of the GPS satellites they will never appear directly overhead and will rest mainly on the horizon [Howard, 2005]. This geometry creates situations where high Vertical Dilution of Precision (VDOP) ratings occur, which indicates a poor vertical solution [Leva, 1994]. Figure 2.19 shows an example of the north-south reach of the GPS satellites. As can be seen in the figure, the satellites never reach above latitude of 60 degrees. With the GPS satellites sitting on the horizon, the visible constellation is often changing and creates an environment with a high potential for multipath and increased ionospheric delays [Cannon et al., 2003].

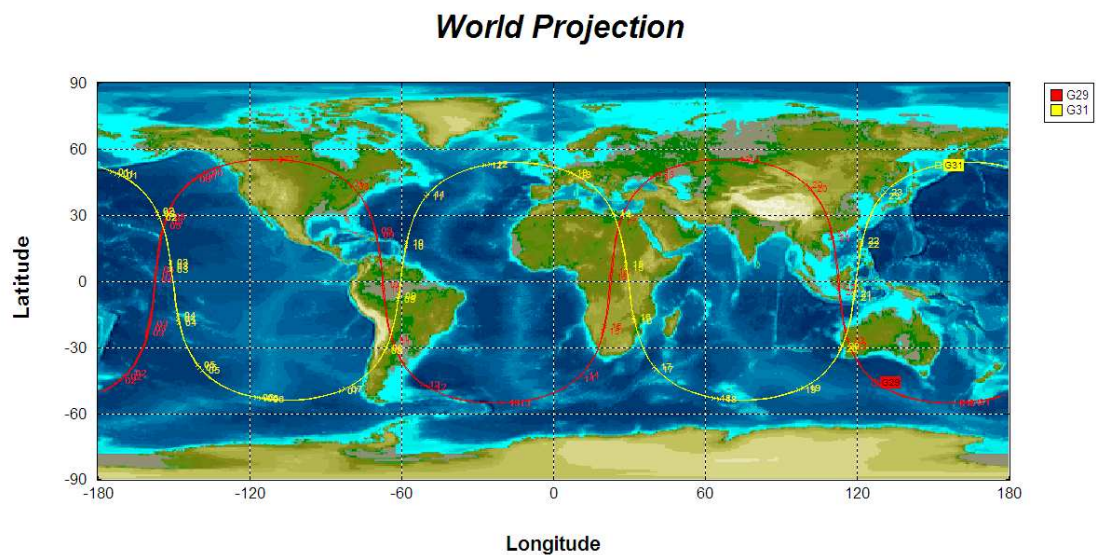


Figure 2.19 – The North-South Extent of Two GPS Satellites

2.5.1 CNav GcGPS

CNav GcGPS utilizes technology from the Jet Propulsion Laboratory to provide a worldwide GPS positioning solution with accuracies of the order of a few decimetres [Roscoe Hudson and Sharp, 2001]. It was developed as a partnership between C&C Technologies and NavCom Technology Inc. to aid hydrographic, offshore oil field exploration, survey and construction industries [Roscoe Hudson and Sharp, 2001].

The CNav space segment consists of geostationary communication satellites that provide Real-Time Gipsy (RTG) corrections to GPS receivers around the world at latitudes between approximately 75 degrees north and south [C & C Technologies, 2008]. With an upper reach in latitude of 75 degrees north, the survey within Oliver Sound is pushing the limits of the CNav correction coverage area. When this limitation is combined with varying topography which obstructs southern visibility, CNav corrections are intermittent at best.

Wert et al. (2004) and Hughes Clarke et al. (2005) demonstrated that CNav observations may be used to observe tidal signatures during a hydrographic survey to a limited accuracy and reliability. The issues that are encountered in surveying a site similar to the head of the Oliver Sound fjord are that the steep fjord walls hinder the ability of the real time CNav correction signals to reach the vessel and limit visibility of the GPS constellation. CNav observations alone are therefore insufficient for observing

the signature of the tides within the Oliver Sound fjord, but they can be used to confirm the phasing of high and low water at various sites within the model domain where visibility was sufficient to receive corrections. In areas where no corrections were received, the data was post processed as discussed in section 2.5.2.

Tidal signatures can be observed in the vessels CNav elevation data if it is referenced to mean sea level instead of the ellipsoid. Therefore the CNav elevation data must be reduced to the best available approximation of mean sea level, the geoid. Large geoidal undulations exist in the area of Oliver Sound and the filtered version of the EGM96 geoid-ellipsoid separation model delivered in the CNav signal is not sufficient to fully account for them. As the undulations are quite short in wavelength, the GPS-H v2.01 separation model, developed through the Geodetic Survey Division of Natural Resources Canada, was used to transform ellipsoid heights to geoid heights [Geodetic Survey Division, NRCan, 2004]. Hughes Clarke et al. (2005) demonstrate that very little difference exists between using the full EGM96 or the GPS-H separation models when processing CNav elevations to observe tidal signatures. GPS-H uses the HT2_0 height transformation which allows for direct transformation of NAD83 (CSRS98) ellipsoidal heights to Canadian primary vertical control CGVD28 orthometric heights [Geodetic Survey Division, NRCan, 2004]. The CGG2000 geoid model was adjusted to the CGVD28 orthometric heights to allow for interpolation between control points in the transformation.

The effects of atmospheric pressure changes on the water level during a GPS observation period were calculated using pressure data from the nearby community of Pond Inlet. The GPS observations were divided into day long segments and the pressure change over that day was used to calculate the inverse barometer effect. The equation for the effect was taken from Wunsch et al. (1997) and was used to calculate the relative water level change due to pressure over each period. It works out that 1 mbar of atmospheric pressure fluctuation generates approximately 1 cm of water level change [Wunsch and Stammer, 1997]. An example of the calculation is shown in table 2.12.

Water Level Change (m)	Change in Pressure ($\Delta\rho$)	Water Density ρ_o (kg/m ³)	Gravity g (m/s ²)
-0.009929	1	1027	9.80665
-0.019858	2	$\eta = \frac{-\Delta\rho}{(\rho_o * g)}$	
-0.029787	3		
-0.039716	4		
-0.049645	5		
-0.059574	6		
-0.069504	7		
-0.079433	8		
-0.089362	9		
-0.099291	10		

Table 2.12 – Inverse Barometer Effect Calculation Showing Change in Water Level with Pressure Change

Squat effects were removed from the data using a developed squat model for the CCGS Amundsen. The squat model was developed during trials aboard the CCGS

Amundsen using the CNav GPS system [Hughes Clarke et al., 2005]. Squat effects on the Amundsen can be in the magnitude of up to 30 cm.

2.5.2 GPS Processing

The GPS data Analysis and Positioning Software (GAPS) package was developed at UNB and allows the user to process, using Precise Point Positioning (PPP), and analyse GPS positional data. PPP is a technique where a single receiver is used to determine its coordinates using precise satellite orbits and clocks [Leandro and Santos, 2006]. The software is web-based and gives the user a report outlining the confidence levels associated with the navigation track along with figures for Neutral Atmospheric Delay, Vertical Ionospheric Delay, Carrier Phase and Pseudorange residuals and Code Multipath. Processing can be done using the software in either static or kinematic modes. In this case, as the vessels are constantly moving, kinematic mode was used. Leandro et al., 2006, state that kinematic positioning uncertainties are approximately 5 cm in the horizontal and 15 cm in the vertical. A more detailed discussion of the GAPS package can be found in Leandro et al. (2006).

The advantage of using PPP over the traditional RTG used by CNav is that the PPP technique uses actual observed satellite and clock errors while RTG uses estimates of the errors. The actual correction of the satellite and clock errors is more accurate than the estimated ones and therefore PPP provides an improved positioning solution over RTG. In a kinematic environment one can expect vertical uncertainties on the order of 15 cm

with PPP and 30 cm with RTG [Leandro and Santos, 2006; Global Offshore Consulting, 2006].

CHAPTER 3. EXPERIMENTAL DESIGN

A hydrodynamic model has been developed for the constricted waters of Bylot Island, including Pond Inlet, Eclipse Sound, Navy Board Inlet and the many fjords which branch off these waters. The purpose of the model is to predict the change in phase and amplitude of the tide as it propagates up to the head of the Oliver Sound fjord. The developed model will herein be referred to as the Bylot Model.

3.1 Constructing the Grid

In order to create a grid of the enclosed waters of the Eclipse Sound region for input to the model, two primary sources of data were required. The first was an accurate coastline of the area which resolved the fjords and islands in the region. The second was the best available bathymetry for the model domain to ensure that the effects on the tide from changes in bathymetry were accurately reproduced.

A coastline for the model was digitized using Ocean Mapping Group software and Landsat 7 orthorectified satellite imagery. The Landsat imagery has a resolution of 30 metres and is freely available from Natural Resources Canada through the GeoGratis Website [Earth Sciences Sector, NRCan, 2006]. The resolution of the satellite imagery

was sufficient to accurately represent the coastlines of the islands and fjords within the model domain.

Bathymetry for the area was obtained from the Canadian Hydrographic Service (CHS) and the Ocean Mapping Group (OMG). The OMG has been collecting data since 2003 on the CCGS Amundsen through the constricted waters behind Bylot Island. Data collected by the OMG include multiple transits through the region (2003, 2004, 2005 and 2006), a survey of Pond Inlet (2005) and a survey of Oliver Sound (2006). The CHS have performed multiple surveys within the region of the model domain. They have surveys at the entrances of Pond Inlet and Navy Board Inlet, within Milne Inlet, a single beam line of data down each of the fjords and evenly spaced soundings over the entire region for navigational charts.

The process of constructing the hydrodynamic model grid was documented and simplified to aid in future model creation. The process is documented in Appendix A and a number of Matlab routines are listed which were either created or built off older FORTRAN programs. The general procedure is outlined in section 3.2.

3.2 Grid Creation Process

The first step in the grid creation process is to create a TIN. The TIN is a series of nodes connected with vertices. Each node has position and elevation information attached to it. In this case, a TIN was created which covered the water area of the region and the depth at each node was recorded. The coastline derived from Landsat imagery was used as the boundary of the TIN and the bathymetric data from the Ocean Mapping Group and the CHS was used to assign a depth to each node. The available bathymetric coverage is shown in figure 3.1 while the interpolated depths are shown in figure 3.2. The resulting TIN is shown in figure 3.3.

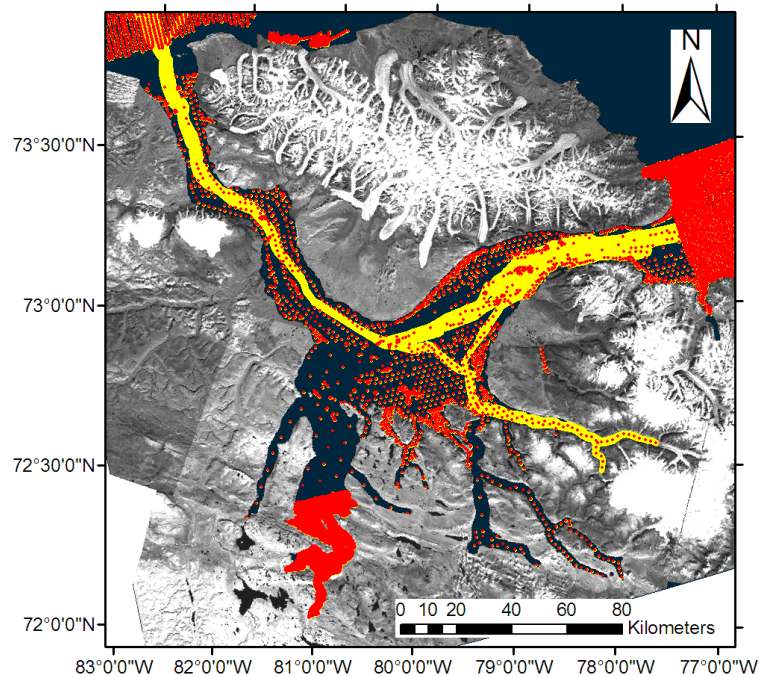


Figure 3.1 – Source Bathymetry (Red = CHS Soundings, Yellow = Amundsen Multibeam Data)

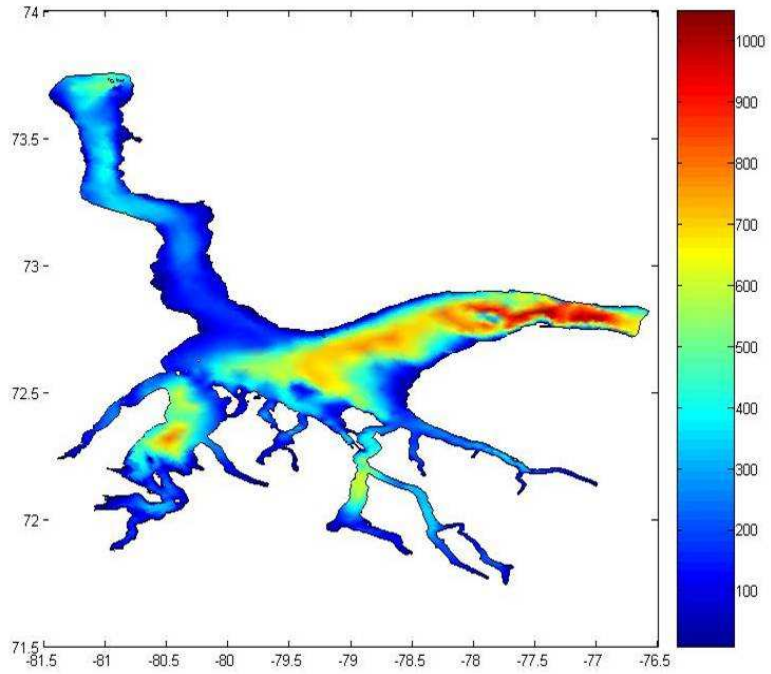


Figure 3.2 – Interpolated and Gridded Bathymetry (Depth in metres)

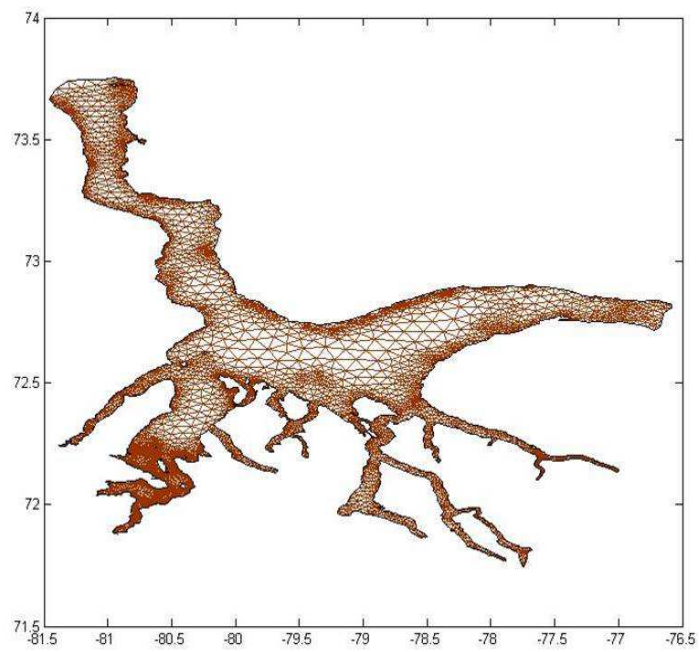


Figure 3.3 – Resulting TIN from Coastline and Bathymetry

Depths within the grid, as shown in figure 3.2, go down to over 1056 metres with an average depth of 182 metres. A total of 10596 nodes form 17979 elements to cover the model domain, as shown in figure 3.3. The mesh stretches approximately 200 km north-south by 200 km east-west.

Before the grid is ready to be input to the modelling software, a number of modifications must be made to format the grid properly. These include altering the location and density of some of the nodes within the TIN, removing unused nodes from the files and reordering nodes. Boundary conditions must also be set to give the model information on how to force the flow. In this case, tides from the Arctic8c model were used along the open boundaries to drive the model simulation.

3.3 Running the Model with the Constructed Grid

The hydrodynamic model developed for the constricted waters of Bylot Island was nested within the Arctic8c model and the constituents from which were used to power the model at open boundaries. The Arctic8c model includes constituents for the M2, S2, N2, K1 and O1 tidal harmonics. The outline of the developed grid and the existing lower resolution Arctic8c grid are shown in figure 3.4.

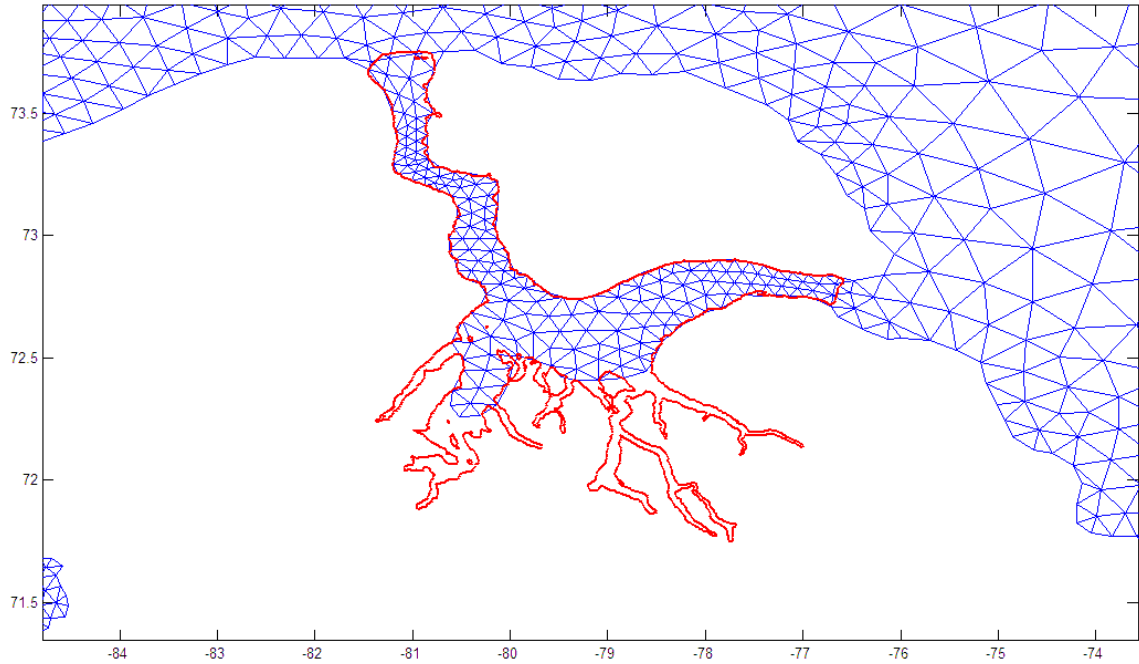


Figure 3.4 – Outline of Developed Bylot Model Grid for Constrained Waters of Bylot Island Overlaid on Existing Arctic8c Grid

The Arctic8c model tidal amplitude and phase for each constituent was extracted by interpolation along the open boundaries of the model for input to the developed hydrodynamic model. Open boundaries include those sections of the digitized model coastline that border water instead of land. It is these sections of the model that are driven to produce the tidal simulation.

3.4 Results

Due to an initially poor distribution of the nodes within the grid and the size and shape of the open boundaries, a series of edge effects were plaguing the model simulation output at the beginning of grid development. Figure 3.5 shows the model simulation

output amplitude of the M2 constituent over the entire model domain using one of the initial grids. On the eastern side of the domain there is an unusual amplification of the tides ramping up from 0.2 m at the open boundary to over 6 metres. In the bottom corner of the eastern boundary there is also an unusual jet of amplification.

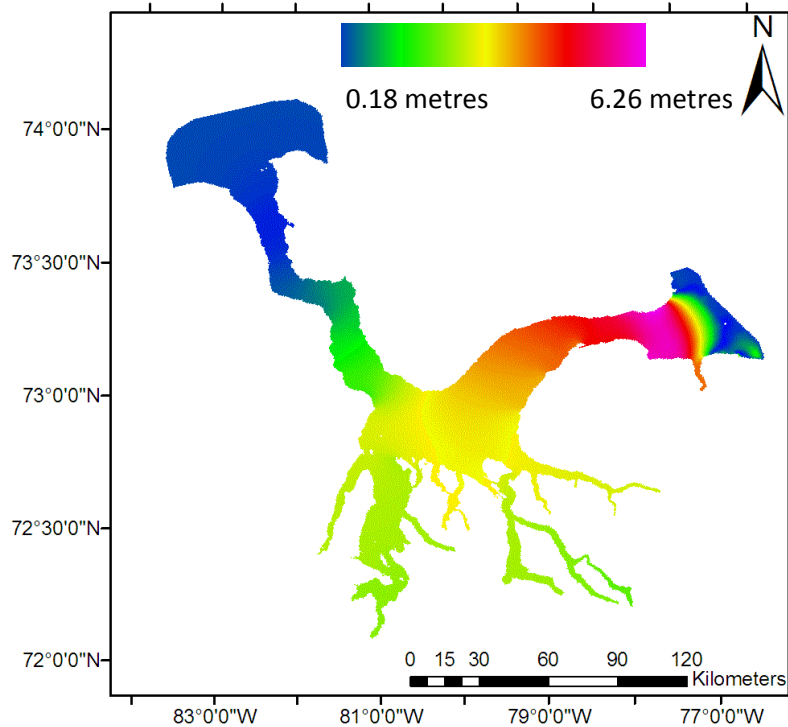


Figure 3.5 – Initial M2 Amplitude

In an effort to cure the strange effects near the eastern open boundary the limits of the model input grid were altered as shown in figure 3.6. This produced more reasonable results, but a strange amplification was still occurring near the eastern open boundary as you enter Pond Inlet. The amplitude of the M2 constituent decreases from 0.5 metres to almost 0 metres and then increases back up to over a metre before falling again to approximately 0.25 metres as you pass through Pond Inlet.

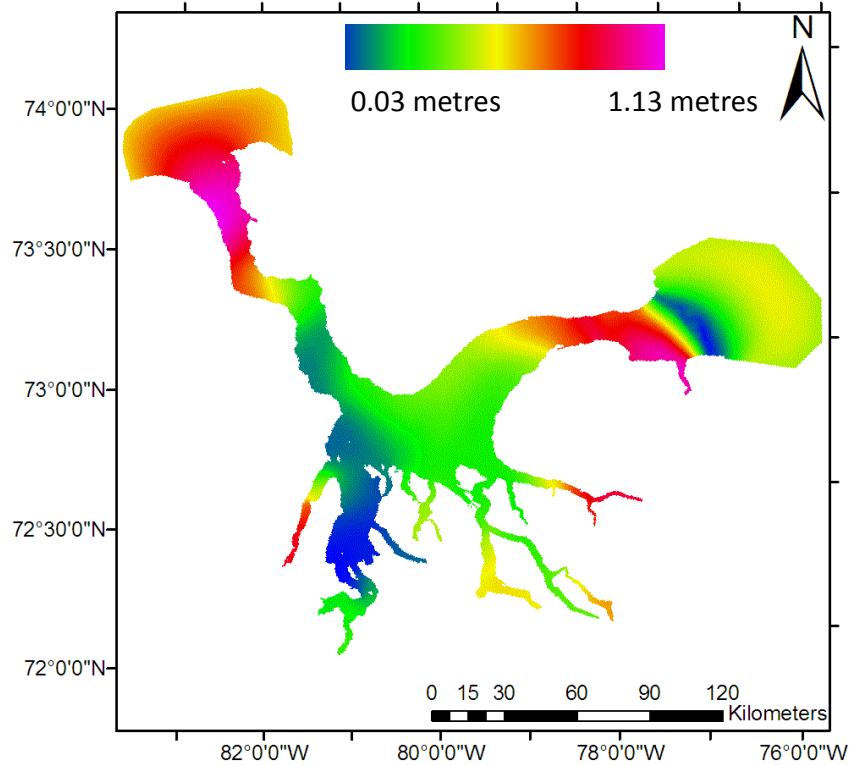


Figure 3.6 – Altered Eastern Boundary Initial M2 Amplitude

From observing the output from the existing Arctic8c model through the region, figure 2.13, and from examining the physical characteristics of the seabed, figure 3.2, it was determined that neither one of the initial model simulation outputs were likely correct as there was no dramatic changes in the seabed morphology which could have caused either result. The open boundaries at each end of the model were altered once again, as shown in figure 3.3. Cutting the grid off at each end of the area essentially removed the troubled areas from the model domain. The model simulation results of the final grid are shown in figures 3.7 through 3.11.

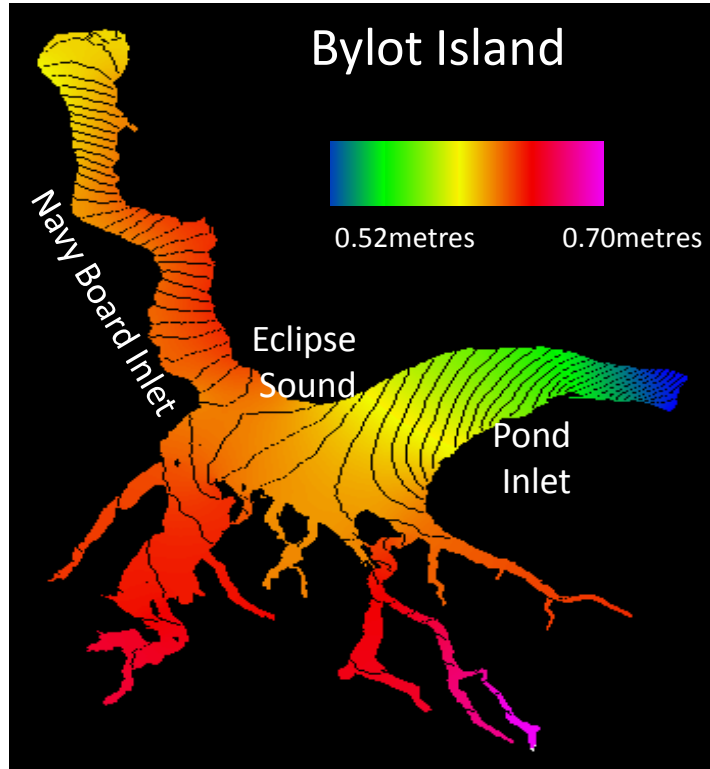


Figure 3.7 – M2 Amplitude with co-tidal lines. Phase contours at 0.5 degrees which equates to approximately 1 minute.

The M2 amplitude varies from 0.52 metres to 0.70 metres with a maximum at the head of one of the most southerly fjords. The gradient of the phase change is quite strong moving through Pond Inlet and Navy board inlet, but is more relaxed in Eclipse Sound and within the fjords. Both the S2 and N2 constituents, shown in figure 3.8 and 3.9, describe similar trends to the M2 constituent.

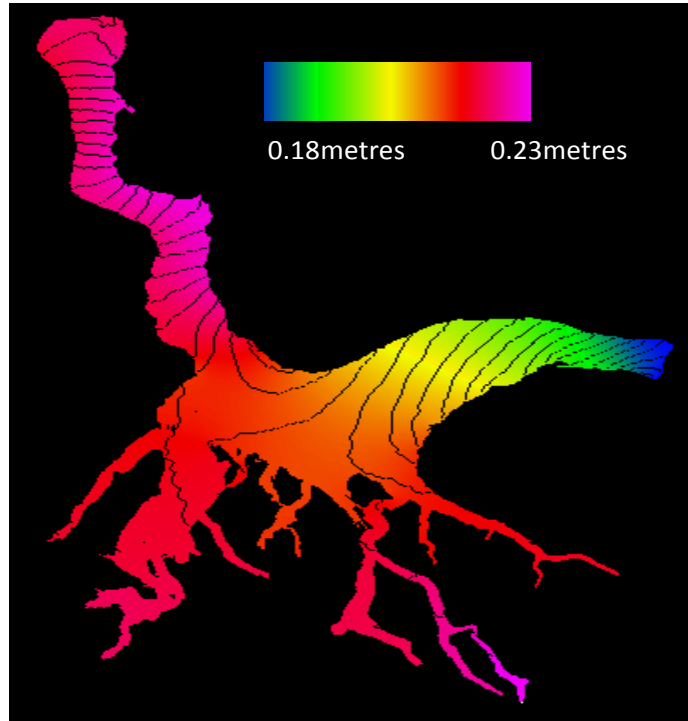


Figure 3.8 – S2 Amplitude with co-tidal lines. Phase contours at 0.5 degree which equates to approximately 1 minute.

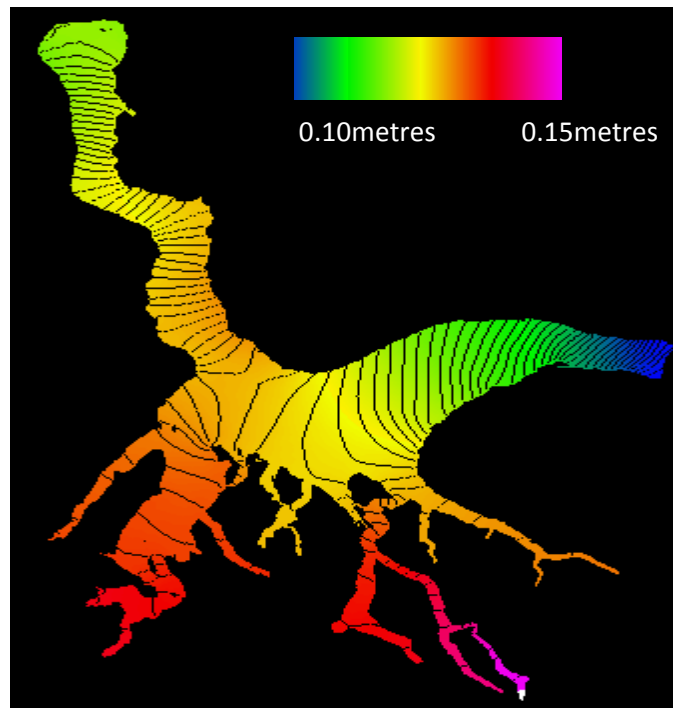


Figure 3.9 – N2 Amplitude with co-tidal lines. Phase contours at 0.5 degree which equates to approximately 1 minute.

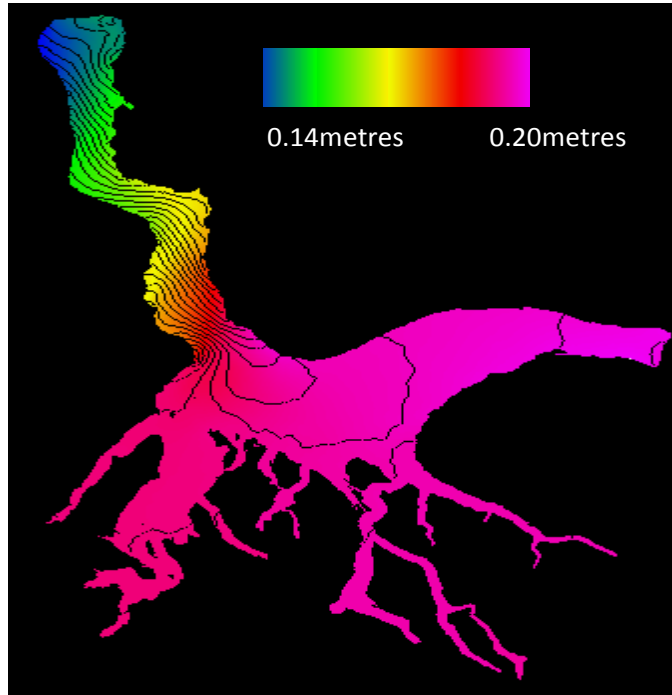


Figure 3.10 – K1 Amplitude with co-tidal lines. Phase contours at 0.5 degree which equates to approximately 2 minutes.

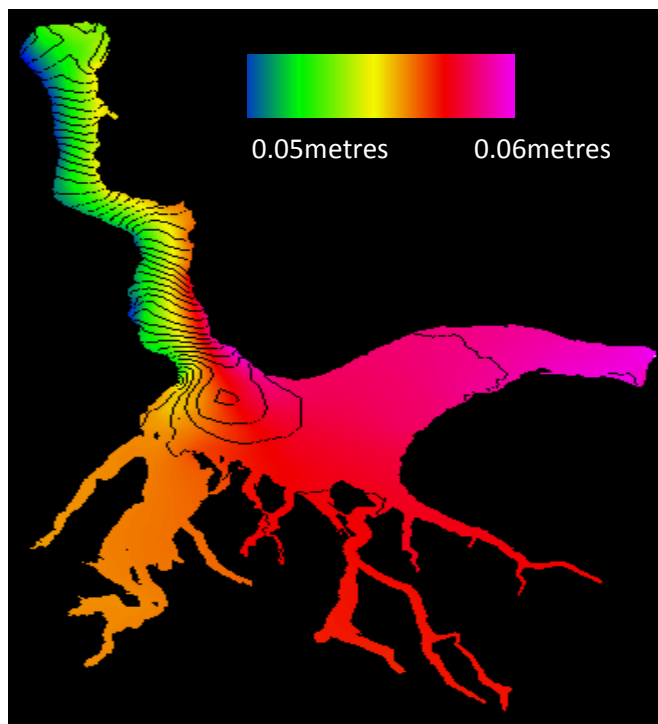


Figure 3.11 – O1 Amplitude with co-tidal lines. Phase contours at 0.5 degree which equates to approximately 2 minutes.

The K1 and O1 constituents, as shown in figures 3.10 and 3.11, show almost no amplification or phase change in the southern portion of the grid. It is only within Navy Board inlet that phase and amplitude changes can be observed.

3.5 Applications of the Developed Hydrodynamic Model

While the primary purpose behind the development of this hydrodynamic model is the extraction of tidal constituents for the purpose of tidal prediction, other uses related to hydrography are apparent. The shape and complexity of the narrow channels and fjords within the model grid domain cause variations in tidal phase and amplitude throughout the model, as shown in section 3.4, therefore using a single chart datum based on historical tidal records in the region to reduce bathymetric data is not appropriate. A chart datum based on historical records at existing predicted tide stations will not sufficiently represent a level below which the tide rarely falls within the model domain. Three potential solutions to this problem are discussed here.

The first possible solution is to use the Indian Spring Low Water (ISLW) determination as a vertical datum. The ISLW is a level for chart datum suggested by Sir George Darwin for Indian waters [Great Britain Hydrographic Office, 1969]. It is constructed by subtracting the sum of the amplitudes of the principal semi-diurnal and diurnal tidal harmonic constituents, M2, K1, S2 and O1, from Mean Sea Level.

The hydrodynamic model outputs tidal amplitudes for each input constituent at every node in the model mesh. The four major constituent amplitudes can then be summed to provide a value for the ISLW at each node within the hydrodynamic model. Instead of creating a vertical datum represented by a plane based on a single tide station, a constantly varying datum can be constructed for the entire survey area with the ISLW value at each node.

The second solution is to use a modified version of the ISLW chart datum. As the new datum should be related to the existing chart datum evaluated at the historic tide station for the area, a scaling factor can be applied to the new datum. A historic tide station must be selected within the model domain and the ratio between the ISLW chart datum at that station and the existing chart datum, lower low water large tide, should be determined. The resulting multiplier can be applied to the ISLW determination at each node within the model.

The third solution is to use a method developed by Charles Hannah at the Bedford Institute of Oceanography (BIO). It uses the ISLW determination, but adds the influence of the N2 constituent and uses a multiplier of 0.85 to bring the calculated value close to existing chart datum.

The result from using any of these solutions is a continuously varying chart datum which covers the entire model domain. The new datum takes into account natural factors of amplification of the tide and allows for a more precise determination of the lower low

water large tide level without the added time and expense involved with installing new tide gauges along the complex and rugged shore.

CHAPTER 4. ANALYSIS

Analysis was performed on the developed hydrodynamic model output to assess the validity of the output solution. The model output was compared to the existing Arctic8c hydrodynamic model solution, predicted tides at the three CHS tidal benchmarks in the area and to CNav GcGPS derived tides from vessel transit. The output model tides were also applied to overlapping multibeam data from the Heron and the Amundsen to assess the practical usability of the model output.

4.1 Model Results vs. Arctic8c Model

A comparison can be constructed for areas of common overlap between the developed model grid and the existing Arctic8c grid coverage for tidal amplitude and phase. The difference in constituent amplitude between the developed model simulation and the Arctic8c solution is shown in figures 4.1 through 4.5. For the semi-diurnal constituents of M2, S2 and N2 the largest discrepancies exist in the south west corner of the area, towards Milne Inlet. For the diurnal constituents of K1 and O1 the largest discrepancies exist in the south east corner of the area, near the entrance to Oliver Sound, although the differences are small and figures 4.4 and 4.5 exhibit some digital noise in the Navy Board Inlet region due likely to rounding errors. The amplitude differences are very small (less than 2cm) over the common areas with the exception of M2 in Milne Inlet where the differences approach 7cm.

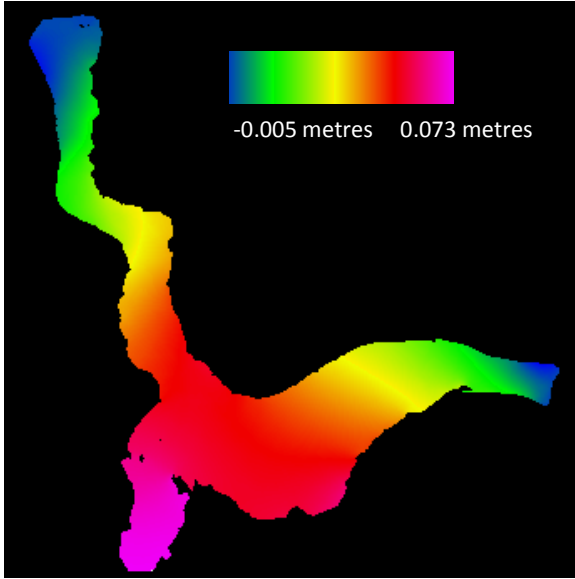


Figure 4.1 – Arctic8c Model Subtracted from Developed Model. Comparison of M2 Amplitude

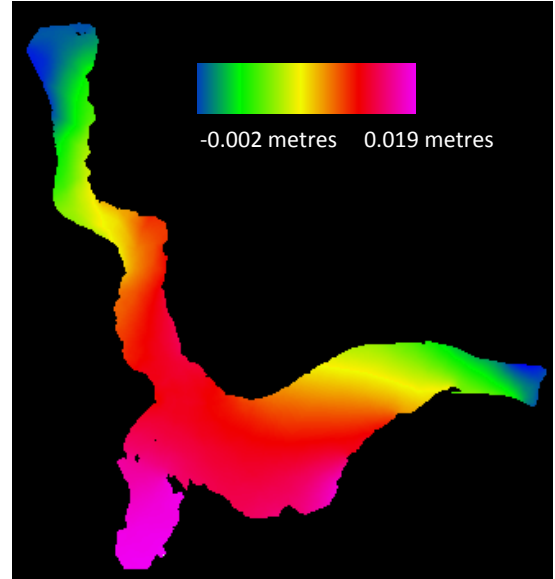


Figure 4.2 – Arctic8c Model Subtracted from Developed Model. Comparison of S2 Amplitude

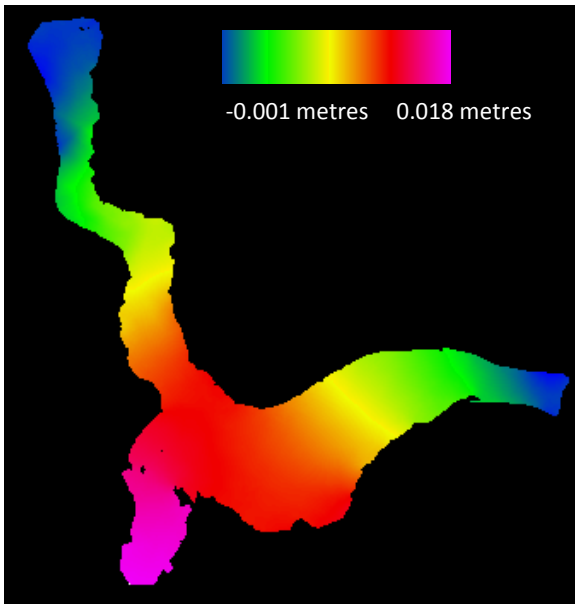


Figure 4.3 – Arctic8c Model Subtracted from Developed Model. Comparison of N2 Amplitude

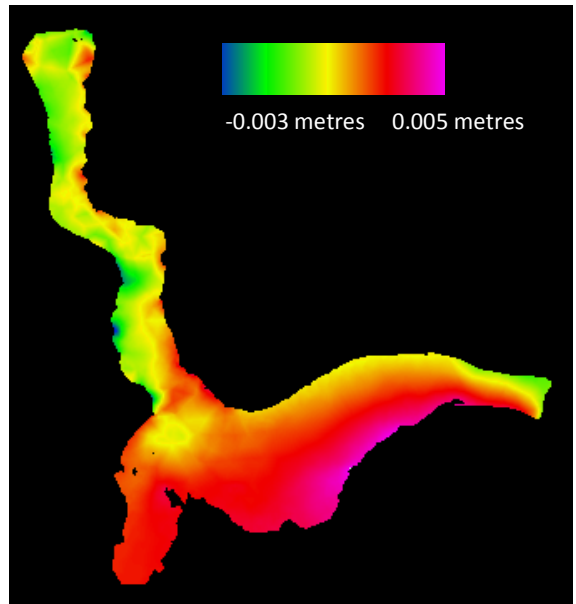


Figure 4.4 – Arctic8c Model Subtracted from Developed Model. Comparison of K1 Amplitude

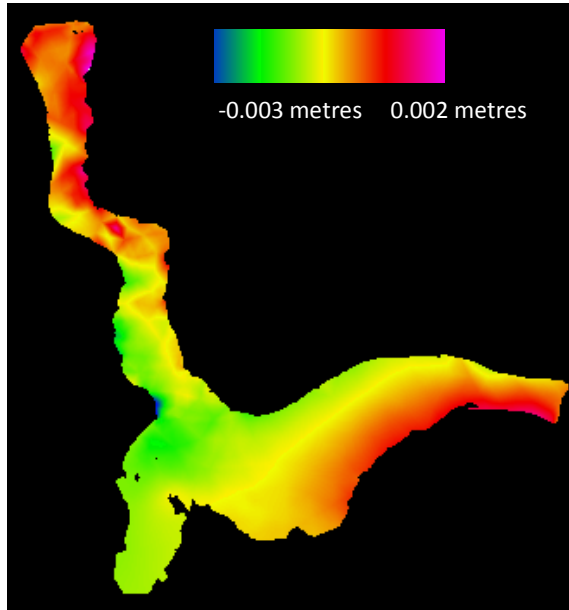


Figure 4.5 – Arctic8c Model Subtracted from Developed Model. Comparison of O1 Amplitude

The difference in constituent phase between the developed model simulation and the Arctic8c solution is shown in figures 4.6 through 4.10. For the semi diurnal constituents of M2, S2 and N2 there is an obvious phase lag in the Eclipse Sound region between the developed model and Arctic8c. The largest deviation is associated with the N2 constituent, at 24.3 degrees, while the closest match is with the K1 constituent with a maximum deviation of -2.30 degrees.

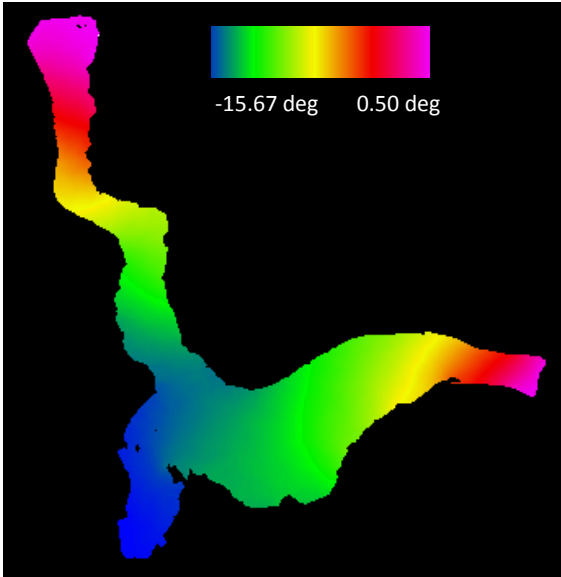


Figure 4.6 – Arctic8c Model Subtracted from Developed Model. Comparison of M2 Phase

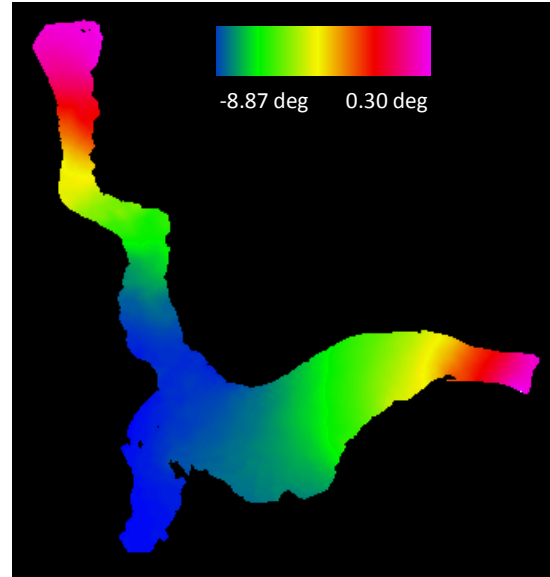


Figure 4.7 – Arctic8c Model Subtracted from Developed Model. Comparison of S2 Phase

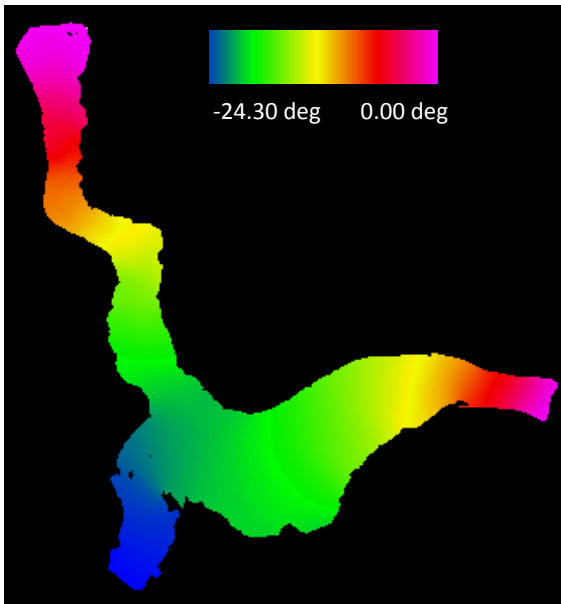


Figure 4.8 – Arctic8c Model Subtracted from Developed Model. Comparison of N2 Phase

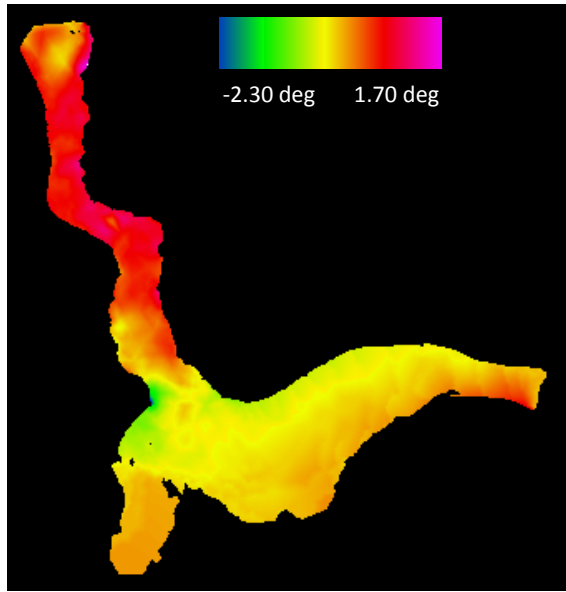


Figure 4.9 – Arctic8c Model Subtracted from Developed Model. Comparison of K1 Phase

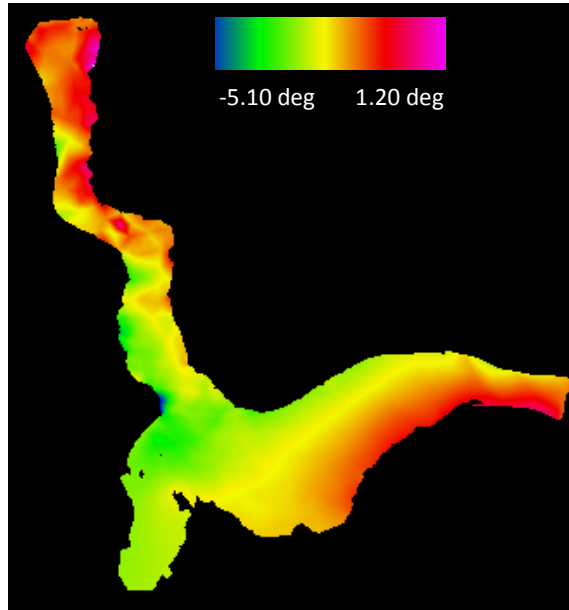


Figure 4.10 – Arctic8c Model Subtracted from Developed Model. Comparison of O1 Phase

4.1.1 Comparison at the Head of Oliver Sound

The potential relative error between using predicted tides from a solution derived from the developed model at the head of the Oliver Sound fjord and a solution at the mouth of the fjord from the arctic8c model was analyzed. This comparison emphasizes the importance of understanding the tidal propagation within the Oliver Sound fjord. Using the constituents of M2, S2, N2, K1 and O1 a tidal prediction was constructed at each location which extended over 10 years and the magnitude of the tide was compared at 1 minute intervals in the prediction. The maximum overall difference and the differences associated with each constituent are shown in table 4.1.

Comparison	Difference (m)
Overall	0.255
M2	0.160
N2	0.052
S2	0.036
K1	0.004
O1	0.002

Table 4.1 – Potential Relative Error Between using a Tidal Prediction from the Developed Hydrodynamic Model and the Existing Arctic8c Grid

4.2 Model Results vs. GPS

The GPS height record of the Amundsen can be compared to the predicted tide constructed from the output of the developed hydrodynamic model to check the model results. The height values from the CNav GcGPS on the Amundsen must be reduced to the geoid and then any effects from vessel squat and the inverse barometer effect must be removed. The resulting height value relates to the height of the GPS antenna above the geoid, which approximates mean sea level.

For the 2004, 2005 and 2007 transits through the model domain, only ASCII NMEA data files were collected aboard the Amundsen. The ASCII files cannot be reprocessed using the GAPS software as it requires the raw data files which include pseudoranges. Therefore data from those years was taken as is, which includes only the real-time CNav corrections. The CNav GPS data from 2006 was collected in raw format and was then processed in GAPS to improve the results using known satellite clock and orbit

information. Post-processing allows for an improved positioning solution over the real-time corrections, as discussed in section 2.52.

The difference data was examined to determine the standard deviation and variance of the data. Any residual trends in the difference were also examined in an effort to determine the existence of missing constituents or issues with the geoid ellipsoid separation model.

4.2.1 Amundsen 2004

In 2004 the CCGS Amundsen transited through the model domain as shown in figure 4.11. The ship spent just over 10 hours transiting through the region on August 19th and 20th, 2004.

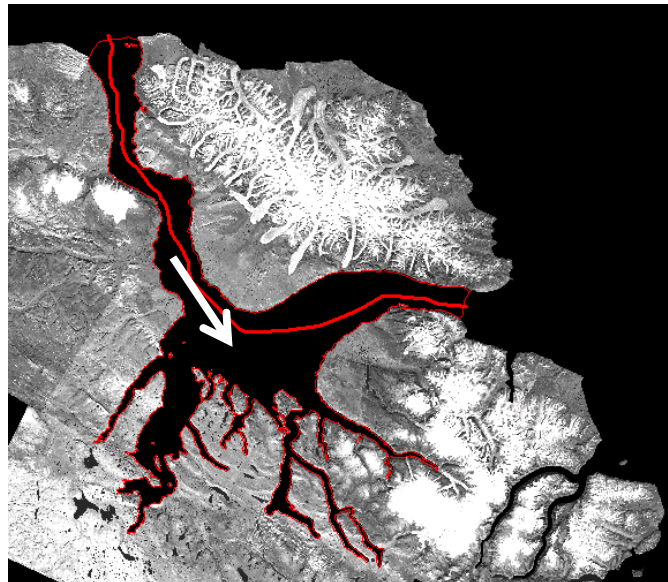


Figure 4.11 – 2004 Amundsen Ship Track through Model Domain with Arrow Indicating Transit Direction

Figure 4.12 shows the velocity of the Amundsen as it transits through the model domain. The velocity was used to calculate the squat value. The vessel was moving for most of the time through the region, but did stop for approximately an hour just after the 6 hour mark of the record.

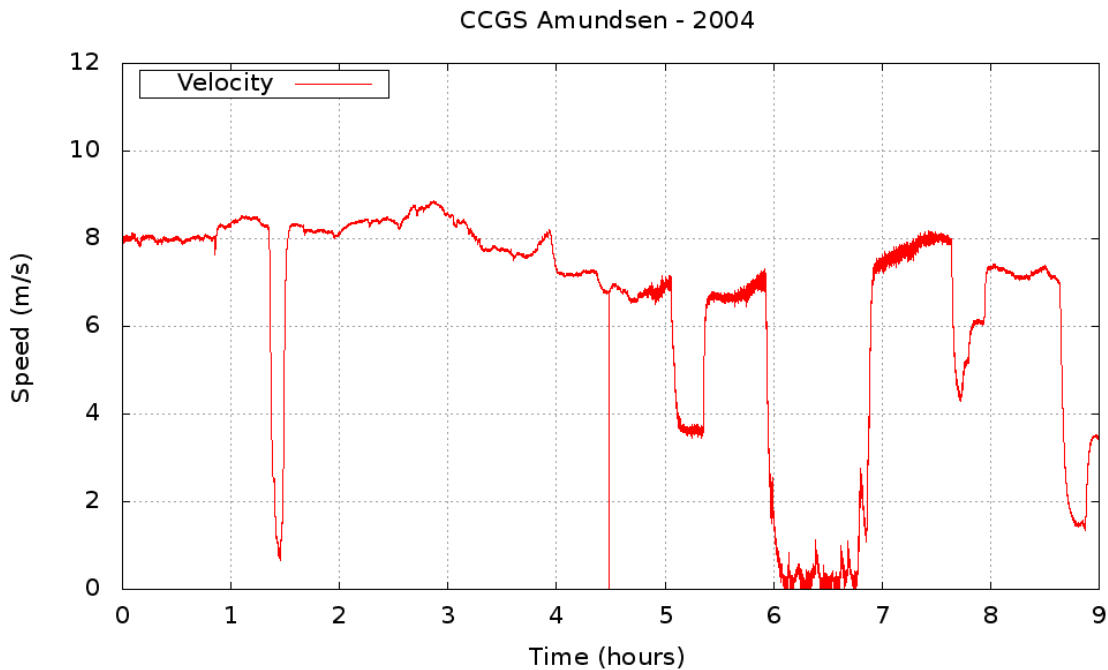


Figure 4.12 – Amundsen Velocity 2004

Figure 4.13 outlines the height of the Amundsen above the geoid. The effects of vessel squat and the inverse barometer effect have been calculated and removed from the data. The effect of the inverse barometer is shown in figure 4.14. The height record in figure 4.13 still does not show a smooth record that is only affected by the tides. Other effects are still apparent in the record, although when compared to the output of the developed hydrodynamic model for the same time and location in figure 4.15, similar

trends can be observed. The hydrodynamic model output in figure 4.15 exhibits a minimum near 5 hours into the record, which is also the location of the minimum in the height record shown in figure 4.13. Figure 4.15 also compares the output from the developed hydrodynamic model grid to the output from the Arctic8c grid for the five constituents of M2, S2, N2, K1 and O1.

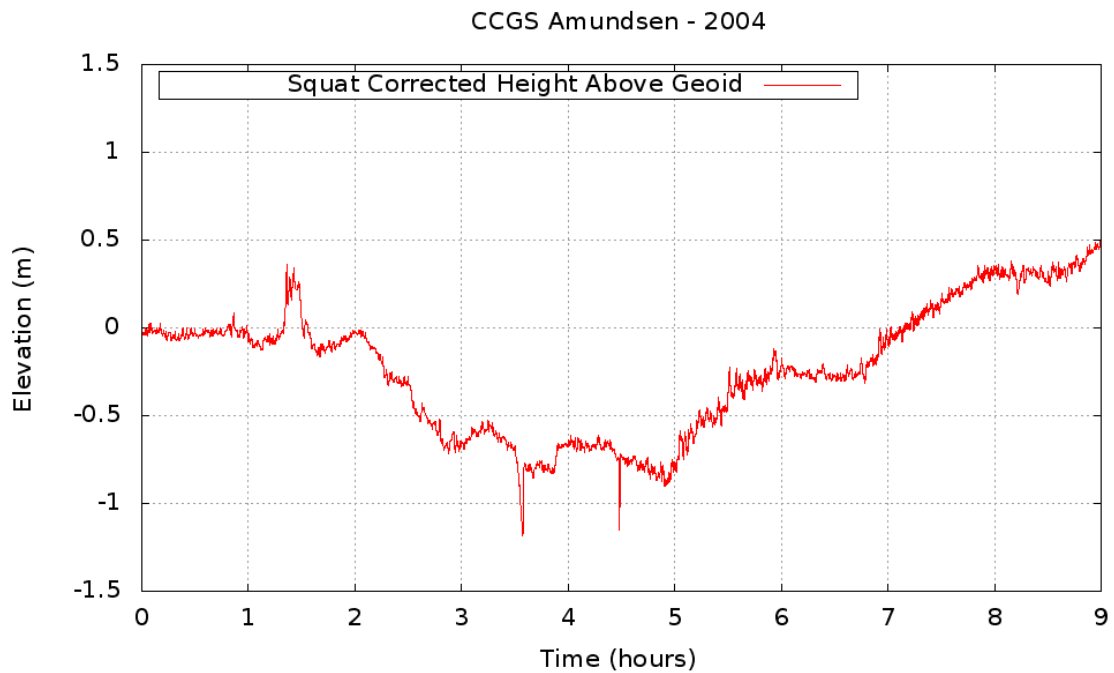


Figure 4.13 – Amundsen Height above the Geoid Corrected for Pressure and Squat

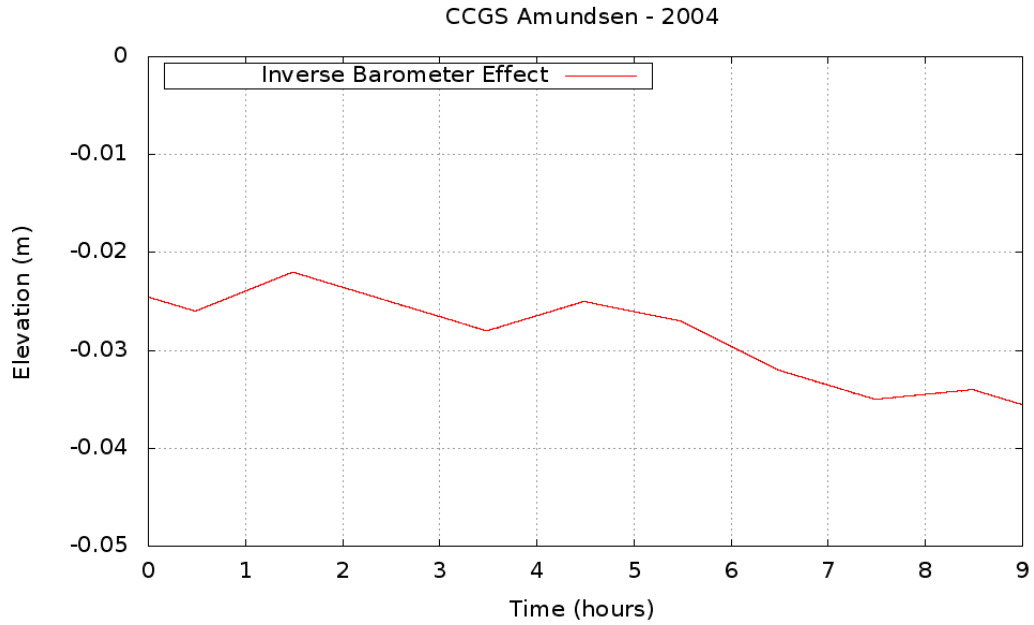


Figure 4.14 – Amundsen 2004 Inverse Barometer Effect

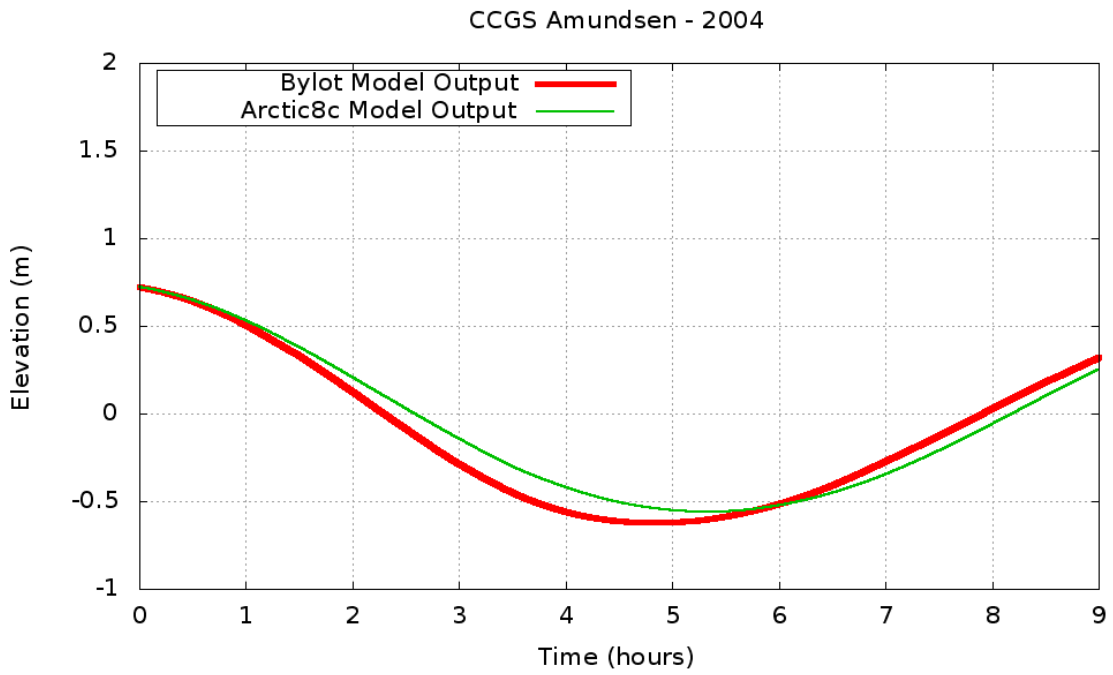


Figure 4.15 – Hydrodynamic Model Output Corresponding to 2004 Ship Track

The model output was subtracted from the vessel height record and is shown in figure 4.16. The dip in the centre of the record has been removed but other artefacts are still observed in the data. A near linear trend can be observed over the entire difference record along with shorter period effects throughout. From figure 4.16, the average of the difference is -0.11 metres with a standard deviation of 0.31 metres.

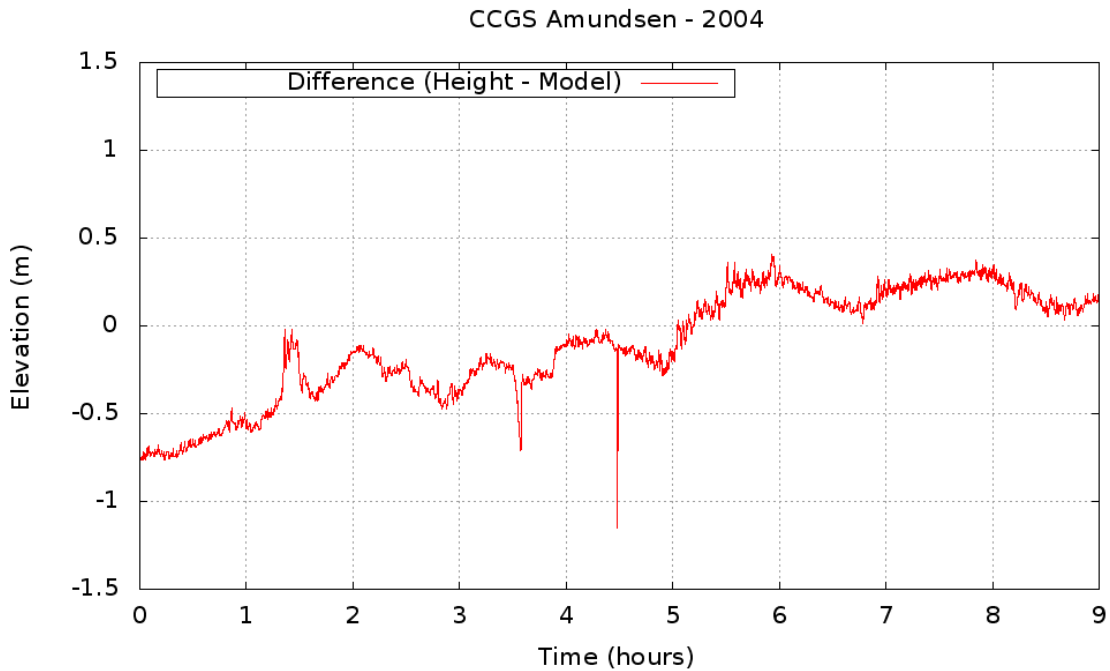


Figure 4.16 – Amundsen 2004 Difference between Corrected Height above Geoid and Model Output

Figure 4.17 shows the number of GPS satellites visible to the GPS receiver during the transit through the model domain. The number of satellites varies from 7 to 10. Figure 4.17 also shows the solution type observed during the transit. A solution type of 2

indicates that the GPS was receiving CNav corrections and a solution type of 1 indicates that corrections were not received and it was operating as a single point system.

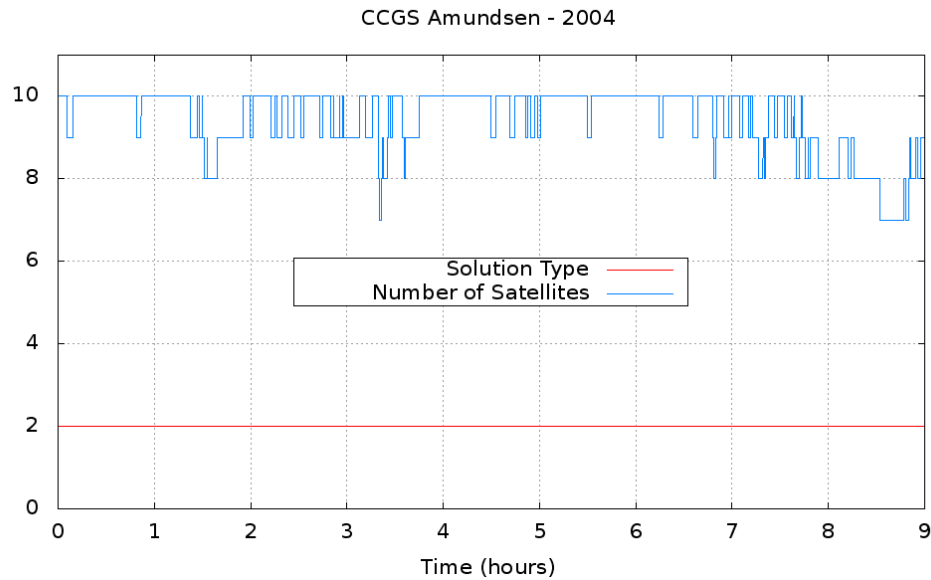


Figure 4.17 – Amundsen 2004 Number of Satellites and Solution Type

4.2.2 Amundsen 2005

The Amundsen spent over 24 hours within the hydrodynamic model grid domain during the cruise in 2005. The majority of the time was spent near the community of Pond Inlet as a survey was performed in the inlet, as shown in figure 4.18. Steep cliffs and large mountains sit directly to the south of the survey area at the entrance to Eclipse Sound in the Pond Inlet waterway. These cliffs partially obstruct the ships view of the GPS constellation and likely fully obstruct the CNav correction satellites for the first 8

hours of observation. The ship was moving for the majority of the time spent within the region although it did stay stationary for approximately 2 hours, as can be observed in figure 4.19.

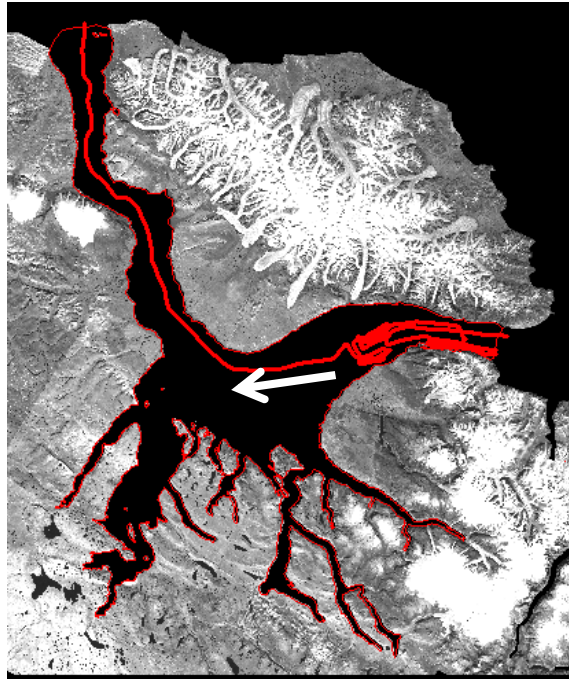


Figure 4.18 – 2005 Amundsen Ship Track through Model Domain with Arrow Indicating Transit Direction

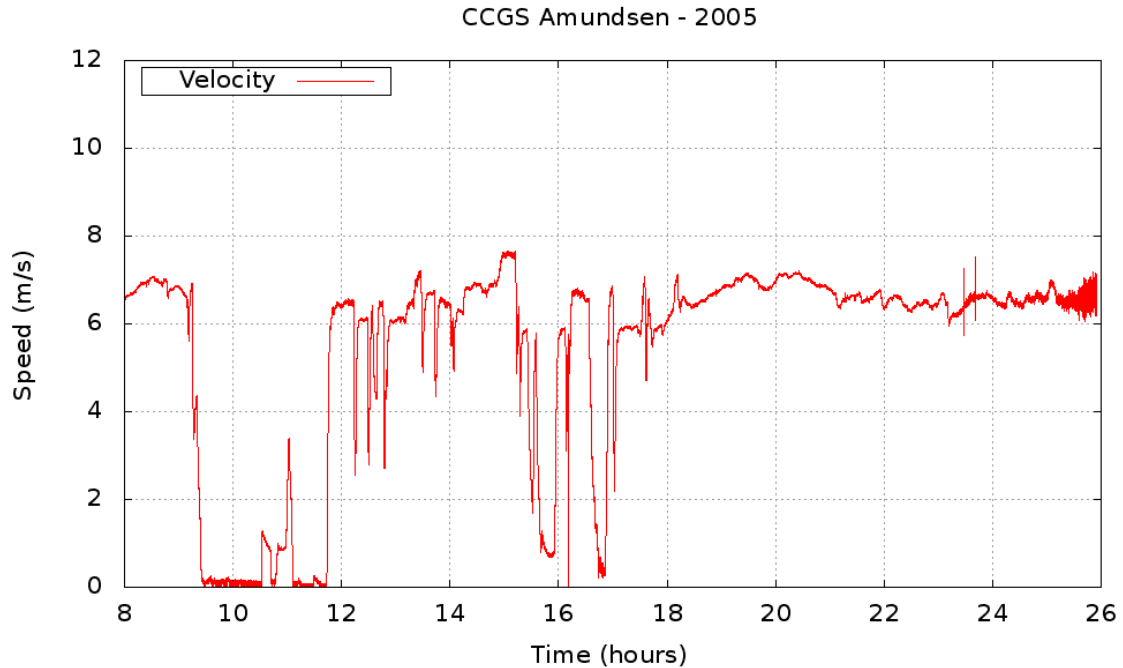


Figure 4.19 – Amundsen Velocity 2005

During the survey in Pond Inlet, the cliffs created obstructions which account for noise in the GPS data observed in the first 8 hours of the GPS record, as can be seen in figure 4.20. The accuracy of the vertical position is not sufficient during this time to make a useful comparison to the model output; therefore that portion of the data was removed from the analysis. The height data was corrected for atmospheric pressure variations using the inverse barometer effect calculation, as shown in figure 4.21. Figure 4.22 shows the output from the Arctic8c model dataset and the developed model for the enclosed waters of Bylot Island for the shortened time period. The difference between the vessel height, figure 4.20, and the model output, figure 4.22, was calculated and the result shown in figure 4.23. The average difference is -0.38 metres with a standard deviation of 0.45 metres.

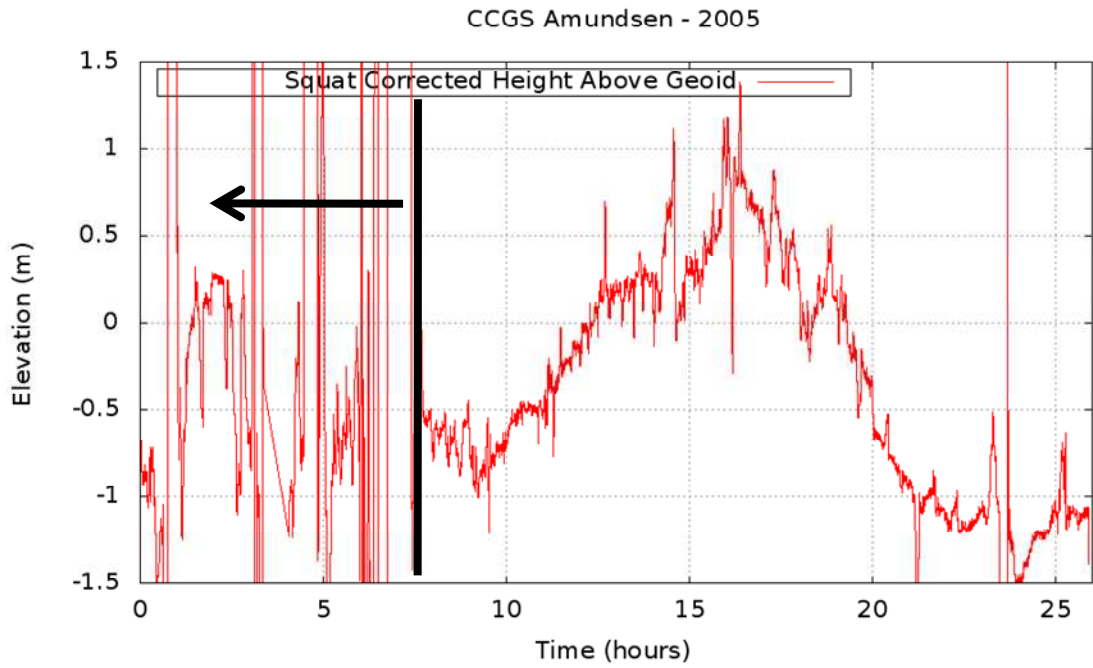


Figure 4.20 – Amundsen Height above the Geoid Corrected for Pressure and Squat. The Area to the Left of the Black Vertical Line was Removed for Analysis

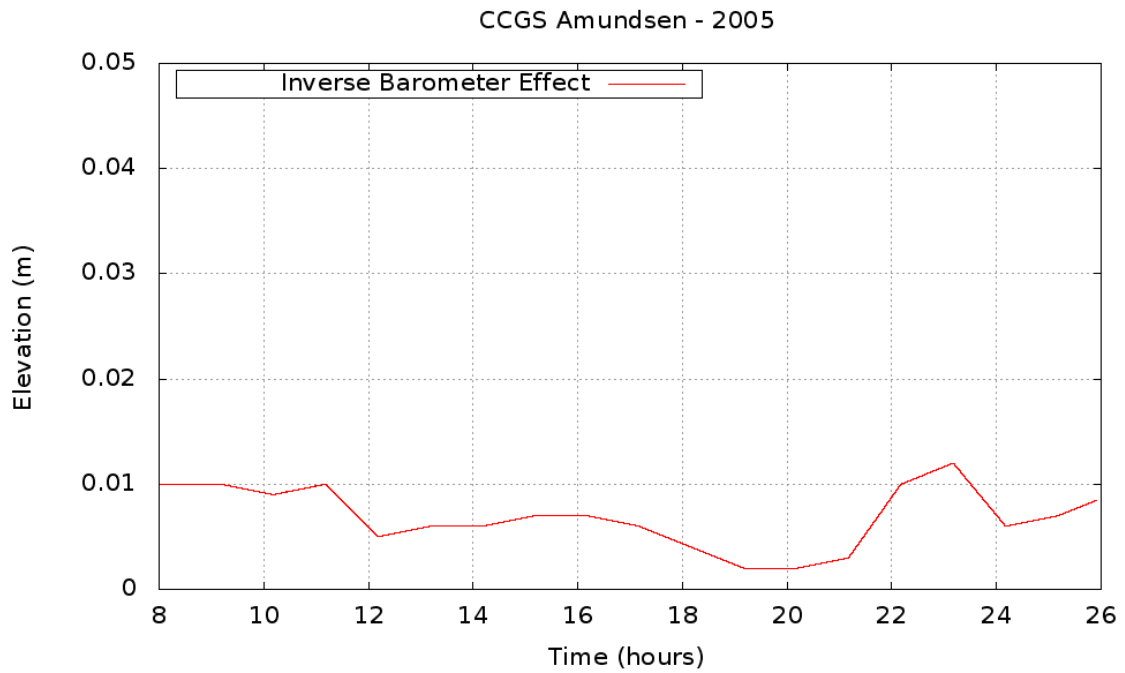


Figure 4.21 – Amundsen 2005 Inverse Barometer Effect

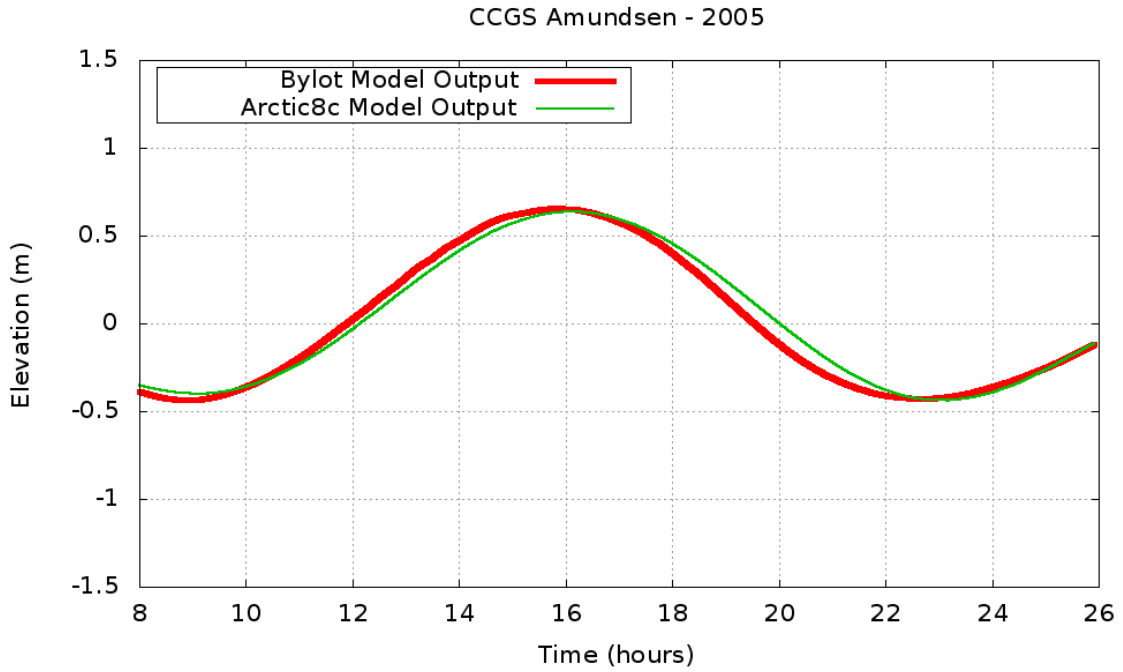


Figure 4.22 – Hydrodynamic Model Output Corresponding to 2005 Ship Track

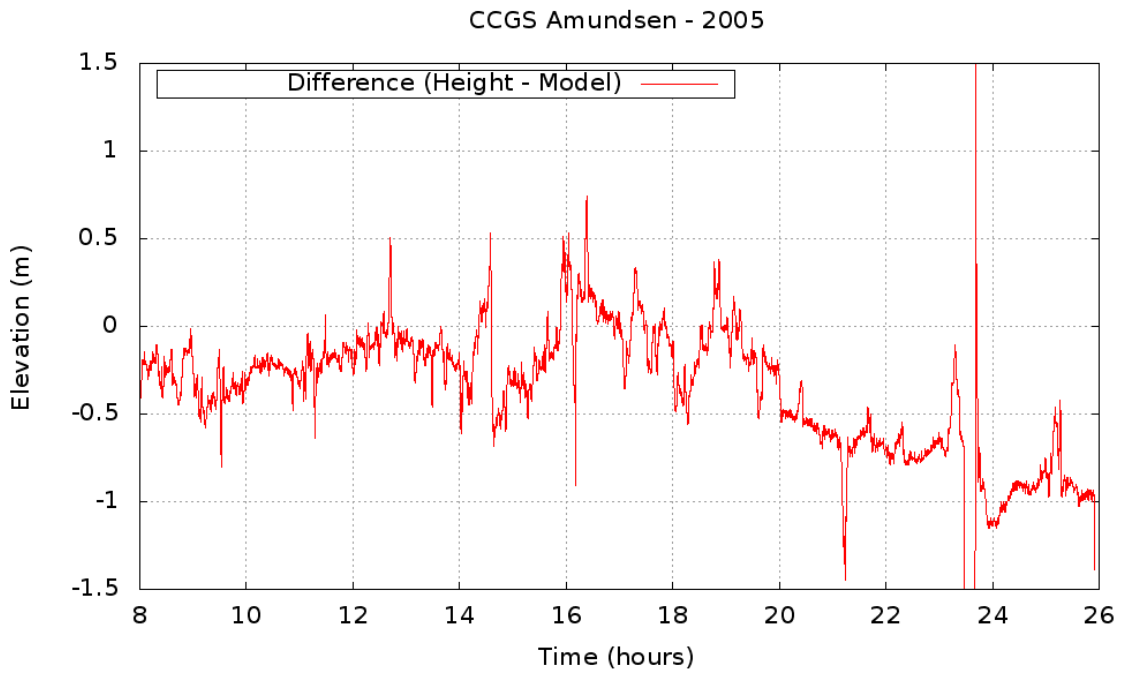


Figure 4.23 – Amundsen 2005 Difference between Corrected Height above Geoid and Model Output

The noise exhibited in figure 4.20 prior to the 8 hour mark clearly correspond to periods in figure 4.24 where the number of visible satellites dips below 4 and the solution type is only 1, which indicates a single point position where no CNav corrections have been received. After the 8 hour mark, once the vessel had moved into open waters, the solution type switches to 2 and the number of visible satellites seldom drops below 7.

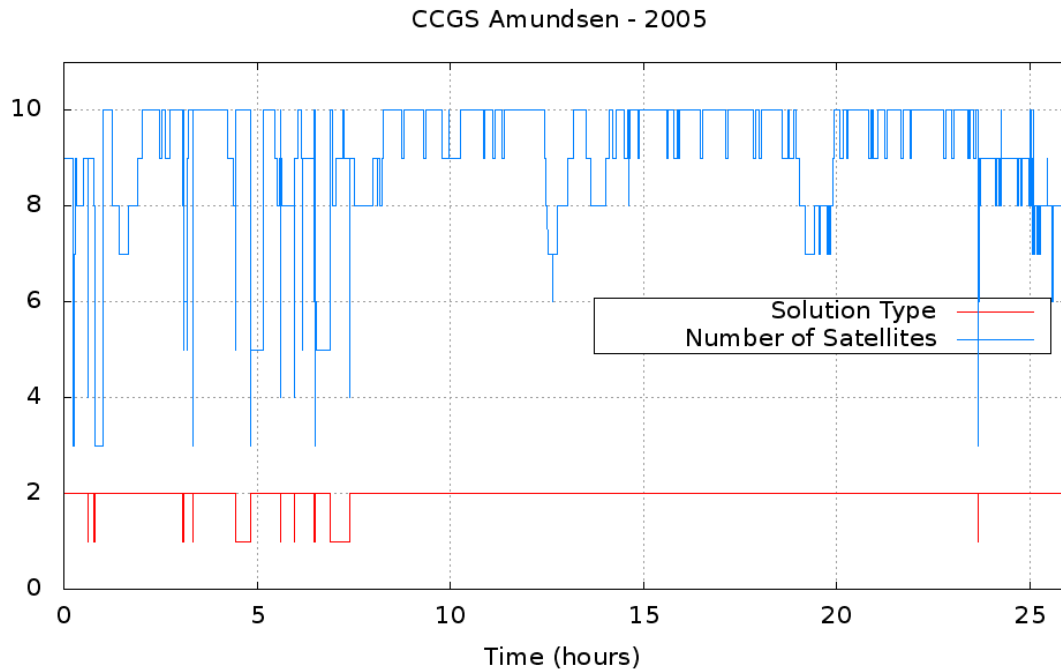


Figure 4.24 – Amundsen 2005 Number of Satellites and Solution Type

4.2.3 Amundsen 2006

In 2006 the Amundsen steamed into the model domain and spent approximately 36 hours surveying within Oliver Sound, as can be seen in the ship track shown in figure

4.25. Therefore the majority of the GPS record for 2006 is from within the Oliver Sound fjord, which is not included in the Arctic8c model data set. The vessel was moving the majority of the time while in the area, but was stationary for periods of 2 to 6 hours, as shown in figure 4.26. This year was also the only time that raw CNav pseudorange data was collected, which allowed for additional signal processing using the GAPS package. As the fjord walls were extremely steep and essentially blocked southward visibility, additional processing was required to interpret the signal. Figure 4.27 shows the original GPS height output while 4.28 shows the post processed output. The post processed output was used for all analysis.

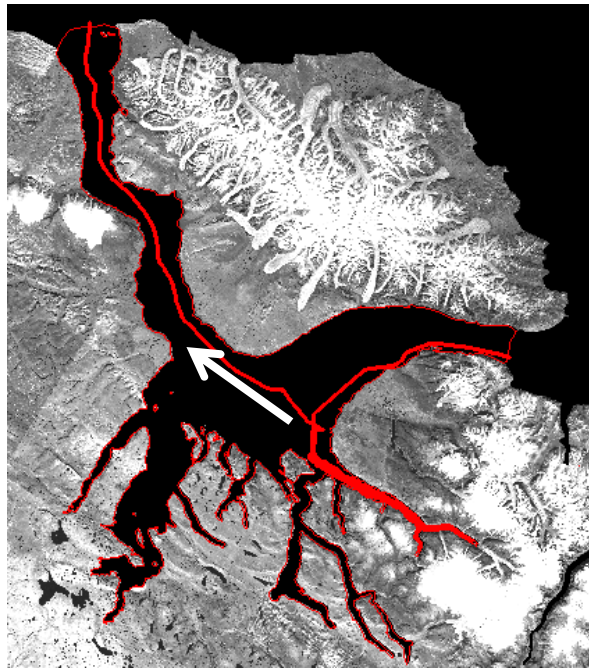


Figure 4.25 – 2006 Amundsen Ship Track through Model Domain with Arrow Indicating Transit Direction

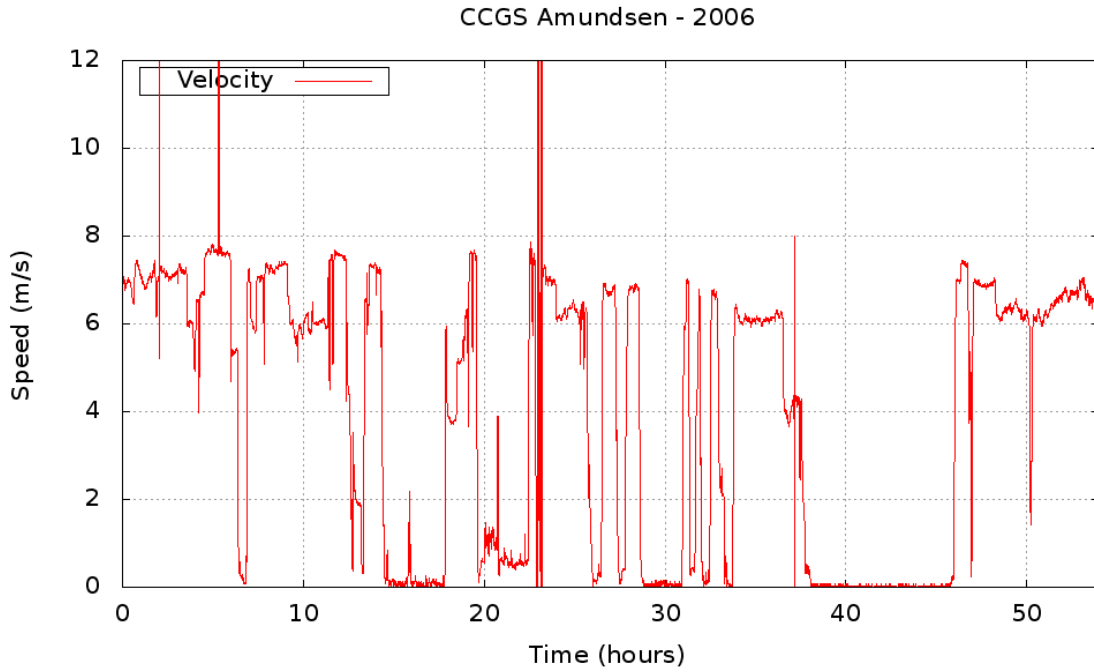


Figure 4.26 – Amundsen 2006 Speed

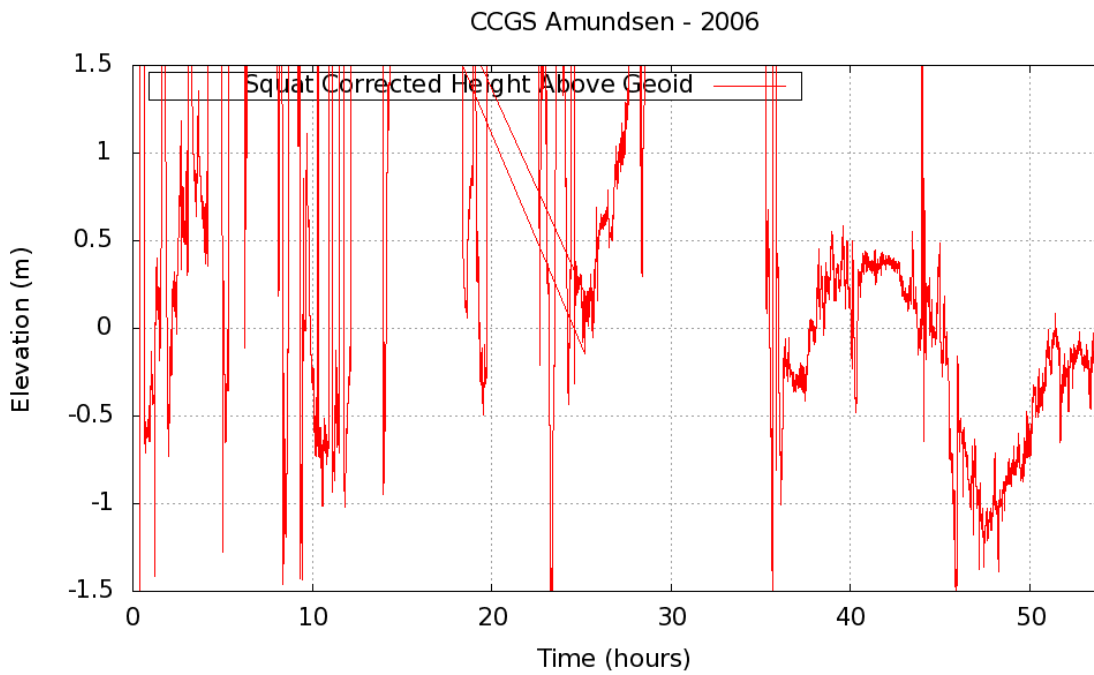


Figure 4.27 – Original Amundsen Height above the Geoid without Post-Processing

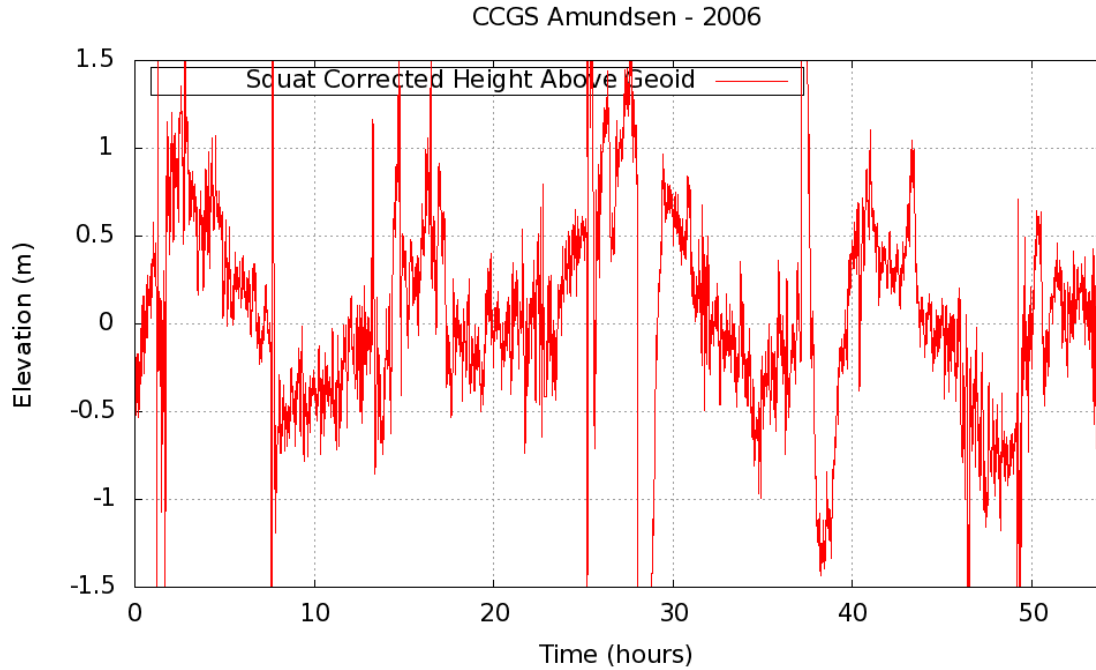


Figure 4.28 – Amundsen Height above the Geoid Corrected for Pressure and Squat with Post-Processing

The outputs from the Arctic8c model data set and the developed model for the enclosed waters of Bylot Island are shown in figure 4.29. As the Arctic8c model does not extend into Oliver Sound, the tides from the nearest nodes were used, which would be located near the entrance to the fjord. The output in figure 4.29 is shown for the five modelled constituents of M2, S2, N2, K1 and O1.

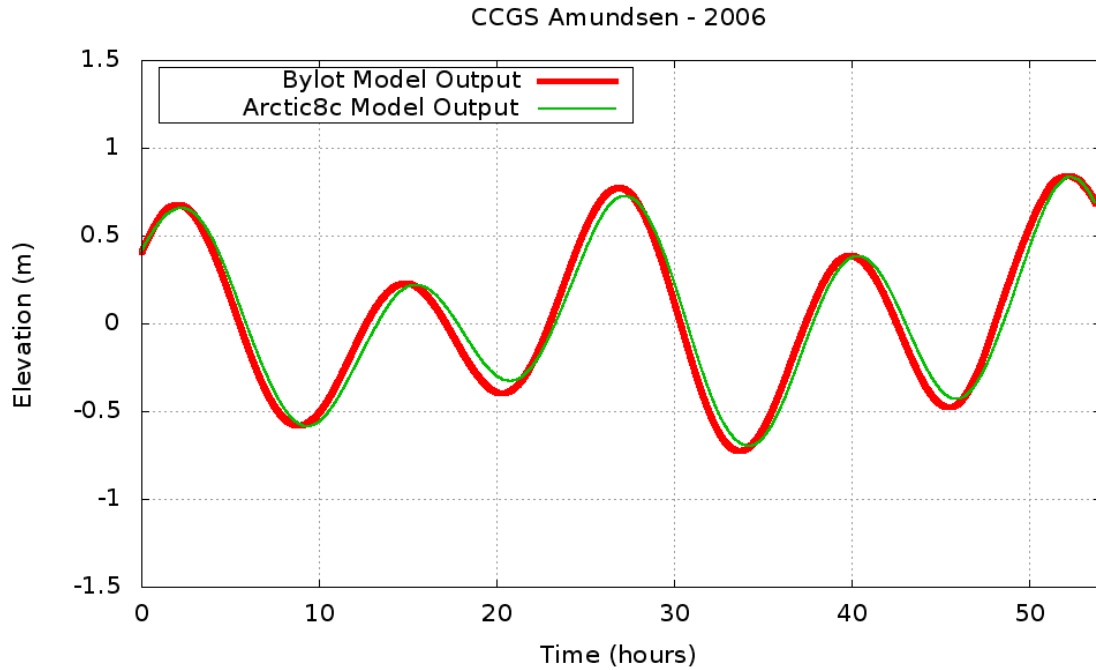


Figure 4.29 – Hydrodynamic Model Output Corresponding to 2006 Ship Track

When the original data, in figure 4.28, is subtracted from the modeled record, in figure 4.29, there are still large obvious fluctuations in the data, as shown in figure 4.30. The differences exist throughout the dataset; therefore it is not simply a case of the model incorrectly simulating the tides in the Oliver Sound Fjord. There is also still a large amount of noise in the data. The average of the difference is -0.07 with a standard deviation of 1.75 metres.

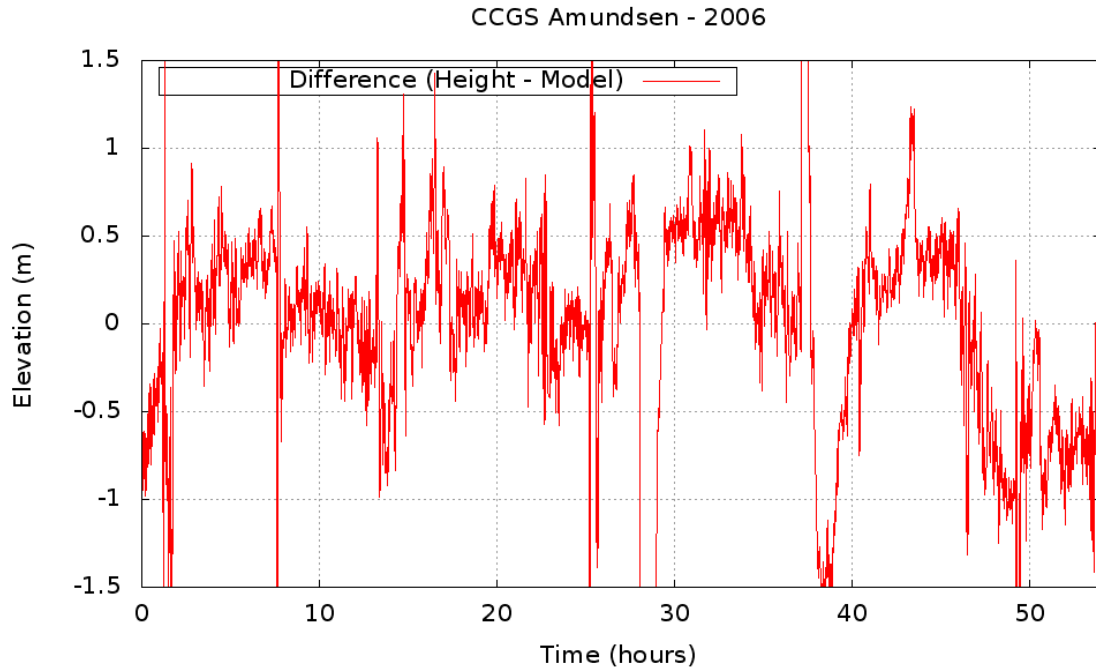


Figure 4.30 – Amundsen 2006 Difference between Corrected Height above Geoid and Model Output

Figure 4.31 shows the number of satellites in view during the survey and the correction type received for the original dataset. The number of satellites can be observed to drop down to 3 at times and the receiver is often in single point mode. Figure 4.32 shows the affect of the changing atmospheric pressure on the vessel height record which was used to reduce the data shown in figure 4.28.

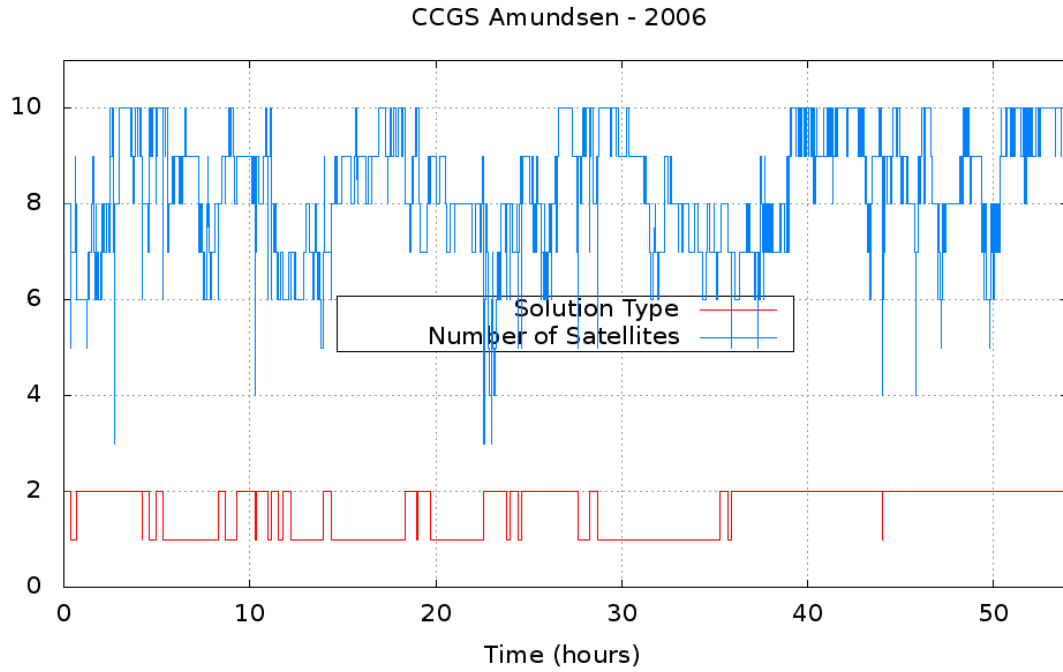


Figure 4.31 – Amundsen 2006 Number of GPS Satellites and Solution Type

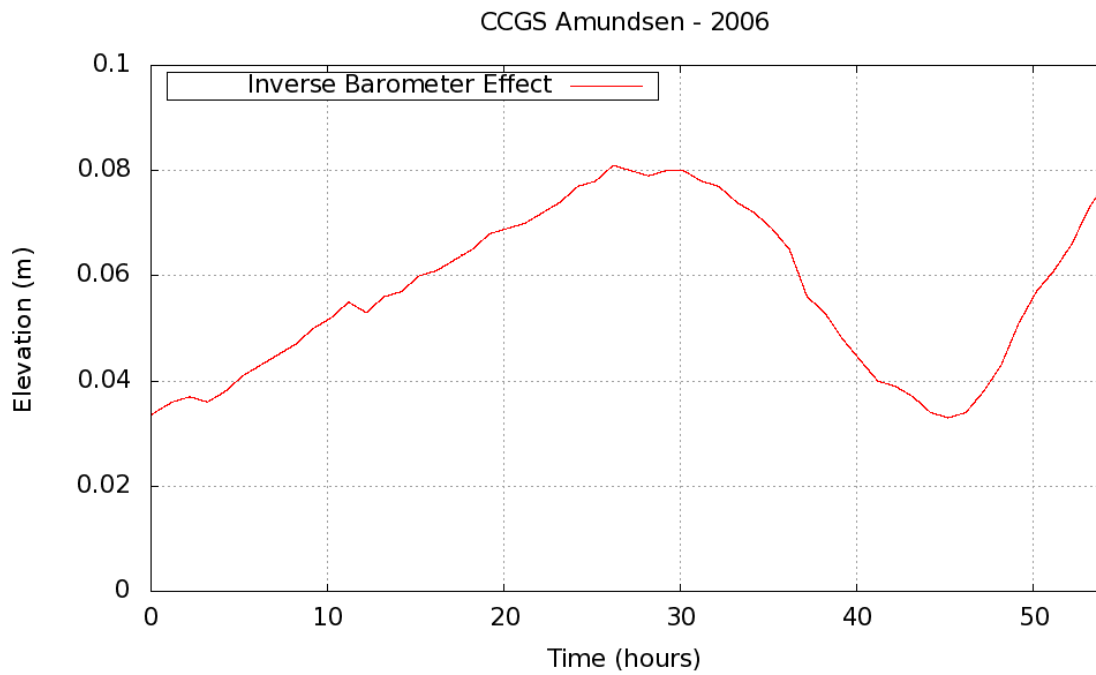


Figure 4.32 – Amundsen 2006 Inverse Barometer Effect

4.2.4 Amundsen 2007

In 2007 CNav data was logged for a short transit as the Amundsen sailed from Pond Inlet out into Lancaster Sound through Navy Board Inlet, as shown in figure 4.33. The transit was mainly in open water, away from steep cliffs that block the view of the CNav correction satellites. The vessel was moving for the entire transit through the area and was only stationary at Pond Inlet, as indicated in figure 4.34.

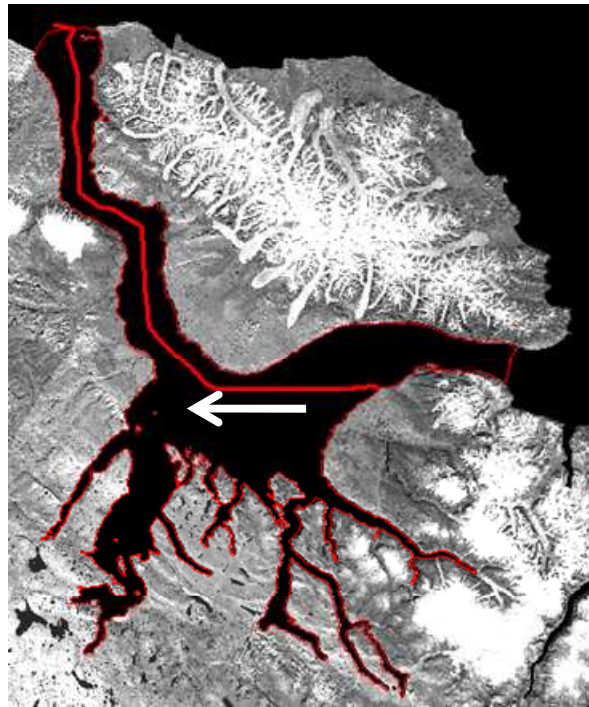


Figure 4.33 – 2007 Amundsen Ship Track through Model Domain with Arrow Indicating Transit Direction

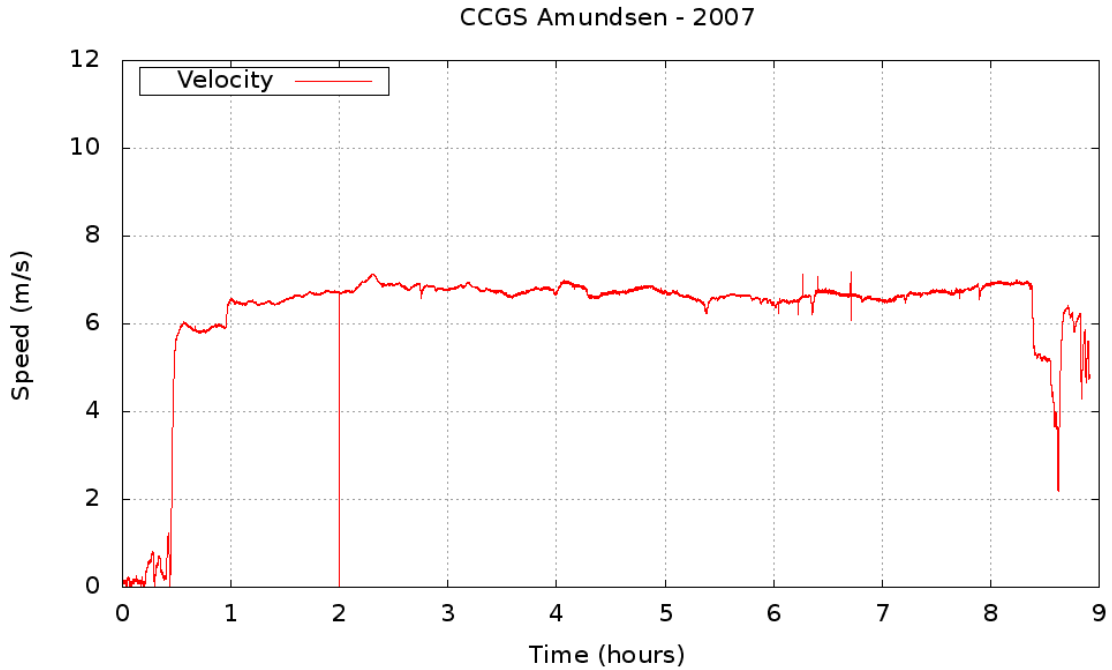


Figure 4.34 – Amundsen 2007 Speed

Figure 4.35 shows the height record of the Amundsen as it travelled through the developed model grid region in 2007. At approximately 6 hours into the record there is a significant jump in the vertical position. Figure 4.36 shows the extent of the vertical step. In examining figure 4.37 it should be noted that it is at this time that the receiver switched to single point mode and was not receiving CNav corrections. After the jump in vertical position, the solution appears to slowly drift back to the correct position over a period of 45 minutes.

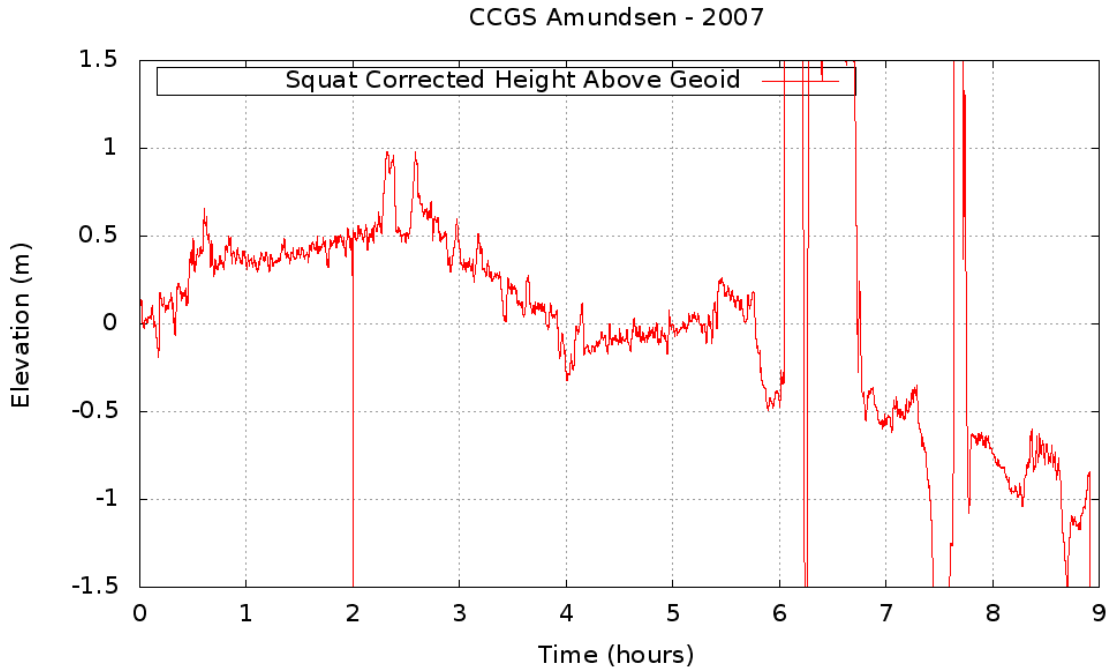


Figure 4.35 – Amundsen Height above the Geoid Corrected for Pressure and Squat

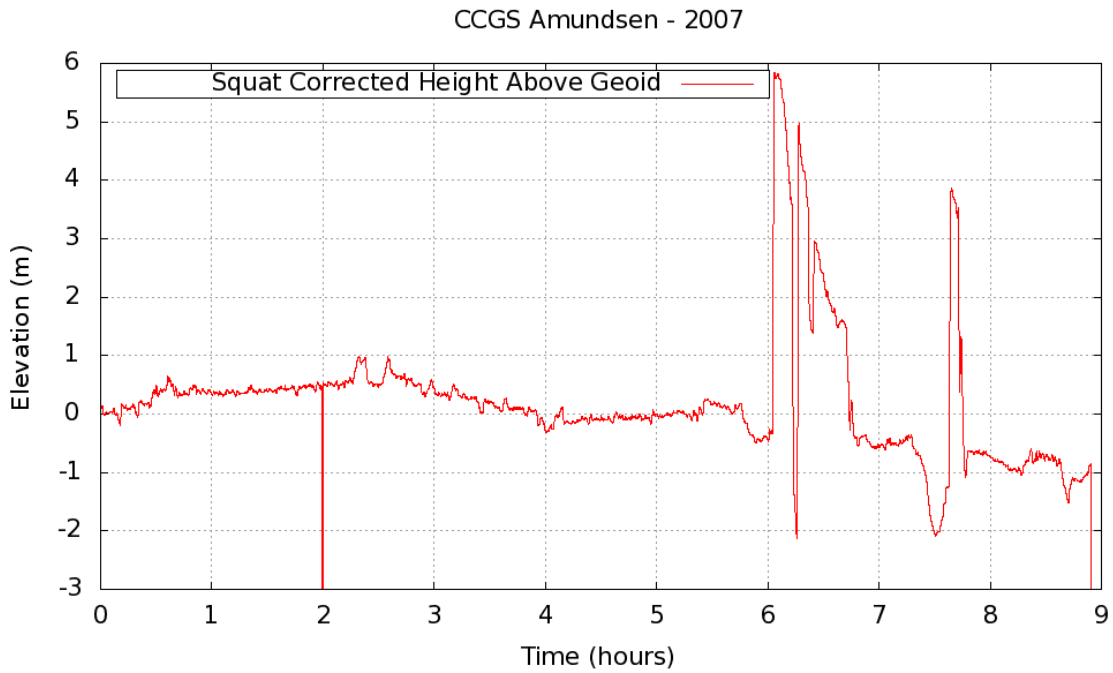


Figure 4.36 – Amundsen Height above the Geoid with Extended Scale

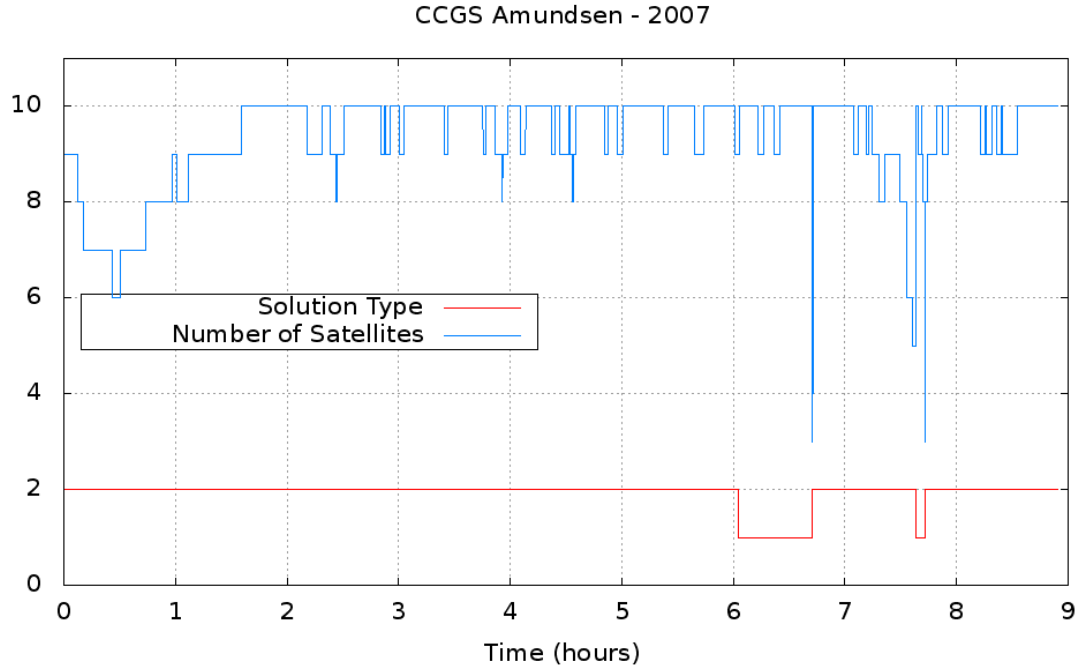


Figure 4.37 – Amundsen 2007 Number of GPS Satellites and Solution Type

The observed height record and the modeled tide from both the Arctic8c model data set and the developed model, as shown in figure 4.38, provide a close match over the first three hours as the vessel is sailing in Eclipse Sound, as shown in figure 4.39. It is over the next hour that the height record shifts downward by approximately 0.75 metres over a period of 1 hour. The average value of the difference is -0.13 metres with a standard deviation of 1.10 metres. The standard deviation is strongly influenced by the large vertical shift at the 6 hour mark in the record. If the standard deviation is calculated up to the 6 hour mark it is reduced to 0.40 metres and if it is calculated to the 3 hour mark it is further reduced to 0.30 metres.

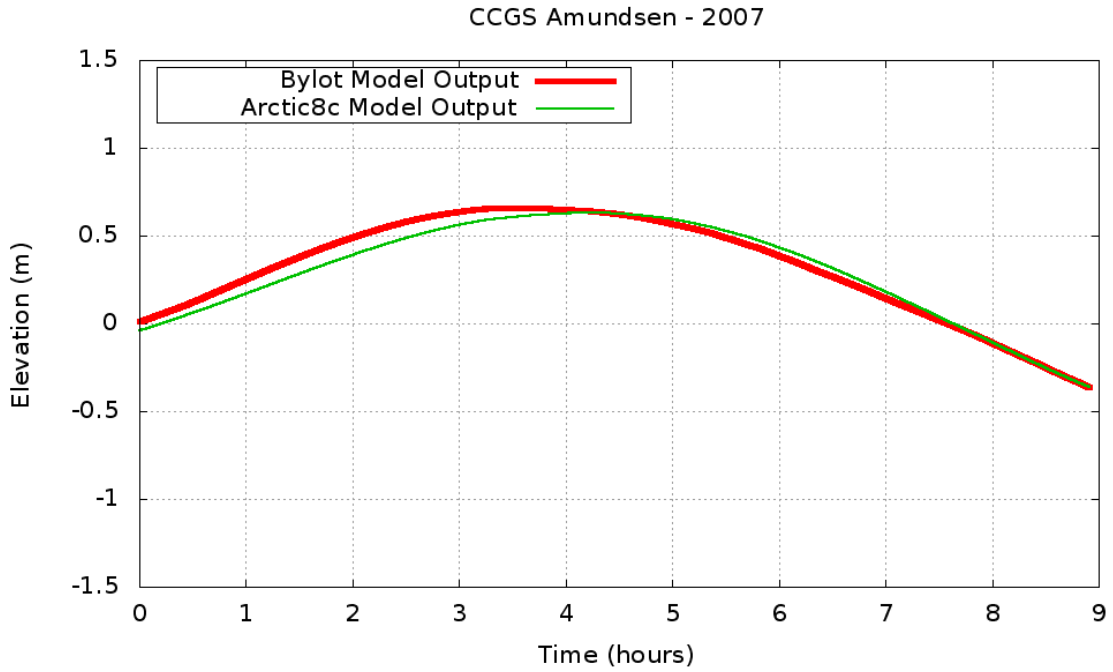


Figure 4.38 – Hydrodynamic Model Output Corresponding to 2007 Ship Track

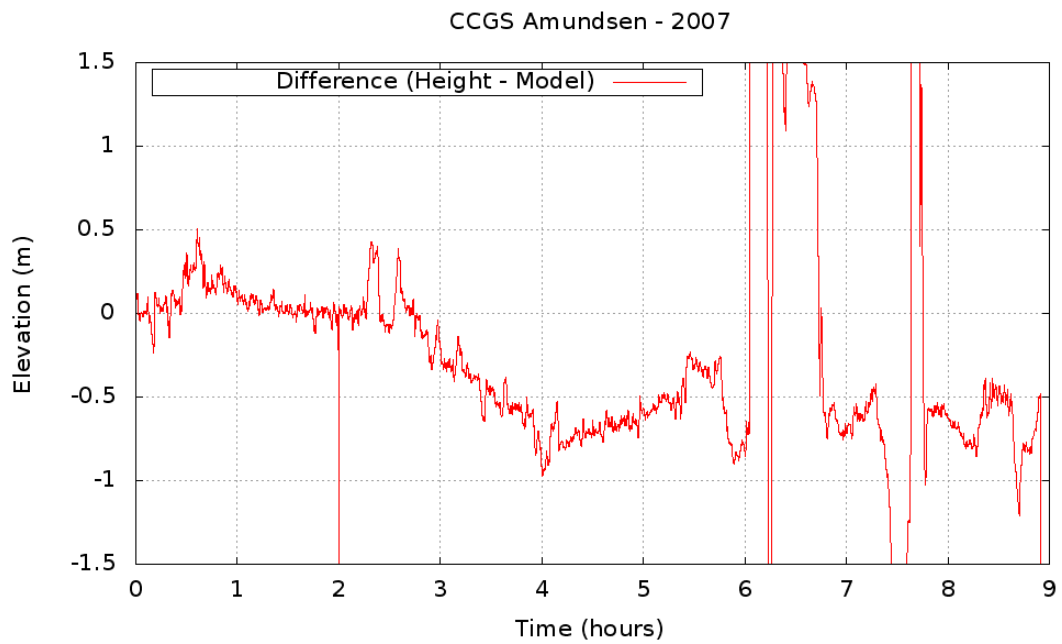


Figure 4.39 – Amundsen 2007 Difference between Corrected Height above Geoid and Model Output

The effects of the changing atmospheric pressure are shown in figure 4.40. The effects over this short of a time span are practically negligible with a maximum variation of 0.005 m.

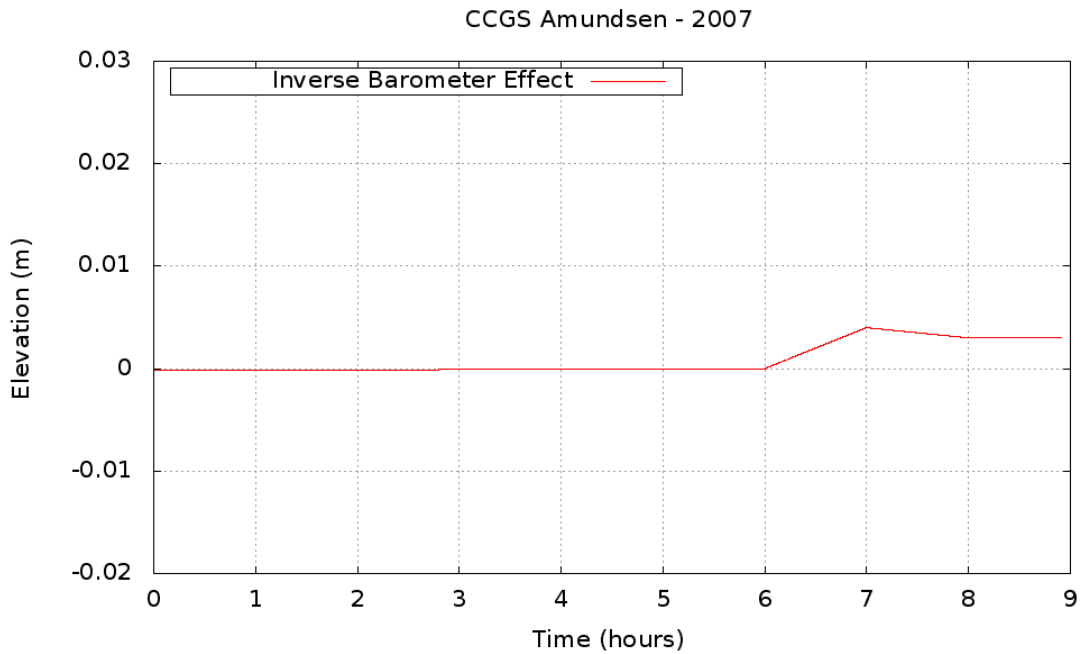


Figure 4.40 – Amundsen 2007 Inverse Barometer Effect

4.2.5 Using CNav to Observe Tides

For each year that the Amundsen has transited through the region described by the domain of the developed hydrodynamic model grid, CNav data has been collected. It is obvious from the analysis in section 4.2 that CNav data alone is insufficient to describe the characteristics of the tides. At times a tidal signature can be distinguished from the record, but there is far too much noise to extract a precise or accurate tidal record. The majority of the noise in the data is caused by the loss of CNav corrections. If a stronger

signal were maintained to prevent the receiver from switching to single point mode then perhaps the quality of the height record could permit extraction of the tides. Other effects are present besides noise in most of the records, such as deviations in the height solution with a higher frequency than the tides or draft changes but with a lower frequency than heave and squat. These anomalies could be related to GPS constellation changes, which occur frequently and rapidly due to the high latitude of the location, unaccounted for atmospheric effects or errors in the geoid ellipsoid separation model.

4.2.6 Apparent Drift within Navy Board Inlet

From examination of the difference figures, from the comparison between the Amundsen height above geoid record and the developed model output, a trend was noted in the Navy Board Inlet section of the domain for the 2004 and 2005 transits. The 2004 transit difference data in Navy Board Inlet is shown in figure 4.41 while the 2005 transit difference data through Navy Board Inlet is shown in figure 4.42. Both figures 4.41 and 4.42 show a downward trend in the data as the latitude increases through the inlet. A trendline can be calculated through each dataset providing the slope of the line. For the 2004 data the slope is -0.562 metres/degree of latitude and the slope for the 2005 data is -0.382 metres/degree of latitude. These drifts in the datasets could indicate that there may be an issue with the geoid ellipsoid separation model not properly resolving the geoid within the area of Navy Board Inlet. Noise in the 2006 and 2007 CNav data, during the Navy Board Inlet transit, did not allow for the calculation of a reasonable trendline through the difference.

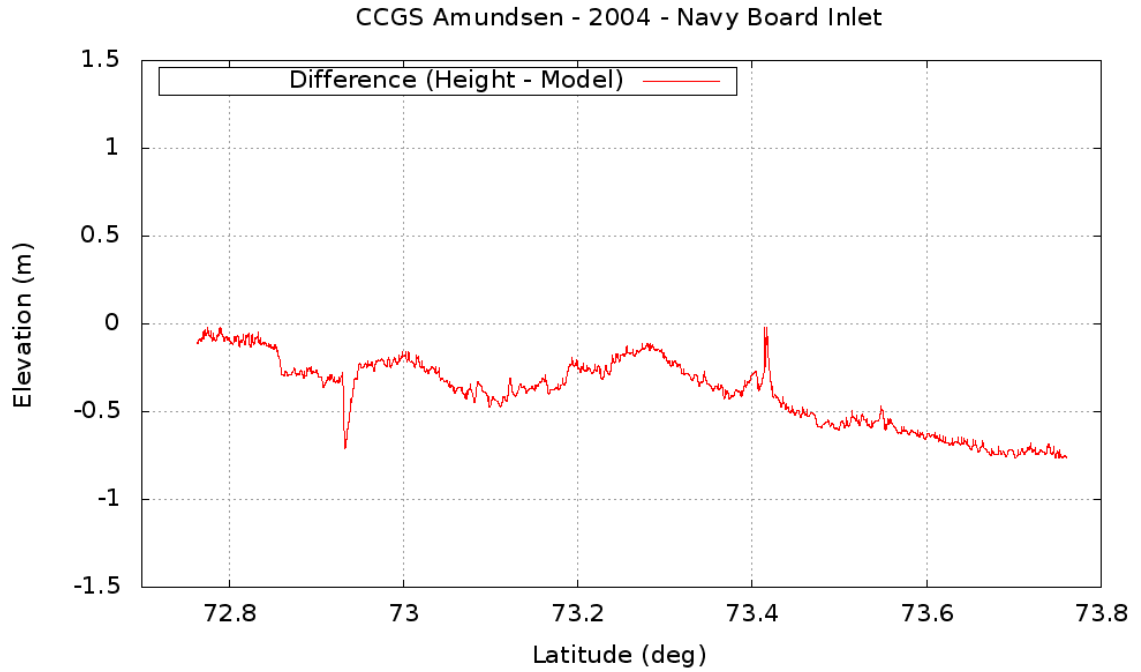


Figure 4.41 – Navy Board Inlet section of the 2004 Amundsen Difference

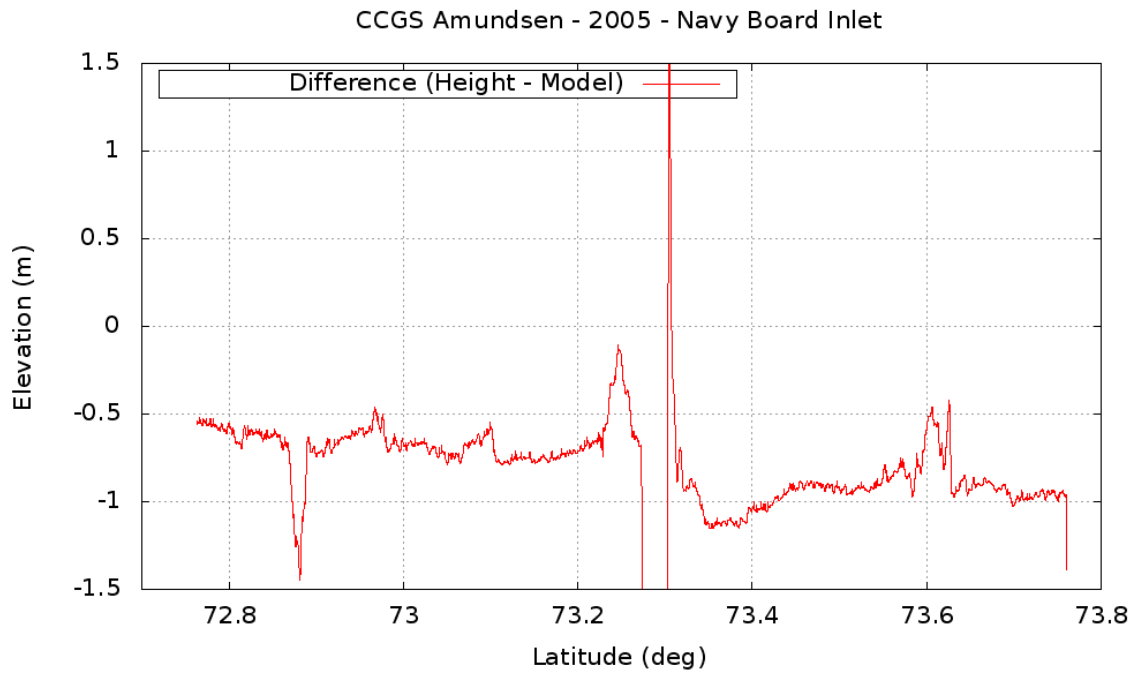


Figure 4.42 – Navy Board Inlet section of the 2005 Amundsen Difference

4.3 Model Results vs. Predicted Tides

As discussed in section 2.1.1, and shown in figure 2.3, there are 3 predicted tide stations that lie within the model domain. The output harmonic constituents from the developed hydrodynamic model grid at the same location as the tide stations can be compared to the predicted harmonics. The accuracy and validity of the predicted tidal harmonics are unknown.

For all three tide stations the original data used in developing the prediction is available online through the Department of Fisheries and Oceans, Marine Environmental Data Service. Using the original data, a new determination of the harmonic constituents can be made using the T_TIDE program. This new determination is compared to the published prediction and the modelled output.

4.3.1 Pisiktarfik Island

At the Pisiktarfik Island tide station the model output was compared to the published predicted harmonic constituents and the output from T_TIDE after reanalysing the original water level record, as shown in figure 4.43. As the original data record at this location was only 15 days long, T_TIDE was unable to determine a value for the N2 amplitude and phase. In figure 4.43 the vertical bars indicates the magnitude of the difference between the three data sources for constituent amplitude and phase. It can be seen that at this station the closest match exists between the T_TIDE output and the

modelled output for amplitude. The output from the model and the published Bluefile provide the closest match for phase.

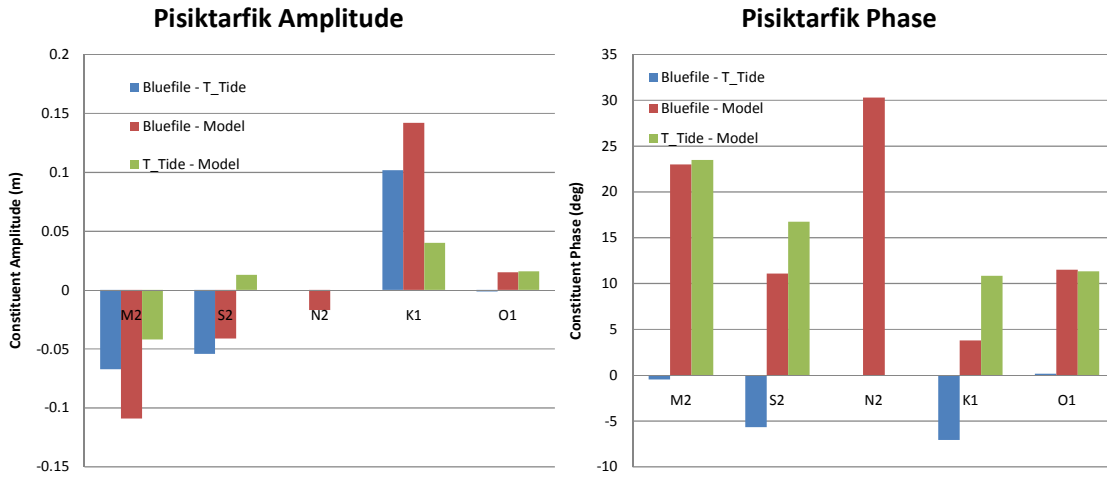


Figure 4.43 – Pisiktarfik Tidal Constituent Comparison

4.3.2 Koluktoo Bay

At Koluktoo Bay the record was long enough to make a comparison with all 5 constituents, including N2, as shown in figure 4.44. The 1964 Koluktoo Bay record was used in the comparison as it was shown to be the most likely to be correct in section 2.1.2. The closest match to the model in this case varied between the T_TIDE output and the Bluefile for amplitude. The closest match was consistently with the Bluefile for phase.

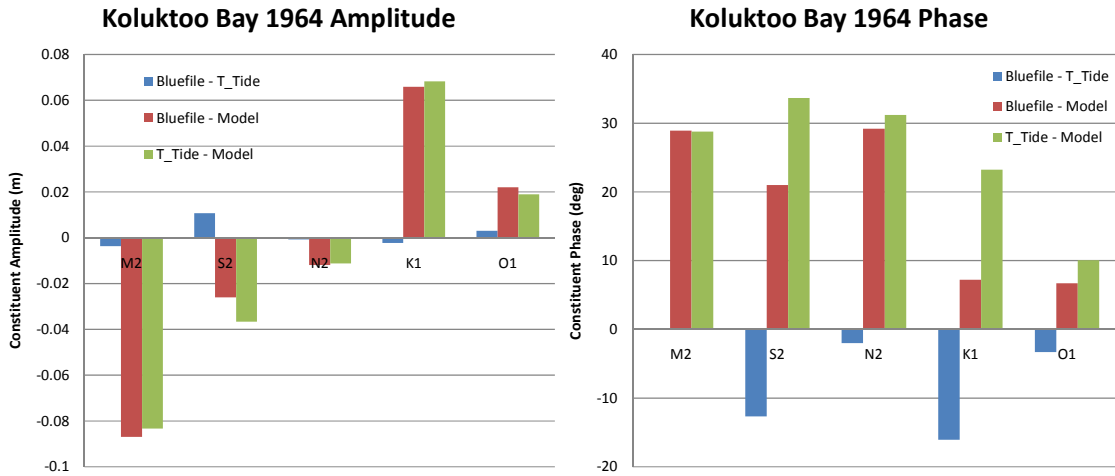


Figure 4.44 – Koluktoo Bay Tidal Constituent Comparison

4.3.3 Milne Inlet

At Milne Inlet the closest match in amplitude varied between the T_TIDE output and the Bluefile, as shown in figure 4.45. The model provided a close match to the predicted amplitude for the M2 constituent with a difference of less than 0.5 cm when compared to both the Bluefile and T_TIDE output. The predicted phase from the Bluefile consistently provided a closer match to the model output than the T_TIDE output.

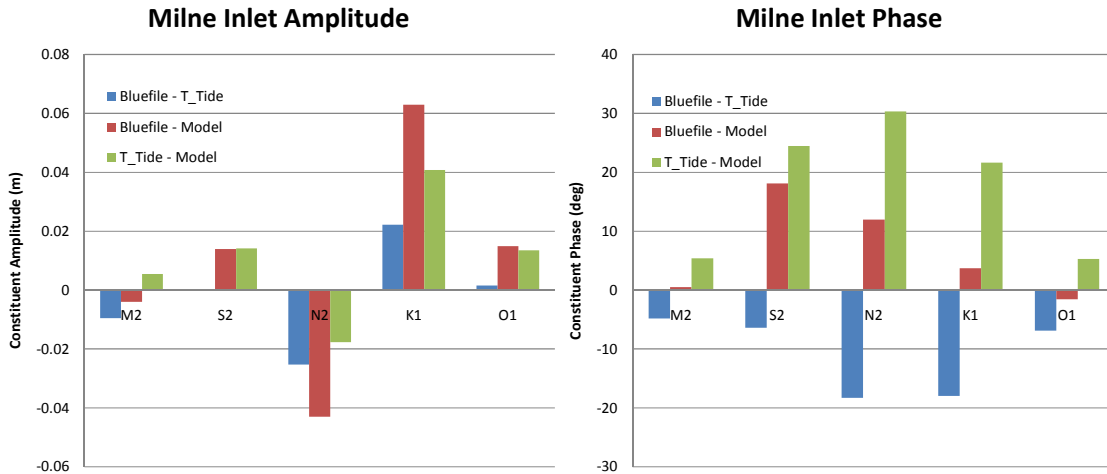


Figure 4.45 – Milne Inlet Tidal Constituent Comparison

4.4 Misfit Analysis

A misfit analysis can be performed that combines the constituent phase and amplitude into a single value [Dunphy et al., 2005]. The equation used for this determination is shown in table 4.2 and illustrated in figure 4.46. The equation examines the constituent amplitude and phase as if they were in the complex plane and combines the imaginary and real parts of the number into a single value which equates to the modulus of the difference between the two complex numbers. Combining the amplitude and phase into a single value allows for comparisons to be made which evaluate how well the constituent was modeled [Dunphy et al., 2005].

Misfit Analysis Equation which Accounts for Amplitude and Phase	$Error = A_o e^{\phi_o} - A_m e^{\phi_m} $	A_o = Observed Amplitude A_m = Modelled Amplitude ϕ_o = Observed Phase ϕ_m = Modelled Phase
---	---	--

Table 4.2 – Misfit Calculation

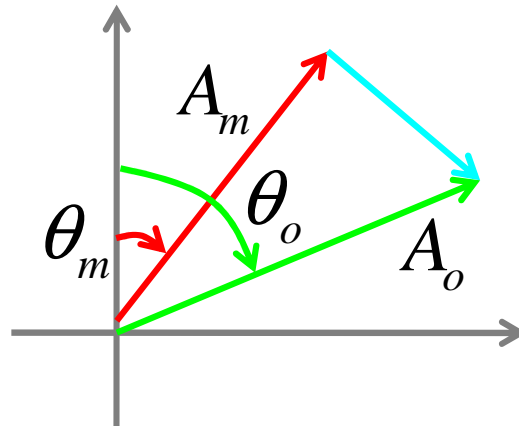


Figure 4.46 – Misfit Calculation

4.4.1 Predicted Tides

Figures 4.47 through 4.49 show the calculated differences associated with each constituent, for the three comparisons at the three tide stations. As there is no true value for the harmonic constituents at the predicted tide stations, the model is compared to both the Bluefile and the output from T_TIDE. A comparison of T_TIDE and the Bluefile determinations is also included.

From figure 4.47, at Pisiktarfik Island the lowest overall misfit was observed when comparing either the Bluefile or T_TIDE and the developed model for the O1 constituent. The largest overall misfit is from comparing the developed model output to either the

Bluefile or T_TIDE for the M2 constituent, where a misfit of 27 cm appears. Determining the second most significant misfit depends on whether the model is compared to the Bluefile or T_TIDE. For the Bluefile comparison, the second largest result comes from the K1 constituent followed by the N2 and S2 constituents. For the T_Tide comparison, the second largest result comes from the S2 constituent followed by the K1 constituent. The water level record at Pisiktarfik was not long enough to determine the amplitude and phase of the N2 constituent in T_TIDE, therefore it was omitted from the analysis. Overall the T_TIDE determination provides a lower misfit when compared to the model output.

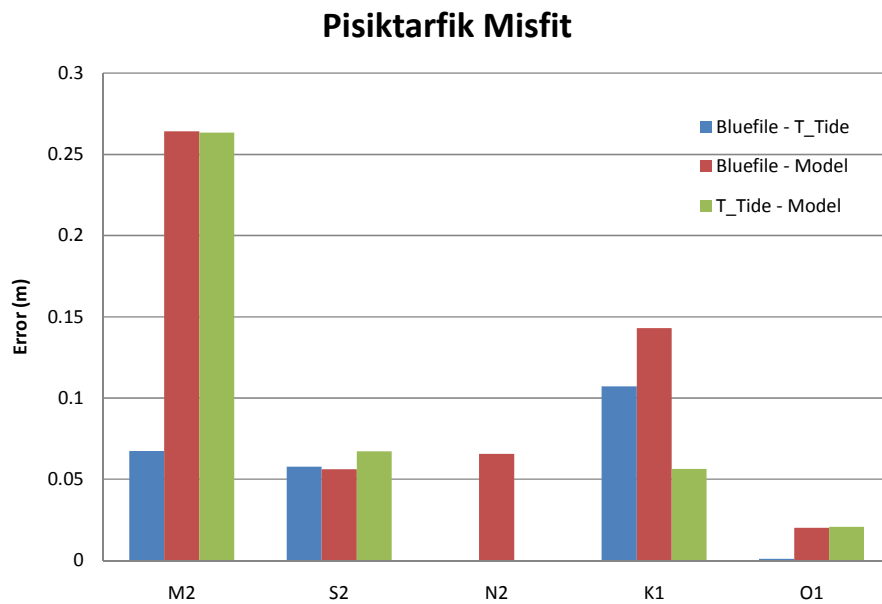


Figure 4.47 – Pisiktarfik Misfit Analysis

At the Koluktoo Bay station, the tidal data from 1964 was analysed using T_TIDE. From figure 4.48, the Bluefile generally provided a closer match to the modelled data in

1964 than the T_TIDE output, although the T_TIDE output and the Bluefile provide a close match when compared together. The largest discrepancy between the model and either the Bluefile or T_TIDE constituents is still with the M2 constituent, at over 30 cm, and the lowest with the O1 consistent.

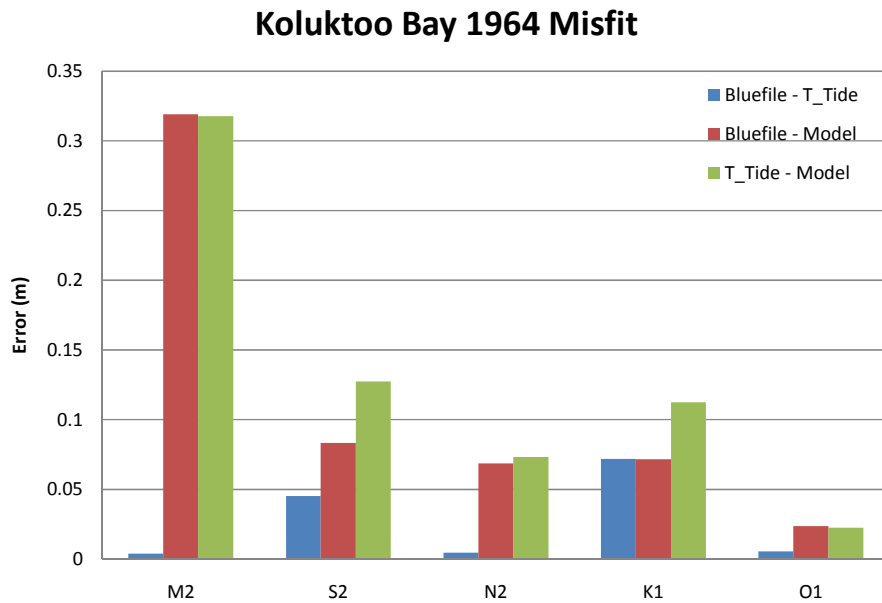


Figure 4.48 – Koluktoo Bay 1964 Misfit Analysis

At the Milne Inlet station, figure 4.49 displays a vastly different trend than the Pisiktarfik and Koluktoo Bay stations. The largest misfit in this case comes from comparing the S2 constituent derived from the model to either the Bluefile or T_TIDE output, although it is less than 10 cm. For the developed model and Bluefile comparison the second largest misfit comes from the K1 constituent followed by the N2 and O1 constituents with the smallest misfit occurring with the M2 constituent. For the developed

model and T_TIDE comparison the second largest misfit also comes from the K1 constituent but is then followed by the M2, N2 and O1 constituents.

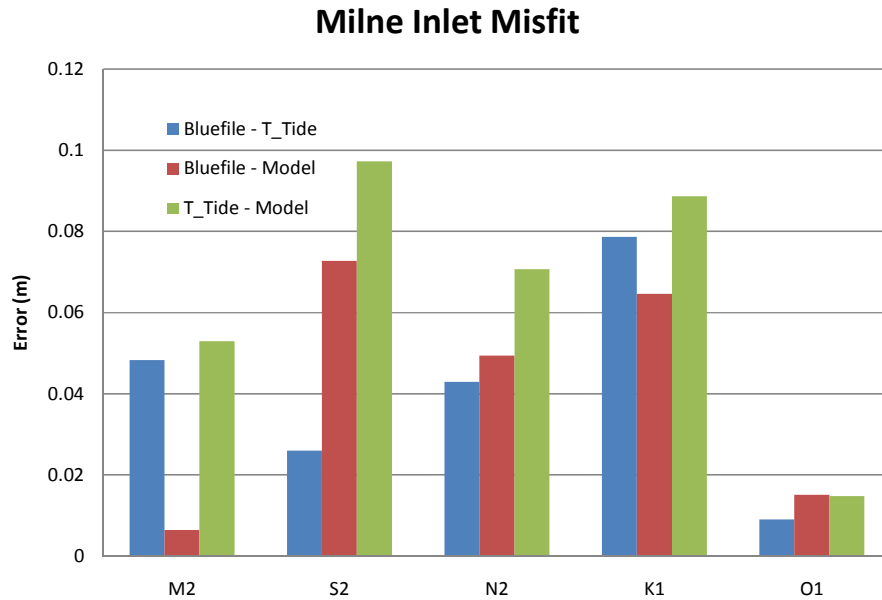


Figure 4.49 – Milne Inlet Misfit Analysis

4.4.2 Arctic8c Model

The misfit of the Arctic8c model and the developed Bylot grid was calculated over the common domain of the two grids. Figures 4.50 through 4.54 show the misfit for each of the five modelled constituents.

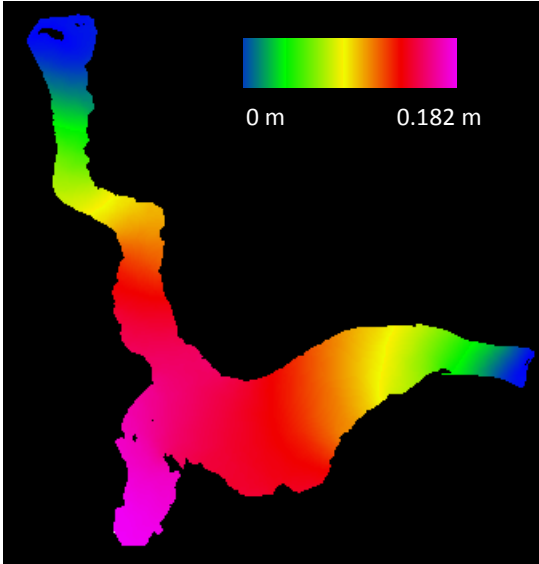


Figure 4.50 – M2 Component of Misfit between Arctic8c Model and Bylot Model

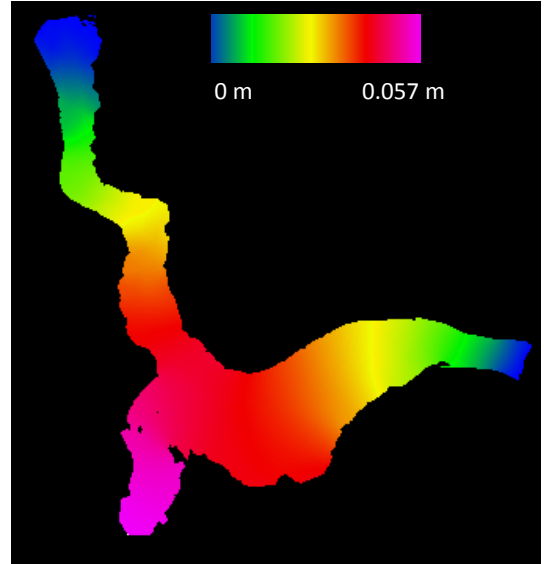


Figure 4.51 – N2 Component of Misfit between Arctic8c Model and Bylot Model

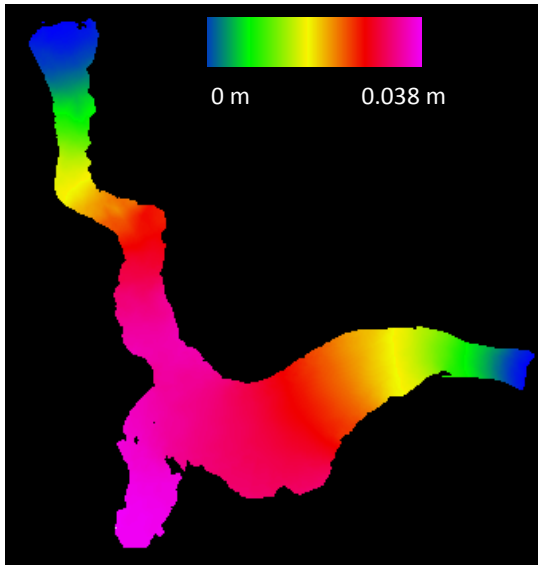


Figure 4.52 – S2 Component of Misfit between Arctic8c Model and Bylot Model

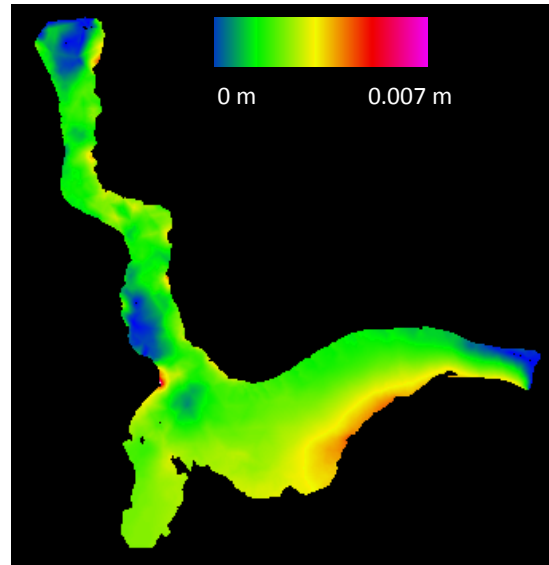


Figure 4.53 – K1 Component of Misfit between Arctic8c Model and Bylot Model

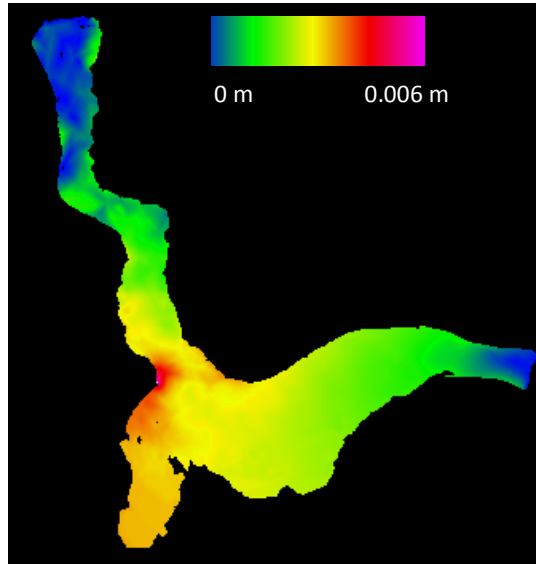


Figure 4.54 – O1 Component of Misfit between Arctic8c Model and Bylot Model

From figures 4.50 through 4.5, the maximum misfit exists with the M2 constituent at a magnitude of 18.2 cm near the entrance to Milne Inlet. The second largest misfit is with the N2 constituent at 5.7 cm, while third is S2 with 3.8 cm. The diurnal constituents of K1 and O1 show negligible misfits of less than 1 cm.

4.5 Model Applied to Multibeam

The modelled predicted tides can be applied to overlapping multibeam data lines to determine if any improvement has been made to the vertical separation between them. Multibeam data from the 2006 surveys by the Amundsen and the Heron in Oliver Sound have been used in the analysis. In each case a small area over which two lines overlapped was chosen and the average difference in that area was calculated. The average

differences were calculated before and after predicted tides from the developed model were applied for the five constituents of M2, S2, N2, K1 and O1.

4.5.1 Amundsen EM300 Data

The Amundsen multibeam data was divided into 5 areas, as shown in figure 4.55, for comparison. The comparison results are shown in table 4.3.

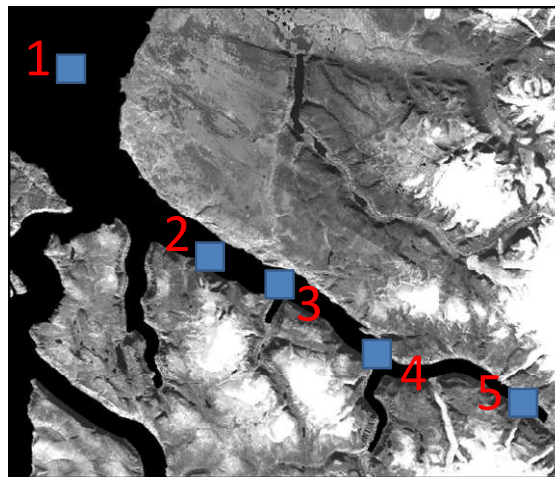


Figure 4.55 – Amundsen Multibeam Comparison Locations

Area	Date – Line 1	Date – Line 2	Average Difference without Tides (m)	Average Difference after Tides Applied (m)	RMS Difference without Tides (m)	RMS Difference after Tides Applied (m)	Improvement?
1	Sept 4 th , 2006 02:00:11	Sept 5 th , 2006 20:57:52	1.0062	-0.0057	1.2080	0.6682	Yes
2	Sept 4 th , 2006 03:23:51	Sept 4 th , 2006 17:42:20	0.2685	-0.2804	1.0578	1.0607	No
3	Sept 4 th , 2006 18:06:00	Sept 5 th , 2006 03:04:13	1.3583	0.3960	1.8304	1.2892	Yes
4	Sept 4 th , 2006 04:17:01	Sept 4 th , 2006 21:23:50	0.1803	0.0837	1.1406	1.1293	Yes
5	Sept 4 th , 2006 05:05:31	Sept 4 th , 2006 11:36:49	0.1004	0.3541	0.5937	0.6839	No

Table 4.3 – Amundsen Multibeam Comparison Results

As can be observed in table 4.3, for 3 out of 5 comparisons applying the modelled predicted tides provided a significant improvement in relating the data from overlapping lines. Area 5, located at the head of Oliver Sound, did not improve with application of the tides. This could indicate that the model does not correctly model the head of the fjord or the comparison values maybe pushing the capabilities of the accuracy of the EM300 multibeam system in shallow depths.

A comparison between two lines of data from the Amundsen EM300 is limited by system range resolution and external errors which propagate into a final sounding

solution. The manufacturer states an accuracy of 0.2% of water depth RMS for the system, which in these water depths approaches the offset between the lines [Kongsberg Maritime, 2003]. The depth of each comparison location and the associated 0.2% RMS value is listed in table 4.4.

Location	Depth (m)	0.02% (m)
1	200	0.40
2	275	0.55
3	300	0.60
4	300	0.60
5	115	0.23

Table 4.4 – 0.2% Water Depth Accuracy for the Five Comparison Locations

4.5.2 Heron EM3002 data

The Heron worked mainly at the head of the Oliver Sound fjord but for less time than the Amundsen, therefore finding overlapping data that was more than a few hours different in time was difficult. The two locations chosen for the Heron multibeam data comparison are shown in figure 4.56. The comparison results are shown in table 4.5.



Figure 4.56 – Heron Multibeam Comparison Locations

Area	Date – Line 1	Date – Line 2	Average Difference without Tides (m)	Average Difference after Tides Applied (m)	RMS Difference without Tides (m)	RMS Difference after Tides Applied (m)	Improvement?
1	Sept 5 th , 2006 01:34:01	Sept 5 th , 2006 05:15:28	0.6070	-0.2145	0.6364	0.2875	Yes
2	Sept 4 th , 2006 11:32:17	Sept 5 th , 2006 04:23:36	-0.8743	-0.6476	0.9094	0.6936	Yes

Table 4.5 – Heron Multibeam Comparison Results.

Both locations from the Heron comparison showed improvements after the application of the modelled predicted tides. The manufacturer states a depth resolution of the EM3002 system at 1cm, which is significantly less than the differences observed between the overlapping lines [Kongsberg Maritime, 2004]. The other issues which could contribute to sounding uncertainty are sound speed errors and long period heave. A large number of sound speed profiles were collected during the Heron survey and errors related

to using incorrect sound speed profiles will be significantly less than the offset between the overlapping lines [Beaudoin, 2008].

The long period heave is an artefact of the Heron's F180 motion sensor and can introduce errors in the depth determination of the EM3002. The artefact can be in the order of 20 cm or more and could influence the calculated difference between two overlapping multibeam lines. Figure 4.56 displays an example of the motion record from a line of EM3002 data and shows the heave in the first row, the long period low pass filtered heave in the next, followed by the high pass filtered actual heave and finally the speed of the vessel. The horizontal scale in figure 4.57 is time and minute intervals are represented by the bold vertical bars.

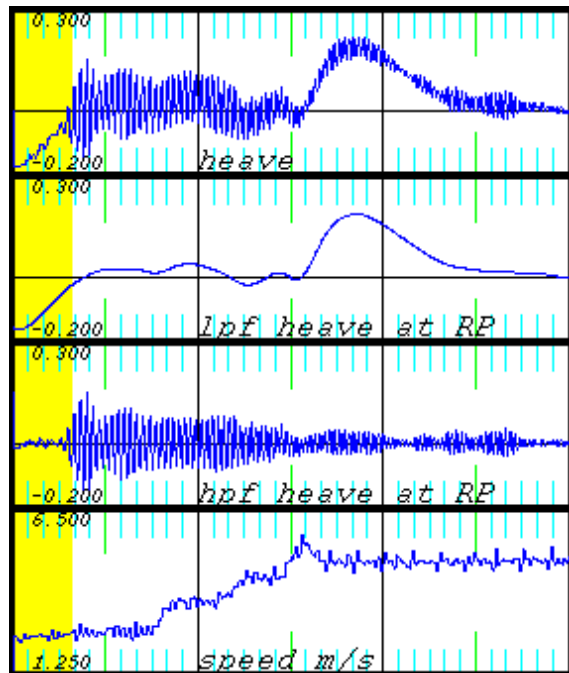


Figure 4.57 – Three Minutes of Raw Heave Data, Long Period Heave, Actual Heave and Speed from the Heron

CHAPTER 5. RECOMMENDATIONS

A number of steps should be taken in the future to further the understanding of the accuracy of the developed hydrodynamic model for the Pond Inlet, Eclipse Sound and Navy Board Inlet regions. Further checks of the model against actual observations and repeatability test will help prove the viability of using hydrodynamic models as a source of tidal information.

In the late summer and early fall of 2008, the Canadian Coast Guard Ship “Henry Larsen” will be transiting through and working in the modelled area on the Northern tip of Baffin Island. The Heron will be onboard the Larsen and will be deployed to collect multibeam data within Oliver Sound, as it did in 2006. During the Larsen transits and the multibeam surveys the Heron will be collecting raw CNav observations. This additional source of CNav data will allow for the benefits of post-processing to be examined and will allow for more testing of the CNav solution versus the modelled tides. A PPK base station will also be set up in the area which should give both a precise vertical solution for tidal analysis and control for CNav comparison. The possibility of setting up pseudolites at control points along the shore of the fjord to minimize the positional uncertainty could also be examined in the future, as could the deployment of GPS buoys throughout the area to determine the Geoid-Ellipsoid separation within the region.

The multibeam data from the Heron will also provide more options for overlapping lines to compare the advantages of applying the modelled predicted tides. Cross lines will be run over new data collected in 2008 and over data collected in 2006.

Tide gauges should be installed within the model domain to check the model output. The existing tide gauge data is from the mid 60's and new data would allow for improved comparisons. A distribution of gauges throughout the area and up into the adjacent fjords, such as Oliver Sound, will allow for an improved understanding towards the effects of the fjords on the amplification and propagation of the tides. Installing tide gauges may be part of the 2008 Larsen program.

Once additional physical data is collected for comparison to the model, the parameter values used to construct the model could be improved. Realistic conditions could be introduced to the modelled simulation such as ice friction, varying bottom frictions, and wind and river inputs. The model could also be run in spherical coordinates instead of Cartesian to observe any changes in the effects of changing the effects of coriolis over the model domain.

CHAPTER 6. CONCLUSIONS

A hydrodynamic model grid and simulation covering the area of a long term monitoring project on the northern tip of Baffin Island, Canada, has been developed. The model simulation will aid in measuring decimetre level changes in the seabed morphology over time through prediction of the amplitude and phase of the five major tidal harmonic constituents within the area. The model accounts for the modification of the tidal wave by the fjords, inlets, islands and sills in the area and is applicable anywhere within the enclosed waters of Bylot Island.

The absolute accuracy of the modelled tidal constituents is still unknown. Comparisons have been made in chapter 4 which give an indication of the uncertainties to expect in the model, but in all cases the subject matter being compared is flawed in some sense. The Arctic8c grid of Dunphy et al. [2005] is coarse and uses low resolution bathymetry within the modelled region, the CNav GPS data is noisy and exhibits unusual drifting trends and jumps in the height records, the predicted tides were all developed from short records in the 1960's when recording methods were more prone to errors, and the multibeam data has physical system limitations which limit its accuracy.

The CNav GPS data that is collected on board the Amundsen and Heron while working and transiting through the model domain is a useful tool in helping to determine the proper phasing of high and low water, but is still plagued with noise and reliability

issues. As future data collection volumes increase the benefits of post processing will become more apparent and new methods of improving the accuracy of the system will undoubtedly increase the usability of the vertical component of the data. In this study the CNav data that was collected in open water provided a much smoother and less noisy solution, such as in the 2007 CNav height record.

The comparison of overlapping multibeam lines is limited by the uncertainty in the sounding position from factors such as range resolution, horizontal positioning uncertainty, long period heave and draft changes. If there was a change in the vessel draft between when the two overlapping lines, that unknown difference in draft would propagate into the vertical difference between the two lines and would affect the comparison. Any long period heave that was not accounted for in the heave sensor would also propagate as an error into the difference between two overlapping lines in the same fashion as the draft error. Horizontal positioning uncertainty would have the affect of shifting the same sounding along a horizontal plane in some direction. This is of particular concern when working along steep slopes, such as the edge of a fjord, and when horizontal positioning uncertainties are large, such as when CNav corrections are lost.

While the model simulation was developed to provide tidal amplitude for hydrographic surveys, it could also be used for other purposes within the area. One example is monitoring the feeding patterns of Narwhals. It has been shown that Narwhals swim within the Milne Inlet area with the tidal currents; therefore an improved

understanding of the tidal currents could lead to an improved understanding of the Narwhal and their feeding behaviour [Marianne et al., 2006]. The model simulation outputs tidal currents at every node within the model domain.

The procedure of developing a hydrodynamic model grid and running a simulation to obtain predicted tides should be studied and compared to recent water level records throughout the modelled area before it becomes a regular component of Arctic data processing. Initial results look promising and in many complex coastal regions a nested hydrodynamic model grid would likely produce better results than the presently available data. If the developed model is assumed to be correct, from section 4.1.1, the error resulting from using just the output of the Arctic8c grid at the head of the Oliver Sound fjord could result in an error of 25 cm. In shallow coastal waters, the IHO S44 special order depth accuracy constraint is just over 25cm; therefore the error budget is almost used entirely by the influence of tidal errors [IHO, 1998]. The development of a hydrodynamic model simulation should improve the ability to detect changes in the seabed morphology through comparison of overlapping multibeam data for long term monitoring projects in remote areas where tidal control is limited.

BIBLIOGRAPHY

- Bartlett, J., J. Beaudoin, and J. E. Hughes Clarke (2004). "CCGS Amundsen: A New Mapping Platform for Canada's North." Lighthouse, Journal of the Canadian Hydrographic Association, (No. 65),.
- Beaudoin, J. (2008). Research Assistant & System Manager, Fredericton, New Brunswick, Canada.
- Beaudoin, J., J. E. Hughes Clarke, J. Bartlett, S. Blasco, and R. Bennett (2008). " Mapping Canada's Arctic Seabed: Collaborative Survey Processing and Distribution Strategies." Proceedings of Canadian Hydrographic Conference and National Surveyors Conference, Victoria, BC, May.
- C & C Technologies (2008). "C-Nav GPS: Confidence Through Diversity." C & C Technologies, Lafayette, LA, USA
- Cannon, E., G. Lachapelle, M. Vinnins, S. Dosso, and G. Heard (2003). "High Latitude Attitude." GPS World, (October).
- Chaffey, J. D., and Greenberg, D. A. (2003). "resolute: A Semi-Automated Finite Element Mesh Generation Routine." Rep. No. 225 Canadian Technical Report of Hydrography and Ocean Sciences, Ocean Sciences Division, Bedford Institute of Oceanography, Department of Fisheries and Oceans, Dartmouth, Nova Scotia, Canada.
- Department of Oceanography (2003). "Numerical Ocean Modeling." Navy Operational Ocean Circulation and Tide Models. [On-line] February 16, 2007.
<http://ioc.unesco.org/oceanteacher/OceanTeacher2/other/NOMModeling/modeling/index.html> .
- Doodson, A. T. (1921). "The Harmonic Development of the Tide-Generating Potential." Proceedings of the Royal Society of London. Series A, Containing Papers of a Mathematical and Physical Character, 100(704), pp. 305-329.
- Dunphy, M., Dupont, F., Hannah, C. G., and Greenberg, D. (2005). "Validation of a Modeling System for Tides in the Canadian Arctic Archipelago." Rep. No. XXX Canadian Technical Report of Hydrography and Ocean Sciences, Ocean Sciences Division, Bedford Institute of Oceanography, Department of Fisheries and Oceans, Dartmouth, Nova Scotia, Canada.
- Earth Sciences Sector, NRCan (2006). "GeoGratis Datasets Search." Natural Resources Canada. [On-line] August 10, 2006.
<http://geogratings.cgdi.gc.ca/geogratings/en/product/search.do?locate=true> .

- Foreman, M. G. G. (2006). "Ocean Sciences Research activities IOS Tidal Package." [On-line] 9/9, 2008. http://www.pac.dfo-mpo.gc.ca/sci/osap/projects/tidpack/tidpack_e.htm .
- Forrester, W. D. (1983). Canadian Tidal Manual. Department of Fisheries and Oceans. Canadian Hydrographic Service, Ottawa, Ontario.
- Funnell, W. R. J. (2005). "Finite-element method." Dept. BioMedical Engineering, McGill University. [On-line] 3/8/2008, 2008. <http://audilab.bmed.mcgill.ca/AudiLab/teach/fem/fem.html> .
- Geodetic Survey Division, NRCan (2004). "The GPS-H v2.01." Natural Resources Canada. [On-line] March 5, 2007. http://www.geod.nrcan.gc.ca/software/gpsht_e.php .
- Gill, A. E. (1982). Atmosphere - Ocean Dynamics. Vol.30, 1st ed., Academic Press, New York.
- Global Offshore Consulting (2006). "CNav 2050." [On-line] 8/13, 2008. <http://www.goc.no/default2.aspx> .
- Godin, G. (1972). The Analysis of Tides. University of Toronto Press, Toronto.
- Great Britain Hydrographic Office (1969). "Tides and Tidal Streams." Chapter Two in Admiralty Manual of Hydrographic Surveying, 118pp.Somerset, England.
- Howard, H. (2005). "Effects of a Polar Orbital Plane on High-Latitude GPS Positioning." Colorado Center for Astrodynamics Research. [On-line] 9/23, 2008. <http://ccar.colorado.edu/~nerem/zipfiles/howard/> .
- Hughes Clarke, J. E., P. Dare, J. Beaudoin, and J. Bartlett (2005). "A stable vertical reference for bathymetric surveying and tidal analysis in the high Arctic." Proceedings of U.S. Hydrographic Conference, San Diego, California, March 2005. pp. 1.
- IHO. (1998). "IHO Standard for Hydrographic Survey." Special publication No. 44, 4th edition, International Hydrographic Organization.
- Ip, J., and Lynch, D. (1995). "Comprehensive Coastal Circulation Simulation using Finite Elements: Nonlinear Prognostic Time-Stepping Model, QUODDY3 User's Manual." Rep. No. NML95-1, Thayer School of Engineering, Dartmouth College, Hanover, New Hampshire, U.S.A.
- Jones, J. E., and A. M. Davies (2007). "A high-resolution finite element model of the M2, M4 M6, S2, N2, K1 and O1 tides off the west coast of Britain." Ocean Modelling, 19(1-2), pp. 70-100.

- Kongsberg Maritime (2004). "EM3002 Multibeam echo sounder." Horten, Norway.
- Kongsberg Maritime (2003). "EM300 30 kHz multibeam echo sounder." Horten, Norway.
- Kwong, S. C. M., A. M. Davies, and R. A. Flather (1997). "A three-dimensional model of the principal tides on the European shelf." *Progress in Oceanography*, 39(3), pp. 205-262.
- Leandro, R. F., and M. C. Santos (2006). "Wide area based precise point positioning." *Proceedings of Institute of Navigation - 19th International Technical Meeting of the Satellite Division, ION GNSS 2006, Sep 26-29 2006*. Institute of Navigation, Fairfax, VA 22030, United States, Fort Worth, TX, United States, pp. 2272-2278.
- Leffler, L. E., and D. A. Jay (Submitted). "Enhancing tidal harmonic analysis: Robust (hybrid L1/L2) solutions." *Continental Shelf Research*.
- Legrand, S., E. Deleersnijder, E. Hanert, V. Legat, and E. Wolanski (2006). "High-resolution, unstructured meshes for hydrodynamic models of the Great Barrier Reef, Australia." *Estuarine, Coastal and Shelf Science*, 68(1-2), pp. 36-46.
- Leva, J. L. (1994). "Relationship between navigation vertical error, VDOP, and pseudo-range error in GPS." *IEEE Transactions on Aerospace and Electronic Systems*, 30(4), pp. 1138-1142.
- Li, L., J. C. Zuo, and P. L. Li (2003). "Tidal Simulation in the East China Sea with Finite Element Method." *Proceedings of Proceedings of the Thirteenth (2003) International Offshore and Polar Engineering Conference, May 25 2002-May 30 2003*. International Society of Offshore and Polar Engineers, Honolulu, HI, United States, pp. 2147-2153.
- Lynch, D. R., J. T. C. Ip, C. E. Naimie, and F. E. Werner (1996). "Comprehensive coastal circulation model with application to the Gulf of Maine." *Continental Shelf Research*, 16(7), pp. 875-906.
- Marianne, M., M. Auger-Méthé, and M. Humphries (2006). "Tidal influences on narwhal movements and pod size." *Proceedings of ArcticNet ASM, Victoria, BC, December*.
- Naimie, C. E. (1996). "Georges Bank residual circulation during weak and strong stratification periods: prognostic numerical model results." *Journal of Geophysical Research*, 101 pp. 6469-86.

- Nave, C. R. (2006). "Standing Waves." Department of Physics and Astronomy, Georgia State University. Atlanta, Georgia. [On-line] 8/11, 2008. <http://hyperphysics.phy-astr.gsu.edu/Hbase/waves/standw.html> .
- Ocean Processes Numerical Modeling Laboratory (2005). "OPNML User's Guide" University of North Carolina at Chapel Hill, Department of Marine Sciences. Chapel Hill, North Carolina, U.S.A. [On-line] December 5, 2006. http://www.opnml.unc.edu/OPNML_USERS_GUIDE/OUG_driver.html.
- Pawlowicz, R. (2007). "Rich Pawlowicz's Matlab Stuff." [On-line] 5/27, 2008. http://www.eos.ubc.ca/~rich/#T_Tide .
- Pawlowicz, R., B. Beardsley, and S. Lentz (2002). "Classical tidal harmonic analysis including error estimates in MATLAB using T_TIDE." *Computers & Geosciences*, 28 pp. 929.
- Roscoe Hudson, J., and T. Sharp (2001). "Globally Corrected GPS (GcGPS): C-Nav GPS System." Proceedings of Dynamic Positioning Conference, Houston, Texas, U.S.A., 2001.
- Simons, T. J. (1980). "Circulation models of lakes and inland seas." Rep. No. 203, Canadian Bulletin of Fisheries and Aquatic Sciences, Ottawa.
- Stewart, R. H. (2005). "Introduction to Physical Oceanography." Department of Oceanography, Texas A&M University. College Station, Texas. [On-line] 05/22, 2008. http://oceanworld.tamu.edu/resources/ocng_textbook/contents.html .
- The NOM Group (2003). "OC2910 - Numerical Ocean Modeling Concepts." [On-line] 5/2008, 2008. <http://iodeweb5.vliz.be/oceanteacher/resources/other/NOMModeling/modeling/index.html>.
- Turnbull, I. D. (2006). "Impact of the Inverse Barometer Effect on Iceberg Drift in the Ross Sea Region, Antarctica." Proceedings of AGU Fall Meeting, San Francisco, CA, USA, 11/12/2006.
- Wert, T., P. Dare, and J. E. Hughes Clarke (2004). "Toward Real-Time Tides from C-Nav GPS in the Canadian Arctic." Proceedings of ION GNSS, Long Beach, California, U.S.A., 2004.
- Wendt, J. F. (1992). "Computational Fluid Dynamics, An Introduction." pp. 287. Springer-Verlag, Berlin.
- Wunsch, C., and D. Stammer (1997). "Atmospheric loading and the oceanic "inverted barometer" effect." *Reviews of Geophysics*, 35(1), pp. 79-107.

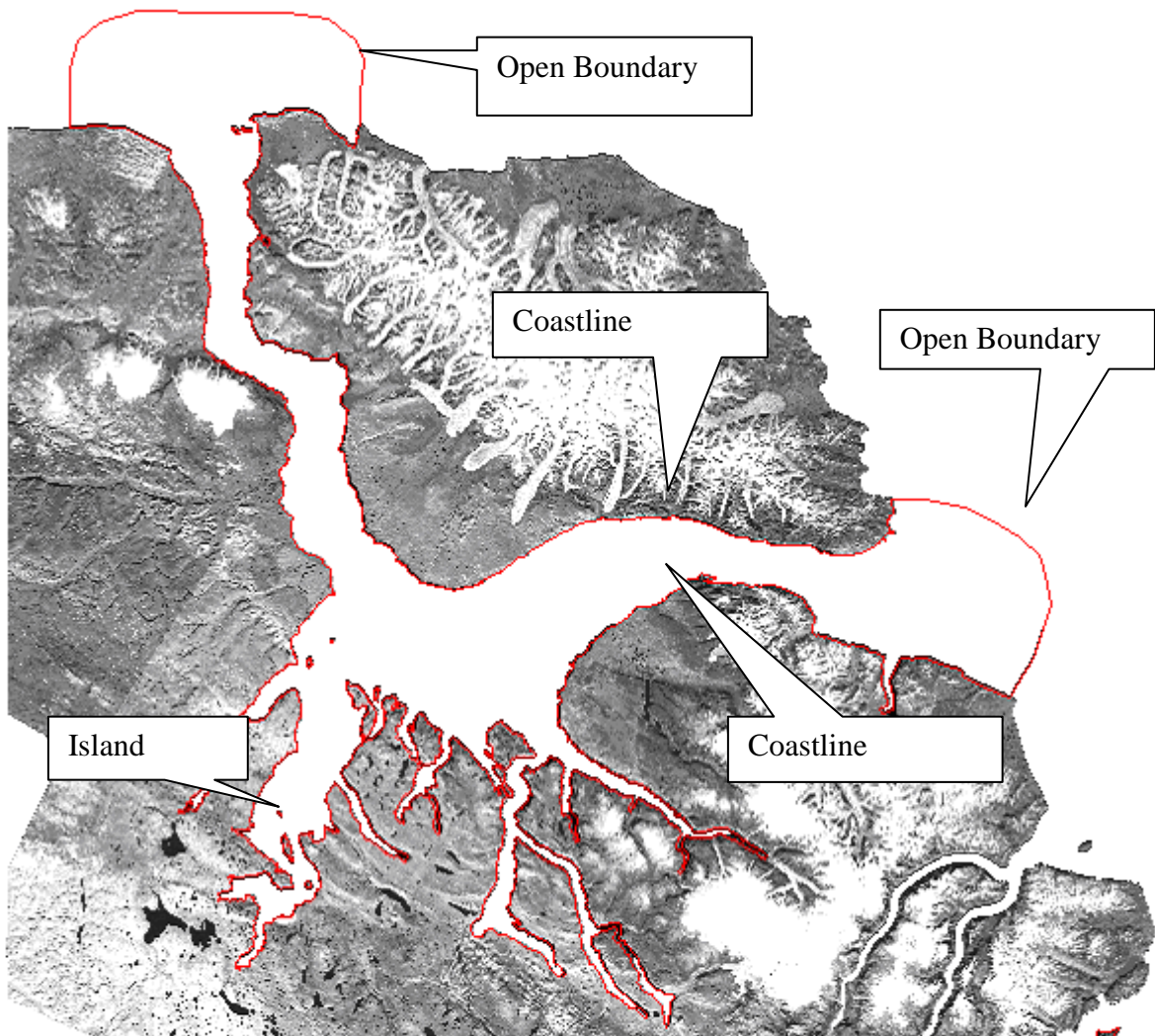
APPENDIX A

Steps Taken in Creating a Quoddy Hydrodynamic Model

1. The first step in creating a Quoddy Hydrodynamic Model is to create a TIN (Triangulated Irregular Network) to input to Quoddy. This can be done using a number of programs that take depth nodes and a boundary file as input. The program examined here is one called [Resolute](#) [Chaffey and Greenberg, 2003]. It can be run on Linux by downloading and installing the [resolute 1.3.tar.gz \(6.0MB\)](#) file from the DFO webpage. The best way to get started with resolute is to read the [pdf manual](#). It provides easy to follow instructions on installation and use of the program.
2. Resolute takes two files as input, a boundary file and a depth file. Both files are simple ascii data files and the format is laid out in the resolute manual. The depth file will have the extension .dat and is in the format Longitude, Latitude, Depth where depth is positive down. The boundary file will have the extension .nod and be of the Trigrid format (see section 5.8, page 18, of the resolute manual).
3. The depth file can be created using OMG (Ocean Mapping Group) software by generating a floating point (r4) grid of the area of interest, using the resolution that you want to use in your model. A reminder of how to create grids and other useful information can be found within the [processing manuals](#) on Jonathan Beaudoin's website. Once an r4 grid is created, it can be converted to an ascii file of depth points in the format Long, Lat, Depth using the OMG program *r4toASCII*.

```
r4toASCII -lola floatfile.r4 asciifile.dat
```

4. The boundary file can be created by digitizing the coastlines and open boundaries of the area of interest. This involves digitizing the mainland coastline and boundary lines as one file and then all island coastlines as separate files.



Eclipse Sound and Area Satellite Image with Digitized Boundary

Using OMG software, digitizing is performed in *jview*. A base image of the coastline in the area must exist already so that digitizing is possible. To open *jview* and begin digitizing the following command is run:

```
jview SatelliteImage.ext -geomask
```

Open a small window in *jview* and begin digitizing the coastline by clicking the middle mouse button. The digitized coastline coordinates will be written to an output file called *mask.file*, but only when *jview* is closed; therefore *jview* should be closed often to save your work. Take note that when *jview* is shut down and started again it will overwrite your previous *mask.file* file; therefore when you

close *jview* to save your work, you must rename the mask.file file (ex: mv mask.file Coast1.geomask). When the entire mainland coastline and open boundaries have been digitized it must be compiled into a single file. The mask file will have the initial coordinate as its final coordinate in its list which should be removed. The island coastlines will each have their own geomask files.

When all coastlines have been digitized, they can be compiled into the .nod (Trigrig) file format (see section 5.8, page 18, of the resolute manual). In that format the <# of nodes> is equal to the total number of digitizing points for all the coastlines and the <# of boundaries> is the total number of self contained boundaries. Notice also that the format requires that the boundary points be in the x y z format, or Longitude Latitude Depth in our case; therefore the geomask files must be rearranged to this format. For the boundary files the depth (z) can be set to 0.

5. To create a TIN using resolute, the *make_triangle_mesh* script that is included with the resolute program must be modified slightly and run to create the grid. The “Input boundary node file” and the “Input depth data file name” fields must be modified to correspond to your boundary file and a depth file names. The “Desired root name of depth mesh file” and the “Desired root name of output neighbour file” fields can be changed to correspond to desired output file names. Other parameters in the *make_triangle_mesh* script can be modified by following the instructions in the resolute manual.
6. The output of the TIN generation process can be viewed used the *showme* command that comes with Resolute.

```
showme output_file_prefix
```

7. Three of the output files from the resolute TIN creation are needed for input to Quoddy, the .bat, .nod and .ele files. The files need to be converted from Trigrig to NML format.
 - The .bat file should be edited so the node numbers start at 1.
 - The .ele file should be edited to remove the header line, the element numbers (1st column) should be incremented by 1 so that the numbers begin at 1 and the node numbers should all be incremented by 1, to correspond to the node numbers in the .bat file.
 - The .nod file is created from the .node file by removing the header information, the attribute numbers and the boundary flags. The node number column must be incremented by 1 to correspond with the other

files.

- The nod file must also be converted from x, y coordinates back to longitude, latitude coordinates. This can be done using the *invproj* command included with PROJ. The first column of node numbers in the new .nod file should be removed so that the coordinates are the only thing in the file. The node numbers can be put back in later. The *invproj* command is run using the info from the filename.node.proj file as follows:

```
invproj +proj=lcc +lat_1=7.227438e+01
        +lat_2=7.340681e+01 +lon_0=-
        7.828313e+01 +lat_0=7.284059e+01
        file.nod > fileLonLat.nod
```

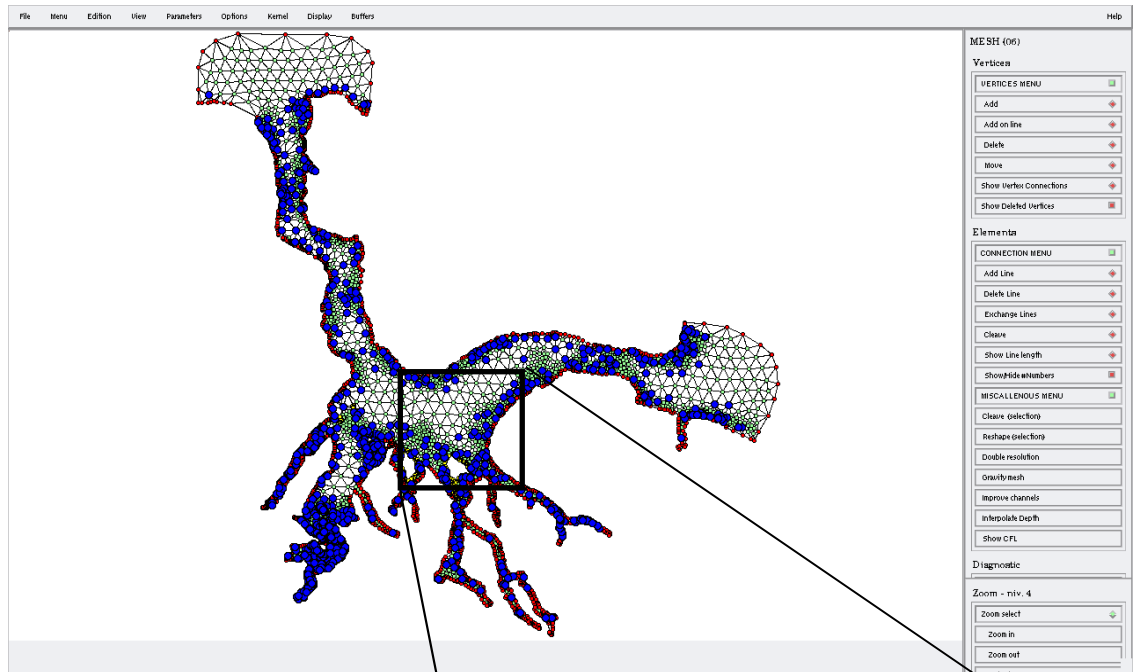
8. Once the three files for Quoddy are created, ensuring that they all have the same filename prefix, they can be edited using a program called Genesis. The TIN that Resolute creates will not be perfect and it must be edited before being input to Quoddy. Depending on the complexity of the TIN, editing can be the most time consuming task in the development of the input files for the hydrodynamic model.
9. The first step in working with Genesis is to move the '.startup' file to the working directory (directory where the Quoddy files are located). The '.startup' file must be edited to correspond to the project area. Fields such as the zoom extents field, the coastlines file location, the tmp working directory, etc. must be modified. The command *xscanp* can then be run from the working directory to open Genesis (as long as during the installation of Genesis, the *xscanp* script was put into a directory in the system path).
10. Once Genesis is up and running, the Quoddy files can be loaded using the following procedure.
 - Go to the **Mesh** menu and select **(Mesh) Elements**
 - Turn on the three menus to the right of the screen
 - Go to the **Options** menu, select **Mesh & Nodes** and then turn on **Rescan boundaries when loading**.
 - The Quoddy files that were created in previous steps can now be loaded into Genesis. Go to **File → Open** then select the **Quoddy** button at the bottom of the new window and open the Quoddy files that were created.

The mesh that was created in Resolute should now show up in Genesis. If the mesh does not look correct or if you turn on **Display Deleted Vertices** and there are many deleted vertices, then you may want to re-run Resolute using different parameters in the *make_triangle_mesh* script. Genesis will have trouble loading the mesh if there are too many vertices connected to a node.

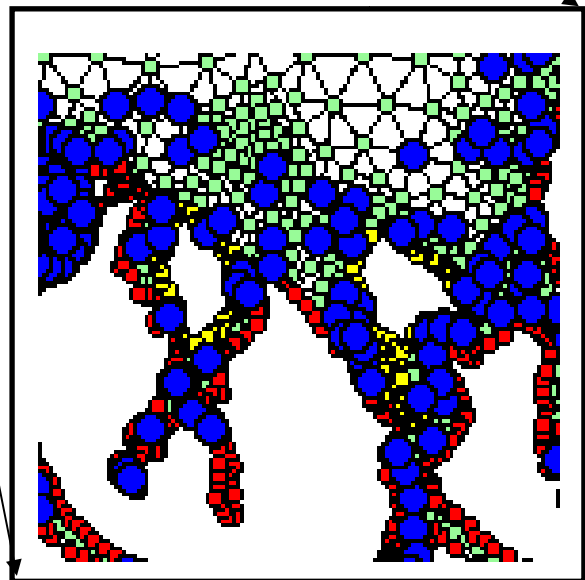
11. Ideally each triangle in the TIN mesh should be an equilateral triangle to ensure the best geometry for input to Quoddy. Having only equilateral triangles would cause each node to have six equally spaced vertices attached to it. This perfect situation will never occur in the model, but it is desirable to get as close to it as possible. Therefore, to modify the mesh that was created in resolute, a filter will be applied that flags all nodes that have more than seven and less than five neighbouring nodes. This will create a cleaner model that has triangles that are closer to the ideal geometry. Filtering is performed as follows.

- Go to the **Display** menu and select **Mesh & Nodes**
- Turn on the **Filter Nodes** options, remove the **CFL Condition**, set the **Minimum Neighbours** to 5 and the **Maximum Neighbours** to 7 and click **ok**.

The display should now show exterior boundary nodes in red, island boundary nodes in yellow, interior nodes in green and any node that failed the filter conditions in blue. Boundary nodes can have less than 5 vertices but not more than 7, as a special case.



Resolute Mesh Loaded into Genesis with Filters Applied



12. The flagged blue nodes will have to be edited so that they have between 5 and 7 vertices attached to them. Some boundary nodes and elements will also have to be modified as the program sometimes does not work properly when connecting

sequential boundary nodes. Stiff elements must also be removed from the mesh. Stiff elements are triangles that are made up of entirely boundary nodes (no interior nodes). Editing the nodes can be very time consuming and the program can be quite temperamental at times, so it's best to save your work often. Saving with an incremental filename is also useful if you need to go back to a previous editing point (ex. file1a.ext, file1b.ext ...).

13. To begin editing, zoom into an area of interest, by enabling the **Zoom Selected** button on the right side of the display. Draw a box over the area and then click **Zoom In**. The nodes and elements must be rearranged and altered so that they fall within the filter conditions and look correct. Editing is performed using the options in the **Vertices** and **Elements** menus to the right of the display. The most used options are the following.

- **Add on line:** Add a node on an element line to help improve geometry.
- **Exchange lines:** Switch an element to the other two nodes that it could be connected to. This is useful when you want to give a node another element.
- **Cleave:** Split a node into two nodes. This is useful when a node has a too many elements attached to it.
- **Reshape (selection):** Reshape triangles to conform to newly created nodes or elements. It is a good idea to choose this every time an edit is made.
- **Improve Channels:** Splits up stiff elements by adding vertices (node) on the line that creates the stiff element. This could be run while viewing the entire mesh to remove all stiff elements.
- **Delete Vertices, Add line and Delete Line:** All useful commands that are most often used to fix boundaries.

14. After cleaning the mesh in Genesis, there will be a new set of mesh files (.nod, .bat, .ele). The next step is to load the files into Matlab using the [OPNML routines](#) [Ocean Processes Numerical Modeling Laboratory, 2005]. Prior to loading the files into Matlab, the first two lines of the .bat file must be removed. Genesis adds a header to the .bat file that cannot be interpreted by the OPNML routines.

The latitude and longitude's within the .nod file can be converted to x and y. This is done using the *proj* command and the information contained within the "filename.node.proj" file (see Step 7). Choosing whether to use geographic or projected coordinates will affect the settings to be used in Quoddy.

Download the OPNML functions from the web and set them up for use in Matlab. Open Matlab and enter the directory where the mesh files are located. The mesh data is loaded using the *loadgrid* command:

```
Grid = LoadGrid('GridPrefix')
```

The mesh can be displayed using the following commands:

```
drawelems(Grid) < Plots the mesh elements
```

```
plotbnd(Grid) < Plot the mesh boundary
```

```
colormesh2d(Grid) < Plot a color grid of the mesh bathymetry
```

15. The next step is to calculate the CFL condition of each element in the mesh. The CFL condition is a relationship between the size of the element and the water depth. If there any elements that do not satisfy the CFL condition, go back into Genesis and resize the elements at fault. If all elements satisfy the CFL condition, then the script will clean out any unused nodes and create new .nod, .ele and .bat files. The command is as follows:

```
ComputeCFLCleanWrite(0.5) < 0.5 is the CFL condition to be tested.
```

The function will ask you to locate the model file.

The input to this function (0.5 in this case) is the desired time step to be used in the model. It does not tell you what time step to use based on the input grid.

16. After running the ComputeCFLCleanWrite() function, the depths for each node must be recalculated against the original grid. This is done using the *redep* command in the konsole / terminal.

```
repedc reference.nod reference.ele reference.bat newfile.nod  
newfile.nod newfile.ele ouput.nod output.ele output.bat
```

or

```
repedc reference.nei newfile.nod newfile.nod newfile.ele  
ouput.nod output.ele output.bat
```

Load the new redep'd grid into Matlab.

```
RedepGrid = loadgrid('output')
```

17. The next step is to format and sort the grid files. The bandwidth of the file is reduced by reordering the nodes.

Run the following command in Matlab.

```
NewGrid = Reduce()
```

18. The node numbers must be sorted in the boundary file, .bnd, so that the island nodes are numbered clockwise and the main coastline is sorted counter clockwise. This is performed using the Matlab program `DisplayAllPoint.m`. The main coastline will usually be in the correct order and for each island the boundary nodes are coloured in order from green to red. The plot generated by `DisplayAllPoint.m` will help show which islands are incorrectly numbered. If the island boundary is displayed in the wrong direction (i.e. green to red in a counter clockwise order) then the island needs to be reordered.

```
DisplayAllPoint(NewGrid)
```

The last line of the .bel file may need to be deleted if it is simply zeros.

19. Edit the program `Create_Bel.m` using the newly created `island.csv` file to put the nodes in the correct order. Edit the “island renumber” numbers to correspond to the node numbers that need to be reversed and change the boundary node numbers. In Matlab `numbnd(Grid)` can be used to display the boundary node numbers. The program `Create_Bel` is run in matlab.

```
Create_Bel
```

20. The open boundary forcing conditions must be extracted from the reference hydrodynamic model grid. The Matlab program `interp_bdry` performs this task.

21. A header must be added to the boundary condition and .bel files for input to QUODDY.

22. QUODDY is run using the `QUODDY` executable as follows. The output from the program is sent to `bylot.res`, `bylot.inq` is an input file, 1 is the number of cycles for ramp up and `bylot_bnd_M2.s2c` is the tidal constituents along the open boundaries.

```
quoddy > bylot.res
          bylot.inq
          1
          bylot_bnd_M2.s2c
```

The .inq input file is read by QUODDY and contains the grid name and other parameter values to be used in the execution of QUODDY. The following is an example input file:

```

{Comment:}
Bylot Waters
{Case name:}
bylot
{Coordinates: CARTESIAN/SPHERICAL}
CARTESIAN
{Boundary element incidence list:}
bylot.bel
{Initial condition file:}
COLD-START 01 01 2006 0.0
{Echo file:}
bylot.echo
{Simulation parameters:}
SI UNITS          [units]
1.00  1.00  1.00  [x, y, and z scaling factor]
72          [degree latitude]
10.0        [minimum depth]
01 01 2006 536544. [end date (d m y) and time (sec) of simulation]
0.5         [time step (seconds)]
10          [number of vertical nodes]

SETQ5
&input
  MASSVAR = 'ZERO'
  PRESSURE = 'BAROTROPIC'
  CLOSURE = 'MY25'
  AHMIN = 10.
  EKMIN = 1.e-3
  EKQMIN = 1.e-3
  EKHMIN = 1.e-3
  Cd = 0.005
  AKMIN = 0.0005
  IQADVDF = 0
  IHHBC = 1
&end

VERTGRID
&input
  GRID = 'SINE'
  DZBL = 1.0
&end

```

DFT

```
&input
  nperiods      = 1
  nconsts       = 1
  constituents   = 'M2'
&end
```

OUTPUT

```
&input
  outdir        = 'output'
  savefield     = -3726
  field         = 'va','e','z','v'
&end
```

APPENDIX B

Developed Matlab Programs

- ComputeCFLCleanWrite.m
 - Compute the CFL condition, check that criteria are met, clean the file by removing unused nodes and write output to a new file
- Reduce.m
 - Reduce the bandwidth of the input file
- DisplayAllPoints.m
 - Display the mesh and highlight whether numbering is clockwise or counter clockwise for island boundaries.
- Create_Bel.m
 - Orders the island boundary nodes correctly for input to QUODDY

Developed C Programs

- AvgDepth.c
 - Calculate the average depth and RMS depth for an input XYZ file
- Check_Nav.c
 - Output an explanation of the contents of each record in an input .nav file
- dumpTides.c
 - Output a text file of position and tide values from an input nav file
- GAPStoNav.c
 - Convert the output of the GAPS processing software to a .nav file
- GPStoNav.c
 - Convert ASCII position data to a .nav file
- POStoNav.c
 - Convert an ASCII POS file to a .nav file
- pressureNav.c
 - Convert atmospheric pressure record to a .nav file for analysis
- navModel.c
 - Trim a .nav file based on an input map of an area of interest.
- tideError.c
 - Develops a predicted tide series over a specified period of time for two sets of harmonic constituents

Modified

- `appendNav.c`
- `diffTide.c`
- `plotTides.c`
- `tidecor2.42.c`

Church, I., Hughes Clarke, J.E., Haigh, S., and Brucker, S., 2006, *Comparing GcGPS Ellipsoid Height Records, Predicted Tides and a Hydrodynamic Circulation Model for the Pond Inlet, Eclipse Sound and Navy Board Inlet System*. ArcticNet Annual Scientific Meeting, poster presentation, Victoria, British Columbia, Canada.

Church, I., 2006, *Towards a Nested Finite-Element Hydrodynamic Model to Predict Phase and Amplitude Modification of Tide within Narrow Fjords*. Geomatics and Geodesy Student Technical Conference, oral presentation, Fredericton, New Brunswick, Canada.